WHP Cruise Summary Information

WOCE section designation	A10
Expedition designation (EXPOCODE)	06MT22_5
Chief Scientist(s) and their affiliation	Reiner Onken, IfMK
Dates	1992.12.27 – 1993.01.31
Ship	METEOR
Ports of call	Rio de Janeiro, Brazil to Cape Town, Africa
Number of stations	112
Geographic boundaries of the stations	23°38.10''S 47°29.90''W 15°0.12''E 30°2.30''S
Floats and drifters deployed	1 float and 6 drifters (see 7.4.4 & 7.4.5)
Moorings deployed or recovered	none

Contributing Authors
In order of appearance

W.Balzer, M. Rhein, T.J. Müller, W. Zenk, R. Onken, U. Rosiak, M. Kalberer, V. Ratmeyer, U. Kuller, M. Bleckwehl, G. Fischer, A. Zimmermann, H. Buschhoff, F. G. Palma, D. Schneider, L. Stramma, J. Waniek, M. Elbrächter, J. Fischer, C. Meinke, U. Papenburg, G. Kroll, U. Send, G. Krahmann, J. Reppin, Th. Mitzka, U. Beckmann, C. Duncombe Rae, W. Erasmi, I. Girod, J. Holfort, U. Koy, P. Meyer, A. Welter, N. Zangenberg, H. Johannsen, K. Johnson, U. Karbach, A. Korves, L. Mintrop, A. Morak, J. Morlang, B. Schneider, C. Zelck, K. Bulsiewicz, G. Fraas, A. Putzka, J. Weyland, J. Brinkmann, M. Krämer, S. Matthias-Maser, R. Tiesel, W.-T. Ochsenhirt, E. Röd, J.C. Jennings, L.I. Gordon

WHP Cruise and Data Information

Instructions: Click on items below to locate primary reference(s) or use navigation tools above.

Table of Contents

* Items not yet available in this DOC file and absent in table of PDF file.

Abstract

From 22 September 1992 to 31 January 1993 the German Research Vessel METEOR performed its 22nd cruise, a journey in the Atlantic Ocean divided into five legs. The main objectives were geological and chemical observations in subtropical regions of the North Atlantic and in the tropical South Atlantic and in the tropical South Atlantic. Additional physical investigations were concentrated in the equatorial regions and at subtropical latitudes of the South Atlantic. These activities were coordinated internationally as part of the World Ocean Circulation Experiment (WOCE). They were supplemented by biological and air chemistry observations and by a component of Joint Global Ocean Flux Study (JGOFS).

1 Research Objectives

The investigations during METEOR cruise no. 22 (Fig. 1a-c, Tab. 1) were aimed for geological and chemical studies in the subtropical North Atlantic and the tropical Atlantic (leg 1) at physical studies of large-scale oceanic transports in the equatorial Atlantic (leg 2) and the subtropical South Atlantic (legs 3, 4, and 5). The circulation measurements are part of the "World Ocean Circulation Experiment" (WOCE). In addition, biological and aerosol observations were carried out.

The main goal of the activities during leg 1 of the Meteor cruise M22 was to improve the understanding of the environmental controls over particle sedimentation in the ocean. This sedimentation is an important component of the global carbon cycle. Several deep-sea moorings with sediment traps for particle sampling that have been deployed earlier had to be retrieved and relaunched during the cruise near the Canary Islands, south of the Cabo Verde Islands, and in the tropical east and west Atlantic. For studies of trace element cycling, suspended particulate matter, sediments and water samples where taken in addition to particles collected by moored sediment traps.

During M 22/2, the circulation and water mass exchange in the tropical western Atlantic was studied. The programme is part of the German distribution to the international WOCE programme. The western boundary current is an important part of the thermohaline circulation, not only for inter-hemispheric water mass transfer, but also for the meridional heat transport. In order to determine the mean transports of the carious water masses and their variability, three current meter moorings were deployed in the boundary current at 44˚ W. Ship-based direct velocity measurements were carried out with two acoustic systems, the ADCP (lowered with the CTD and vessel-mounted) and the Pegasus profiling system. The CTD measurements were complemented by oxygen and freon measurements to determine the water mass boundaries and the spreading pattern of the various water masses and their variability. Additionally XBT's were dropped to improve spatial resolution.

In the South Atlantic, the heat and water mass transports are dominated by the anticyclonic subtropical gyre near the surface. At lower levels the (Sub) Antarctic Intermediate Water and the Circumpolar Deep Water have northward components, and the North Atlantic Deep Water has southward components. At the lowest level the Antarctic Bottom Water passes the South Atlantic on its way from the Antarctic to the North Atlantic. Investigations of the water mass transports in the western South Atlantic were performed during legs 3 and 4. These included studies of the near-surface southward Brazil Current, the Antarctic Intermediate Water on its way north, the deep western boundary current at the continental slope and the overflow of Antarctic Bottom Water across the Rio Grande Rise through the Vema and Hunter Channels. Thirteen deep-sea current meter moorings had been deployed by METEOR in January 1991 between the continental slope and the Vema Channel. Eleven of these moorings were recovered. CTD measurements were also carried out at the moorings' positions for a determination of the water mass contribution, and in the area of the eastern Rio Grande Rise. Seven deep-sea moorings were deployed in the Hunter Channel overflow region. In addition, satellite-tracked ARGOS drifters were launched for near-surface current observations, and RAFOS floats with acoustic tracking for current measurements in the Antarctic Intermediate Water. Four sound sources were deployed in the area. These studies are part of the "WOCE Deep Basin Experiment" (DBE).

The global "WOCE Hydrographic Programme" (WHP) includes a large set of zonal and meridional sections in all oceans, with measurements of temperature, salinity, oxygen, nutrients and anthropogenic tracers. The aim is the determination of global water mass distributions and geostrophic mass and heat transports. The zonal WHP section A10 along 30˚ S was selected for leg M 22/5. Station distances were in the range of 9 to 45 nautical miles on a cruise track from Brazil to southern Africa. The investigations were supplemented by measurements of the carbonate system as a contribution to the "Joint Global Ocean Flux Study" (JGOFS), by biological sampling for the determination of surface plankton, and by studies of atmospheric aerosol particles. Here, particularly the biological constituents, the size distributions and the soluble components of aerosol were determined. In addition the carbon content and the properties of precipitation water found in these extremely clean oceanic regions will be compared to results from urban areas.

Tab. 1: Legs and chief scientists of METEOR cruise no. 22

Leg 22/1
- 22.09.92 - 21.10.92
- Hamburg - Recife/Brazil
- Chief scientist: Prof. Dr. W. Balzer

Leg 22/2
- 23.10.92 - 15.11.92
- Recife - Recife
- Chief scientist: Dr. M. Rhein

Leg 22/3
- 18.11.92 - 30.11.92
- Recife - Santos/Brazil
- Chief scientist: Dr. T.J. Müller

Leg 22/4
- 01.12.92 - 22.12.92
- Santos - Rio de Janeiro/Brazil
- Chief scientist: Dr. W. Zenk

Leg 22/5
- 27.12.92 - 31.01.93
- Rio de Janeiro - Cape Town/South Africa
- Chief scientist: Dr. R. Onken

Coordination:
- Prof. Dr. G. Siedler

Masters (F.S. METEOR):

Legs 22/1-4
- Captain G. Müller

Leg 22/5
- Captain M. Kull

2 Participants

Tab. 2: Participants of METEOR cruise no. 22

Leg M 22/1

Name	Specialty	Institute
Balzer, Wolfgang, Prof. Dr. (Chief Scientist)	Marine Chemistry	UBB
Bleckwehl, Manfred, Dipl.-Ing.	Geology	UBG
Buschhoff, Hella, Techn. Ass.	Marine Chemistry	UBB
Fischer, Gerhard, Dr.	Geology	UBG
Gonzales Palma, Francisco, Stud.	Marine Chemistry	UGC
Kalberer, Markus, Stud.	Environ. Sciences	ETHZ
Kuller, Uwe, Stud.	Geology	UBG
Ochsenhirt, Wolf-Thilo, Techn.	Meteorology	DWD
Rathmeyer, Volker, Dipl.-Geol.	Geology	UBG
Rosiak, Uwe, Techn. Ass.	Geology	UBG
Schneider, Daniel, Stud.	Marine Chemistry	UGC
Tiesel, Reiner, Dr.	Meteorology	DWD
Zimmermann, Andreas, Stud.	Marine Chemistry	UBB

Leg M 22/2

Name	Specialty	Institute
Rhein, Monika, Dr. (Chief Scientist)	Marine Physics	IfMK
Baum, Ekkehard, Dipl.-Phys.	Marine Physics	IfMK
Beckmann, Uwe, Techn.	Marine Physics	IfMK
Eisele, Alfred, Techn.	Marine Physics	IfMK
Elbrächter, Martina, Techn.	Marine Physics	IfMK
Fischer, Jürgen, Dr.	Marine Physics	IfMK
Krahmann, Gerd, Dipl.-Phys.	Marine Physics	IfMK
Kroll, Gerhard, Dr.	Marine Physics	IfMK
Langhof, Hans-Jürgen, Techn.	Marine Physics	IfMK
Meinke, Claus, Dipl.-Ing.	Marine Physics	IfMK
Mitzka, Thomas, Stud.	Marine Physics	IfMK
Ochsenhirt, W.-Th., Techn.	Meteorology	DWD
Papenburg, Uwe, Techn.	Marine Physics	IfMK
Ramos, José, Capitao-Tenente	Observer	DHN
Reppin, Jörg, Dipl.-Oz.	Marine Physics	IfMK
Send, Uwe, Dr.	Marine Physics	IfMK
Stramma, Lothar, Dr.	Marine Physics	IfMK
Tiesel, Rainer, Dr.	Meteorology	DWD
Tinnemeyer, Stephan, Stud.	Marine Physics	IfMK
Treede, Holger, Techn.	Marine Physics	IfMK
Waniek, Joanna, Dipl.-Oz.	Marine Physics	IfMK

Leg M 22/3

Name	Specialty	Institute
Siedler, Gerold, Prof. (Chief Scientist, Nov. 16-18)	Marine Physics	IfMK
Müller, Thomas, Dr. (Chief Scientist, Nov. 18-30)	Marine Physics	IfMK
Bassek, Dieter, Techn.	Meteorology	DWD
Biastoch, Arne, Stud.	Marine Physics	IfMK
Boebel, Olaf, Dr.	Marine Physics	IfMK
Carlsen, Dieter, Techn.	Marine Physics	IfMK
Haag, Christian, Stud.	Marine Physics	IfMK
Johannsen, Werner, Techn.	Marine Physics	IfMK
Kipping, Antonius, Techn.	Marine Physics	IfMK
Kisjeloff, Boris, Techn.	Computer Science	IfMK
Ramos, José, Capitao-Tenente	Observer	DHN
Röd, Erhard, Dr.	Meteorology	DWD
Wehrend, Dirk, Techn.	Marine Physics	IfMK
Schmid, Claudia, Dipl.-Oz.	Marine Physics	IfMK

Leg M 22/4

Name	Specialty	Institute
Zenk, Walter, Dr. (Chief Scientist)	Marine Physics	IfMK
Bassek, Dieter, Techn.	Meteorology	DWD
Biastoch, Arne, Stud.	Marine Physics	IfMK
Boebel, Olaf, Dr.	Marine Physics	IfMK
Bradshaw, Kenton M., Techn.	Marine Physics	WHOI
Carlsen, Dieter, Techn.	Marine Physics	IfMK
Correia, Ivo F., Scientist	Marine Geology	GEOMAP
Diaz Pinaya, Walter H., Stud.	Marine Physics	IOUSP
Gallo Xavier, Andrea, Techn.	Data Bank	Petrobras
Haag, Christian, Stud.	Marine Physics	IfMK
Hogg, Nelson, Dr.	Marine Physics	WHOI
Johannsen, Werner, Techn.	Marine Physics	IfMK
Kipping, Antonius, Techn.	Marine Physics	IfMK
Kisjeloff, Boris, Techn.	Computer Science	IfMK
Moreira Lima, José, Scientist	Marine Physics	Peterobras
Ramos, José, Capitao-Tenente	Observer	DHN
Röd, Erhard, Dr.	Meteorology	DWD
Wehrend, Dirk, Techn.	Marine Physics	IfMK
Worrilow, Scott, Ing.	Marine Physics	WHOI
Schmid, Claudia, Dipl.-Oz.	Marine Physics	IfMK
Zhang, Huai, Scientist	Marine Physics	WHOI

Leg M 22/5

Name	Specialty	Institute
Onken, Reiner, Dr. (Chief Scientist)	Marine Physics	IfMK
Bassek, Dieter, Techn.	Meteorology	DWD
Beckmann, Uwe, Techn.	Marine Physics	IfMK
Brinkmann, Jutta, Dipl.-Met.	Atmospheric Physics	UMZ
Bulsiewicz, Klaus, Dipl.-Phys.	Tracer Oceanography	UBT
Duncombe Rae, Chris, M.Sc.	Phys. Oceanography	SFRI
Erasmi, Wolfgang, Stud.	Marine Physics	IfMK
Fraas, Gerd, Techn.	Tracer Oceanography	UBT
Girod, Ilona, Stud.	Marine Physics	IfMK
Holford, Jürgen, Dipl.-Oz.	Marine Physics	IfMK
Johannsen, Hergen, Techn.	Marine Chemistry	IfMK
Johnson, Kenneth, Dr.	Marine Chemistry	BNL
Karbach, Uwe, Techn.	Marine Chemistry	IfMK
Korves, Annette, Techn.	Marine Chemistry	IfMK
Koy, Uwe, Techn.	Marine Physics	IfMK
Krämer, Martina, Dr.	Atmospheric Physics	UMZ
Matthias-Maser, Sabine, Dr.	Atmospheric Physics	UMZ
Meyer, Peter, Dipl.-Ing.	Marine Physics	IfMK
Mintrop, Ludger, Dr.	Marine Chemistry	IfMK
Morak, Anja, Techn.	Marine Chemistry	IfMK
Morlang, Jürgen, Stud.	Marine Chemistry	IfMK
Putzka, Alfred, Dr.	Tracer Oceanography	UBT
Ramos, José, Capitao-Tenente	Observer	DHN
Röd, Erhard, Dr.	Meteorology	DWD
Schneider, Bernd, Dr.	Tracer Oceanography	UBT
Welter, Alexander, Stud.	Marine Physics	IfMK
Weyland, Joachim, Stud.	Tracer Oceanography	UBT
Zangenberg, Norbert, Dipl.-Oz.	Marine Physics	IfMK
Zelck, Clementine, Dipl.-Biol.	Marine Biology	BAH

Tab. 3: Participating Institutions

BAH	Bundesforschungsanstalt Helgoland c/o Zoologisches Institut und Museum Martin-Luther-King-Platz 3 20146 Hamburg Germany
BNL	Oceanographic and Atmospheric Sciences Division, Bldg. 318 Brookhaven National Laboratory Upton, NY 11973 USA
DHN	Diretoria Hidrografia e Navegacao Niteroi, RJ Brazil
DWD	Deutscher Wetterdienst, Seewetteramt Bernhard-Nocht-Str. 76 20359 Hamburg Germany
ETHZ	Eidgenössische Technische Hochschule Dept. Umweltnaturwissenschaften Zürich Switzerland
GEOMAP	GEOMAP Rua Mexico, 21-150 Rio de Janeiro - RJ Brazil
IfMK	Institut für Merreskunde an der Universität Kiel Düsternbrooker Weg 20 24105 Kiel Germany
IOUSP	Universidade de Sao Paulo Instituto Oceanográfico Cidade Universitária CEP 055 08 P.O. Box 9075 Sao Paulo Brazil

Petrobras	Petrobras/ CENPES (Research and Development Center) Cidade Universitária Q7 Ilha do Fundao 21910 Rio de Janeiro - RJ Brazil
SFRI	Sea Fisheries Research Institute Private Bag X2 Rogge Bay 8012 Cape Town Republic of South Africa
UBB	Fachbereich 2, Meereschemie Universität Bremen P.O. Box 330440 28334 Bremen Germany
UBG	Fachbereich Geowissenschaften Universität Bremen P.O. Box 330440 28334 Bremen Germany
UGC	Facultad de Ciencias del Mar Universitad de Las Palmas de Gran Canaria Campus universitario de Tafira 35017 Las Palmas de Gran Canaria Spain
UMZ	Institut für Physik der Atmosphäre Johannes-gutenberg-Universität Saarstr. 21 55122 Mainz Germnay
WHOI	Woods Hole Oceanographic Institution Woods Hole, MA 02543 USA

3 Research Programme

3.1 Marine Geology and Marine Chemistry, Leg M22/1

For the long-term research project of the SFB 261 aimed at reconstructing the mass budget and current systems of the South Atlantic during the late Quaternary, sample material needs to be taken from the water column, from sinking particles and from the sea floor. The sediment traps deployed during METEOR-Cruise 20 had to be recovered and partly re-deployed; in addition, new trap moorings had to be launched south of Cabo Verde and in the equatorial West Atlantic. Micropaleontological, geochemical and isotopic characteristics of the trap material and of the sediments will be determined both on board and in laboratories at home subsequent to the cruise.

3.1.1 Particle Flux Studies

It was intended to determine the seasonal pattern of particle sedimentation in representative productivity regions of the Eastern and Equatorial Atlantic. For this purpose, sediment traps with time controlled sample changers were deployed at critical stations during cruise M 20 for a period of one year; these traps had to be recovered and redeployed during cruise M 22. New moorings with sediment traps had to be deployed south of Cabo Verde Islands in a highly productive divergence zone and in the equatorial West Atlantic. The moorings in the West Atlantic are part of a SW-NE transect over the equatorial upwelling system. The transect will be completed by an additional mooring to be deployed during M23/3.

The following properties of the trapped material will be investigated: the species composition of the planktonic organisms (pteropods, foraminifera, radiolaria, coccolithophorids, and diatoms), the chemical and isotopic composition of these organisms, as well as the composition of the organic and terrigenous material. The objective of the study is to identify seasonal variations in those components, which play an important role in the sediment formation process. The results are expected to provide a basis for deducing paleo-current systems and paleoproduction conditions from sediment analyses.

The primary aim was to characterize the particle flux in the important production zones and to determine the portion of sinking material (export production) in relation to the productivity of the region. In particular, the idea is to be tested that a smaller portion of material sinks out of less productive regions in comparison to productive regions. In addition, it is important to consider the ratio of carbon in organic form (C_{org}) to carbon in carbonates (C_{carb}) and its variation from one area to the other. This ratio is important for the carbon cycle since the formation of carbonate releases CO_2, while the production of organic matter binds it. A potential correlation between the sedimentation of opal and the productivity of a region will also be investigated.

3.1.2 Trace element cycling

The Marine Chemistry Group at the University of Bremen investigates the vertical transport of trace elements from the mixed layer until their burial in the sediments by participating in the sediment trap program of the Dept. of Geosciences at the University of Bremen. Several productivity regions typical for the Eastern and Equatorial Atlantic are studied within the framework of the German JGOFS program. In the material from the moored sediment traps (consisting mostly of fast sinking particles) a set of selected trace elements (Al, As, Ba, Cd, Co, Cr, Cu, Fe, Mn, Ni, Pb, Se, V, Zn) will be analyzed in home laboratories. During M22/1 samples of suspended material (comprising slowly sinking particles) were obtained on the same stations by using in situ-pumps supplemented by water sampling using GoFlo-bottles. Comparison of both kinds of water column particles with the trace element composition of the sediment, and its relation to the vertical distribution of dissolved trace elements in the water column are expected to provide important clues on transport and sorption mechanisms as well as on the general geochemical behaviour of these elements in the ocean.

For a study of trace element speciation and the their mode of dissolution from dust, suspended particles from the regions of maximal dust input and of maximal precipitation (ITCZ) off Northwest Africa were sampled.

3.2 Physical Oceanography M 22/2

The western tropical Atlantic is a region of special interest in the global circulation. The meridional heat transport takes place by warm surface water and subpolar intermediate water from the Southern Hemisphere moving northward in the upper 800m, and North Atlantic Deep Water (NADW) moving southward between 1200 and 4000 m. In total, the transport of this meridional cell at the equator is estimated at 15 x $10^6 m^3 s^{-1}$ or even higher. The details of the mean water mass exchange across the equator are not well known from observations. Furthermore, the seasonal changes of the upper-layer circulation in this region are insufficiently explored.

The objective during leg M 22/2 was to investigate the transport and the spreading of water masses in the western equatorial Atlantic with regard to their means as well as their annual and longer-term variations. For comparison the results of the fall situation 1990 from cruise M 14/2 and the spring situation 1991 from cruise M 16/3 are available.

Currents were investigated using current meter moorings as well as shipborne acoustic measurement techniques on different time and space scales. Three moorings were deployed along 44° W off the Brazilian coast (K359 - K361). All three moorings are equipped with upward-looking acoustic Doppler current profilers (ADCPs) for measuring the currents in the upper 300m of the water column. From the moorings, results are expected on the mean currents and on transports in the boundary regime and their variability.

The instantaneous current field was measured by two shipborne acoustic measurement techniques. One method used the shipborned ADCP which recorded the currents within the upper 300 m of the water column. The second acoustic method used the Pegasus system. It included a free-falling acoustic instrument that measures the acoustic travel time relative to bottom transponders, which were deployed and distances were measured prior to profiling. Near the ocean bottom the Pegasus dropped an attached weight and returned to the ocean surface. From the recorded acoustic travel time data relative to the bottom transponders a current profile was derived on board of the sip. Because of the complicated vertical structure of the currents near the equator and the non-applicability of the geostrophic method, the Pegasus system is the most suitable instrument to measure current profiles and transport below the depth reached by the vessel-mounted ADCP. Pegasus drops were carried out at 44˚ W, at 35˚ W, and at 5˚ S (see Fig. 1d). Another profiling system used a self-contained ADCP attached to the rosette. This method was explored and found to work well on previous cruises.

The distributions of salinity, oxygen, freon and temperature characterize the water masses in the equatorial boundary current region. Measurements at 60 stations were carried out suing the CTD with oxygen sensor and rosette sampler. From the rosette, water samples were taken to determine freon concentrations and to calibrate the salinity and oxygen measurements. Resolution along the sections was improved by XBT drops between the hydrographic stations. The results of M 22/2 will be compared to the previous measurements of cruises M 14/2 and M 16/3 and further evaluated in cooperation with other groups.

3.3 Physical Oceanography M 22/3-4

The planned work of the Marine Physics group was related to two topics (see Figs. 4 and 5). First, we have investigated the Brazil Current and its hydrographic environment at the shelf edge of Brazil. Second, we studied the deep western boundary currents and the water exchange of Intermediate and Bottom Waters between the Argentine and the Brazil basins. The main objectives of both subprogrammes concerned water transport rates in the southwest of the large-scale subtropical circulation in the South Atlantic. Both programme topics were directly related to the work that was preformed on board METEOR during cruise no. 15. In January 1991 a total of 13 deep-sea moorings was launched between the Brazilian shelf and the Vema Channel. These moorings had to be recovered during cruise no. 22. Both studies represent significant components of the international WOCE programme with its subprogramme Deep Basin Experiment (DBE). The field work was carried out in cooperation with researchers of the University of Sao Paulo, Brazil, and the Woods Hole oceanographic Institution, USA.

Surveys of the 200-300 m deep Brazil Current were conducted using acoustic (ADCP) and electromagnetic (XCP) methods. Near-surface currents have been determined by satellite tracked drifters. All current observations were supplemented by CTD and XBT casts. Beneath the southward Brazil Current flows the Antarctic Intermediate Water with a northward component at 900m depth. Neutrally buoyant RAFOS floats have been used to track the movement of these waters. The deep western boundary current system additionally was observed by CTD profiling.

After the recovery of the earlier launched current meters in the Vema Channel METEOR proceeded towards the Hunter Channel for the deployment of six current meter moorings. The instruments will monitor the water exchange between the two ocean basins. These observations were supplemented by hydrographic surveys. In addition, we moored three sound sources in the southern Brazil Basin. They transmit an 80-second signal daily needed for RAFOS float tracking. At the end of the floats' mission they are expected to surface, and an ARGOS satellite link will be used to retrieve the data.

3.4 Physical Oceanography M 22/5

The main objective during leg 5 was a set of observations by the Marine Physics group of the zonal section A10 along 30˚ S as is part of the "WOCE Hydrographic Programme" (WHP). The primary goal was to map the large-scale three-dimensional distribution of temperature, salinity, and chemical constituents of seawater and to determine heat and water transports. The knowledge of these transports is essential for the understanding of physical processes in the ocean and the atmosphere which are relevant to the change of climate. In addition, these data serve together with other data sets as initial conditions for numerical ocean circulation models and can be used to verify model predictions. As the section through the center of the South Atlantic subtropical gyre is crossing the Brazil Current on the western side and the Benquela Current in the east close to the African continent, the observational programme was intensified there.

In combination with observations from the previous legs the survey started at the South American continental shelf with high resolution CTD measurements in the Brazil Current area. In order to obtain data from independent methods, expendable temperature probes (XBT), acoustic current profilers (ACDP) and free-falling current profilers (XCP) were used to resolve the structure of this boundary current. The same methods were applied in the Benquela Current region. On average, CTD stations were spaced approximately 30 nautical miles apart, with higher resolution in the boundary current regions and over complicated topography. Pressure, temperature, conductivity, and oxygen were measured continuously in the vertical up to the bottom. In addition, 20-40 water samples were taken on every station for the determination of hydrographical and geochemical parameters.

3.5 Marine Chemistry

The investigations on the oceanic carbonate system which started a few years ago in the Chemical Department of the Institut für Meereskunde (IfM) Kiel were continued during M 22/5. The background for these studies is the question of how much of the anthropogenic CO_2 is stored in the ocean. About 6 Gt C are presently emitted per year into the atmosphere as CO_2 by fossil fuel combustion and deforestation. From this, 3 Gt C remain in the atmosphere and cause an annual increase of the atmospheric CO_2 content by about 1.5 ppm, resulting in today's CO_2 content of almost 360 ppm in the northern hemisphere. The remaining 3 Gt C are taken up by the ocean and/or the terrestrial biosphere. The relative effectiveness of these sinks is uncertain. However, this is an important question with respect to the prediction of the future CO_2 content in the atmosphere. Model calculations and estimates based on measurements give a range of 0.5 - 2.5 Gt C for the annual uptake of CO_2 by the ocean. In order to improve our understanding of the ocean as a sink for anthropogenic CO_2, we applied two different experimental approaches:

First, the partial pressure differences of CO_2 ($DpCO_2$) were measured at the air/sea interface. This quantity is the driving force for the CO_2 exchange and, by multiplication with appropriate exchange coefficients, gives the CO_2 flux at the sea surface. The anthropogenic input may then be estimated by balancing the CO_2-fluxes on a global scale. Difficulties with this approach arise from the high spatial and seasonal variability of pCO_2 which is due to different processes: changes in temperature, convection and formation of organic matter. A measuring system (equilibrator/IR-spectrometer) was therefore developed which measures pCO_2 continuously while the ship is steaming.

Secondly, the storage of anthropogenic CO_2 is calculated from the distribution of total carbonate in the water column. Due to elevated CO_2 concentrations in the atmosphere caused by human activity, the total carbonate concentration in surface water today is higher than before the onset of industrialization. Taking into account a correction for carbonate resulting from the oxidation of organic matter, the anthropogenic contribution can be calculated and tracked by using the depth distribution of carbonate. The total carbonate concentrations as well as alkalinity were measured for this purpose in samples from the hydrocasts. In order to enhance data density, two systems were used for the coulometric total carbonate determination and the alkalinity titration.

Additionally, the marine chemistry group was responsible for the determination of nutrients and oxygen on the WHP section. According to WOCE requirements, the full set of samples is analyzed on the basis of WOCE criteria for data precision. The data are used for the identification of water masses as well as for the calculation of anthropogenic CO_2 stored in different water masses.

3.6 Biological Oceanography and Marine Taxonomy M 22/5

This survey was part of a long-term programme to describe the taxonomy, zoogeography and ecology of ichthyoplankton, planktonic Gammaridea and some other selected invertebrates from the entire Atlantic Ocean. Quantitative plankton sampling by uniform methods allows assessments of distribution patterns and particularly of areas of reproduction. A comparison of areas of reproduction with regional hydrographic features allows the evaluation of those physical environmental parameters limiting reproduction or affecting larval survival.

While generally sampling has been carried out from two surface microlayers down to 200m depth, during M 22/5 only neuston sampling was done. More intense surveys in the North Atlantic already allowed to elucidate faunistic boundaries, recently including respective seasonal and even interannual changes. In the South Atlantic, similar investigations have been made in the southeastern and southwestern shelf areas by Argentine and Spanish groups. However, the ichthyoplankton geography of the open subtropical South Atlantic is largely, and the Gammaridea plankton geography is completely unknown.

During the cruise, emphasis was placed on sampling and on the analysis of qualitative as well as quantitative faunistic differences between the shelf, the continental slope, the boundary current regimes and the central southern subtropicalgyre.

3.7 Tracer Studies M 22/5

In addition to the classical hydrographic data, the measurements of anthropogenic tracers provide parameters for water mass analysis. They are particularly important for the determination of water mass transports and mixing processes because of their well-known input history at the ocean surface.

In cooperation with the Marine Physics group measurements were carried out of the CFMs F11, F12, F113, and CCl_4 and samples for ^{3}He, tritium and ^{14}C were taken. CCl_4 is of special interest since the release of this substance to the atmosphere and thus to the oceans started much earlier than that of other tracers. Therefore it is a useful property for characterizing old water masses. Measurable CFM and tritium concentrations are found within the thermocline down to about 1000m depth and particularly in the western boundary current regime.

The zonal section A10 of the WOCE programme crossed the Brazil and Angola Basins and the northern Cape Basin. In the Brazil Basin the North Atlantic Deep Water (NADW) at the continental slope, and the Antarctic Bottom Water (AABW) and Antarctic Intermeditate Water (AAIW) north of the Vema and Hunter Channels were of special interest. The main purpose of the planned work was to monitor the tracer concentrations of these water masses and to compare them with results from earlier cruises further north.

Up to now observations in the Angola Basin and in most parts of the Cape Basin displayed tracer concentrations of deep water masses below the detection limit, except for CCl_4. One question to be answered was whether the CCl_4 (which was found on A9 at 19˚ S at the eastern slope of the Mid-Atlantic Ridge) originates from the Cape Basin. Contributions to ^3He were expected due to tritium decay in Central Water masses and due to admixture of waters of Pacific origin within the deep and bottom waters.

CFMs were measured on the majority of the water samples. Sampling of ^3He and tritium was restricted to about every third station, but had high vertical resolution. No large volume sampling was performed. Small volume ^{14}C sampling was done, and the subsequent analysis will be carried out by the Institut für Umweltphysik of Heidelberg University. The obtained data are part of the expected large WOCE tracer data set for the South Atlantic.

3.8 Atmospheric Physics M 22/5

Aerosol particles (AP) over the South Atlantic are mainly influenced by two sources: seasalt-AP and aged continental background aerosol. Probably mineral AP of the Namib Desert in Southwest Africa could also contribute to the marine AP.

During M 22/5 the size distribution of the marine AP in the size range of 0.005 mm to about 50mm radius was determined.

The ocean is an important source of biological AP. These are able to form ice nuclei and thus contribute to cloud formation. Up to now little is known about the biological portion of the marine AP. Therefore particles of this type were determined in the radius range >0.2 mm.

The capability of AP to take up water vapor is dependent on both size and solubility of the AP. The present knowledge of the solubility of AP is low. Therefore it was important to investigate the size-dependent soluble part of the AP.

Moreover, the carbonaceous part of the AP was analyzed in order to determine the contributions in particle or biogenic AP form.

Rainwater samples from this clean-air region were analyzed with regard to acidity, total concentration of soluble mass, and major anions for a comparison with similar properties in polluted areas.

4 Narrative of the Cruise

4.1 Leg M 22/1 (W. Balzer)

At 12:12 p.m. of September 22 METEOR left the harbour of Hamburg with 33 crew members, 2 meteorologists, 2 scientific guests from the University of Las Palmas (Gran Canaria) and 11 geologists and marine chemists from the University of Bremen. After several hours allowing maximal speed for METEOR the weather changed: as a consequence of permanent headwinds and opposing currents the effective speed was much less than expected all the way until the end of the English Channel. In order to test the instruments for subsequent purposes a profile of the Hudrosweep and the Parasound echo sounder across the Celtic margin was recorded (station 462-92 and 463-92; Fig.2), where a large multinational project of the European Community is to be started in 1993.

After a further test of the in situ camera in the Biscaya, the METEOR sailed directly to the first mooring position 60nm north of the Gran Canaria (station 465-92). Within less than 7 hours the mooring CI1 was recovered and the mooring CI2 was deployed successfully both equipped with 2 sediment traps and a current meter. The long-term mooring CI1 had been deployed during cruise M 20 as part of a cooperative programme of Spanish institutions and Kiel University. At all stations, where moored sediment traps had to be recovered and/or deployed for long-term studies of the seasonality of the particle sedimentation by the geologists of Bremen University, several other devices were deployed regularly: several holes using the multinet in different depth ranges were taken for studies of the plankton composition, an underwater camera was operated for in-situ studies of sinking and suspended particles; for investigations of trace element cycling, in-situ-pumps were used at different water depths to collect suspended particles from 400-900 L seawater, and GoFlo-bottles were taken for contamination-free sampling of dissolved trace elements; mostly at the end of the station work, sediments were sampled using a multicorer to which a CTD-O_2-transparency probe was attached for continuous recordings of seawater properties.

After a short trace element sampling of the top 400 m of the water column near Cape Blanc, a new mooring (Sta.467-92) with sediment traps (CV1) was deployed south of the Cabo Verde Islands at 11° 29.0N, 21° 01.0W followed by sampling of the water column and of the sediment. This programme - as outlined above - took 17 hours at a water depth of 5000 m. During transit to the main study area in the equatorial Atlantic, another short sampling programme for trace elements was performed in the upper water column at 7° 50N, 16° 55W. The stations for trace element work both north of and within the Intertropical Convergence Zone served to investigate the dissolution behaviour of Sahara born particles with and without previous digestive action of slightly acidic rain.

The week spent between 3˚ N and 6˚ S in the Guinea Basin was filled with the recovery of 3 moorings (EA6, EA7, EA8; Sta.469-92, 470-92, 471-92) with 2-4 sediment traps and the re-deployment of the mooring EA9 (Sta.470-92 at 00˚ 01.0 S, 10˚ 48.4 W) supplemented by water column and sediment sampling as mentioned before. These studies of the seasonal particle sedimentation at several positions within the equatorial upwelling region will provide information about the productivity gradients between the centre, the northern and the southern edge of this important upwelling region. These stations extend the 20˚ W-transect of the Joint Global Ocean Flux Study (JGOFS) southwards. Trap deployments near the Canary Islands, near the Cabo Verde Islands and in the Guinea Basin increase the data base from regions with low mixed layer depth but high productivity conditions resulting from equatorial or coastal upwelling. After crossing the Intertropical Convergence Zone and entering the region of SE trade winds, the sea surface temperature cooled down from 29˚ C to 22˚ C, the air temperature near the Equator fell to 21˚ C and the sky was permanently clowdy.

By leaving the last station in the Guinea Basin at Oct.10, the last week of our cruise began with 965 miles of pure sailing to our next mooring position in the northern Brasil Basin. With prevailing clowdy weather, moderate temperatures and showers from time to time we occupied the station (Sta.472-92) in the afternoon of Oct.16, too late to start with the deployment of the mooring. For security reasons this kind of work requires daylight and some extra time for unforeseen events during deployment, and work for moorings was always put to the early morning hours. Work at this station therefore was started with water and plankton sampling and filtering of large water volumes for collecting SPM and with 2 deployments of the in-situ camera. Beginning at 06.15h (ship time) the next morning we deployed the mooring WA1 with 3 sediment traps and a current meter within 3 hours; finally, the multicorer brought well filled tubes of red/brown deep sea clay from a water depth of 5500 m. Because the regular programme of station work was completed without any complications, there was extra time available for time-comsuming in-situ pumping near the sea floor for studies of resuspension processes.

After one day of sailing the Meteor reached at its last and southernmost station of this leg. Following water, plankton and particle sampling during the night, the mooring WA2 was deployed at 7˚ 31.3 S, 28˚ 02.5 W in the early morning of Oct.19. Further deployments of the in-situ camera and of the in-situ pumps, an unsuccessful trial with the multicorer and the recording of a well resolved profile of the T-S-O2-transparency probe in the water column filled the day until we had to leave for Recife at 18.00h. Right in time at 08.54h of Oct.21 we reached at the quays of Recife being happy that we had completed 90% of our programme within the short time for scientific work as compared to the long time needed for sailing roughly 6000 miles.

4.2 Leg M 22/2 (M. Rhein)

Seven members of the scientific crew arrived in Recife on October 20 and started a day later to unload the containers and to install the scientific equipment on METEOR. The scientific crew was completed on October 22 by the arrival of 14 scientists from Kiel and by Prof. Dr. Edmo Campos from the Hydrographic Institute of the University Sao Paulo, Brazil and Captainlieutenant Ramos as the Brazilian observer.

Unfortunately, the plate to mount an ADCP (Acoustic Doppler Current Profiler) in the ship's well was unavailable on board. To build one with the help of the ship's crew was postponed, we first wanted to investigate how good the installed, and recently renovated shipborne-ADCP worked. METEOR left the port of Recife on October 23, 10:00 a.m., heading northward (Fig. 1d and 3).

At sea, the shipborne ADCP registered continually the velocities down to about 300 m depths, and as the ship reached deep water, XBTs were dropped every 10-15 nautical miles (Fig. 1d) to resolve the temperature field down to 750 m depth. Two CTD stations and measurements of the instantaneous current fields with an ADCP attached to the rosette (lADCP) and with the Pegasus Profiling system (Pegasus stations S6, S7) were carried out on October 24, 0:00 at 5˚ 8 S, 34˚ 836' W and 34˚ 854' W. The CTD was mounted in a 24 bottle (10 l) rosette, where 2 bottles had been sacrificed to place the ADCP. Besides temperature and conductivity, an oxygen sensor was used, which was calibrated by oxygen titration of samples from the 10 l bottles. The Freon (F11, F12) measurements from water samples completed the programme. All systems worked well and received reliable data. A short circuit on October 25 destroyed some of the Freon analytical gear, but it could be repaired with the help of the ship's electronic technician. After this event, the Freon measurements worked well during the whole cruise. Only the new broad band ADCP (BBADCP), delivered to METEOR on October 23, and especially dedicated to measure velocities in the deep ocean failed to communicate.

After reaching the 44˚ 8 W section, the transport of the North Brazil Current (NBC) along the Brazilian shelf was surveyed with the shipborne ADCP on October 26 from 1˚ 800' S, 44˚ 824' W to 0˚ 801' N, 44˚ 824' W. On October 27 and 28, after carefully surveying the bottom with Hydrosweep, and after the evaluation of the ship's drift, three moorings were deployed off the Brazilian coast (mooring K359: 0˚ 814.6' N 44˚ 818.6' W; K360: 0˚ 837' N, 44˚ 810' W; K361: 1˚ 811.2' N 44˚ 802.7' W). Each mooring is equipped with upward looking ADCPs, which measure the currents in the upper 300m, and with 7-9 conventional Aanderaa current meters. As surface currents around 2kn were present at the mooring locations, the deployment of the moorings over the stern of the ship was more convenient than over the side.

The CTD- and Pegasus profiling at the 44˚ 8 W section was continued till October 31, where we reached our northernmost position at 6˚ 840' N. Two CTD stations were placed north of the Ceara Ridge (5˚ 842.4' N and 6˚ 804.6' N) to estimate a likely flow of lower North Atlantic Deep Water on this northern path. On the way to 4˚ 80' N, 35˚ 80' W, starting on October 31, 2:00 p.m., the shipborne ADCP was exchanged by an ADCP mounted in the ship's well because the former instrument worked only in the depth ranges to 230-300m, and got no data above 30m. The new ADCP received good signals even in the upper bins above 30m and down to 270-400m. Additionally XBTs were launched every 10nm.

To shorten the time needed to retrieve the Pegasus probe, a terminal showing the acoustic ranging of the probe from the ship has been installed on the bridge. Subsequently, the time for Pegasus retrievals decreased from 40-60 min to 13-20 min.

The 35˚ 8W section was reached on November 12, and began with 4 CTD stations to 2500 m depth. South of 1˚ 8N, the CTD was again lowered to the bottom. A first test of the BBADCP was carried out on November 2. It was lowered to 7m depth to study the appropriate parameter setting for using it when attached to the rosette. The first deep profile with the BBADCP was obtained on November 4 parallel to a Pegasus drop at 0˚ 846 S, 34˚ 859.5' W (S2). But the data showed time gaps by up to half an hour preventing the evaluation of the velocity field below 1500 m. This failure could not be repaired during the cruise.

At the southern end of the 35˚ 8 W section four bottom transponders (at each location two) were deployed at 3˚ 859' S, 34˚ 857' W, (S14) and at 4˚ 830' S, 35˚ 805' W, (S15), November 6 to 7 after surveying the bottom topography with Hydrosweep. Their distances were carefully measured. S14 is located in a 20 sm broad channel which is about 3500 m deep and bordered by elevations up to 18 m depth; the southeast flowing deep water seems to be guided by that channel. The CTD/ADCP work on that section continued till November 7, 07:00 p.m. when we reached the shelf at 5˚ 801' S, 35˚ 800' W.

After proceeding to the 5˚ 8 S section the work began with a shallow CTD station. We repeated the measurements at the Pegasus station S6 (5˚ 839' S, 34˚ 854' W), where profiles already had been taken on October 24. The Pegasus and the shipborne-ADCP data showed distinct vertical structures in the velocity profiles which remained almost coherent for the duration of the stationwork, but disappeared a few miles farther offshore. On the other hand, they were present along our transit route to 44˚ 8 W. To study this phenomenon further, profiles from shipborne-ADCP and data from the lADCP, lowered to 250 m depth, were combined and the ship stayed at the S6 position for another two hours.

On 9 November, the lADCP failed due to water leakage. It could not be fully replaced by the BBADCP, as this instrument was only capable to cover the upper

1500m of the water column. To complete the current field measurements of the 5˚ 8 S section, two additional Pegasus stations at 5˚ 815' S, 32˚ 800' W (S16) and at 5˚ 810' S, 31˚ 830' W (S17) have been installed on November 10. On this section, also Tritium and Helium samples have been taken from the 10 l Niskin bottles. They will be analyzed at the Institut fuer Umweltphysik, Heidelberg. The easternmost CTD station was done at 5˚ 8 S, 30˚ 80' W and on November 11, METEOR headed southwest to 10˚ 8 S 32˚ 830' W. On the way, 4 shallow (1500 m) CTD stations were carried out as well as XBT drops every 10nm. The expected splitting of the South Equatorial Current in a northwest flowing North Brazil Current and a southward flowing Brazil Current was also surveyed with the vessel-mounted ADCP.

The 10˚ 8 S section began on November 13, 1:00 p.m. with deep CTD stations to the bottom and the BBADCP attached to the rosette. The BBADCP profiles were valid for the upper 1500 m. Altogether 10 CTD stations have been carried out on that section, which ended on November 14, 11:00 p.m. The ship headed north towards Recife, where we arrived on November 15, 11:00 a.m.

4.3 **Leg M 22/3** (T.J. Müller)

On November 16, G. Siedler had taken over the chief scientist's duties from M. Rhein. During the following two days the captain and the chief scientist communicated frequently with the German Embassy in Brasilia in order to obtain a decission on the clearance for work in the 200nm zone from the Brazilian government. On November 18, a message was received which said that clearence could not be expected. Upon the request of the German Embassy for G. Siedler to leave the ship and to travel to Brasilia for a discussion about open questions with Brazilian authorities, the chief scientist's duties were transferred to T.J. Müller. About two hours before the ship's departure a telephone message was received through the Brazilian observer indicating that clearence was given.

METEOR left Recife on November 18, at 10:00 p.m. with 10 scientists and technicians from the Institut für Meereskunde Kiel (IfMK), Germany, and with the Brazilian observer from the Diretoria Hidrografia e Navegacao (DHN), Niteroi, RJ, Brazil.

Heading south to the main working area on the Sao Paulo Plateau, a test station was carried out for the vertically profiling CTD/rosette and a new acoustic release system on 13˚ 857.4' S, 36˚ 816.6' W. Then, the westernmost channel of the Victoria-Trinidade Ridge was surveyed with METEOR's multibeam echo sounding system Hydrosweep for determining the sill depth. It turned out that the channel is very narrow, 1 to 2nm, and shallows from the northeast from more than 1800m towards the southwest to less than 1000m. The channel ends here and the sill depth located at 19˚ 837' S, 38˚ 826' W is less than 950m. It is thus possible that Antarctic Intermediate Water can pass this channel on its way north.

During the earlier cruise M 15 in 1991, an anti-cyclonic doming of the upper thermocline was observed just south of the Vitoria-Trinidade Ridge. It could be a topographically controlled permanent feature. A section with three CTD stations and some deep-reaching XBTs (1300m) at 6nm (Fig. 4) nominal distance were carried out. Doming could be observed again, but the signal was very weak.

Proceeding further south to the Sao Paulo Plateau, the large-scale structure of the main thermocline was observed with XBTs spaced horizontally at 20nm. Most of these profiles were taken outside the 200nm zone. On November 25, a mooring carrying a sound source was deployed outside the 200nm zone. It is part of an array aimed at studying the flow field at mid-depth by neutrally-buoyant drifting floats (RAFOS).

After having launched the mooring, a CTD section was carried out, with a total of 25 stations between the 3000m and 200m depth contour normal to the continental shelf with a station distance of 60nm each.

On this section also three Brazil Current meter moorings 333/BE, 334/BM and 335/BW were recovered on November 26 and 27.

METEOR finished the leg in Santos on November 30 at 09:18 a.m.

4.4 **Leg M 22/4** (W. Zenk)

In Santos/Brazil W. Zenk took over as chief scientist from T.J. Müller on November 30, 1992. On the morning of December 2, METEOR left port at 8:00 a.m. (Fig. 5a) and sailed directly towards mooring position 906/DB1 near 28° 8 S, 44° 8 W. In addition to 33 crew members 19 scientists were on board the ship. This number included team members (Fig. 5b) from Kiel, Sao Paulo, Rio de Janeiro, and Woods Hole. The official observer from Brazil, Capt. J.M. Ramos, stayed on board. He had previously joined the ship in Recife (22/2).

The main work was concerned with mooring activities which had begun during the previous leg in the Brazil Current region and continued during most of leg 3. Initially we recovered the Woods Hole moorings 906/DB1-909/DB4 without any difficulties. Unfortunately the acoustic release of 910/DB5 failed, and after extensive unsuccessful release attempts, this mooring had to be given up. On December 2, the sound source mooring 350/K2 was deployed on the western Vema terrace. Next moorings 337/VW and 338/VE were recovered from the western shoulder and the Vema Sill. A second mooring was lost when we were unable to communicate or release 337/VM. We had better luck with 343/DBK and 912/DB6, both situated on the eastern Vema terrace. To summarize, by December 7 eight moorings had been recovered which originally had been deployed in early January 1991 from METEOR (M 15). Further logistical details can be found in the attached mooring inventory (chapter 7.3.3).

In the inner Vema district the narrowly-spaced CTD section from the 1991 expedition was repeated although with a reduced number of stations. Further stations were occupied on the way to the Hunter Channel. Besides CTD observations surface drifters and RAFOS floats were deployed. During the cruise the scientific party gathered at irregular intervals to discuss scientific issues and the next day's schedule. Seminars on various topics of the South Atlantic and applied research methods were given. Contributions werde made by colleages from all three participating countries.

Slowed down by strong easterly winds the Hunter region was approached on December 11. Hours earlier METEOR had occupied the deepest station of the cruise at a depth of 5146 m. Due to poor weather conditions we were unable to perform the intended bathymetric survey with Hydrosweep, the shipborne multibeam echosounder. By December 15, we had managed to launch seven moorings across the Hunter Channel. They consist of a zonal row of six current meter moorings (H1-/H6) and one sound source (K0) mooring. A difficult situation arose when a severe storm appeared in a very short time and the ongoing deployment of mooring H3 could not be finished properly. The problem was solved by a brave zodiac maneuver. On December 13, all work had to be terminated until the storm weakened the next day.

After the mooring work was completed the Hunter region was left, heading due NW. On December 16, an additional mooring was installed close to the bottom on the eastern flank of the Rio Grande Rise.

A final mooring deployment (K3) was performed on the return leg to Rio de Janeiro. In this case we combined near-bottom current meters with a sound source at about 1000m depth. At the end of these activities METEOR sailed on a northwesterly course towards the Brazilian shelf. Underway we launched all remaining RAFOS floats and the satellite-tracked, surface drifting buoys. Further observations of the upper-ocean thermal structure were done by two-hourly spaced XBT drops on the return leg. These data were transmitted through the Global Telecommunication System of the World Meterological Organization (WMO) in a near-real-time. Approaching the shelf nine XCP probes were dropped in order to analyze the vertical structure of the Brazil Current. METEOR called port at Rio de Janeiro in the morning of December 22, 1992.

4.5 **Leg M 22/5** (R. Onken)

METEOR left Rio de Janeiro on December 27, 1992 at 6:00 p.m. The first destination was the test station no. 620/92 located at waypoint A (see Fig. 7). Because METEOR crossed the Brazil Current on its way to the test station, the temperature and velocity structure of this current were recorded with XBT drops and the shipborne ADCP (S-ADCP). On the station all instruments were tested and the scientists familiarized themselves with their usage. As the overside

ADCP (IADCP) was not yet ready for use, another test station was occupied in the early evening. Here, the IADCP passed its first test successfully. Afterwards METEOR headed for waypoint B. Between B and C the Brazil Current was crossed for the second time and was surveyed again with XBT and S-ADCP. METEOR turned at C and hydrographic stations were conducted with a horizontal resolution of 10nm between C and B. To the east of B the interval between the stations increased to 30nm.

30˚ 8 S was reached at waypoint D for the first time. For the next weeks, METEOR sailed eastward along this line (Fig. 6) passing the Vema Channel, the eastern part of the Rio Grande Rise, the northward directed dead end of the Argentine Basin, the eastern extension of the Rio Grande Rise, the southern Brazil Basin, the Mid-Atlantic Ridge, the southern Angola Basin, the Walvis Ridge, and the northern Cape Basin. A northward detour was done over the Walvis Ridge because of the complicated topography. The intervals between stations varied between 9 and 45nm (chapter 7.4.1, Fig. 8) in order to ensure that the water depth between two successive stations should not differ by more than 1000m.

At 11˚ 850' E the 30˚ 8 S latitude was left and the station programme was continued in east-northeast direction for two reasons. On the one hand the section was planned to cut the Benguela Current at nearly a right angle, and on the other hand the 200nm zone of the Republic of South Africa had to be avoided because no application for reasearch permission had been made. Here, the station interval was reduced to 20nm. The last station was located on the African shelf at a water depth of about 200m. Because of a bad weather forecast for the following days, the measurement activities were finished in the afternoon of January 28, although 16 hours of spare time were still available, and METEOR headed for Cape Town and arrived there in the afternoon of January 30.

5 Preliminary Results

5.1 Marine Geology and Marine Chemistry during M22/1

5.1.1 Deployments and Sampling

(U. Rosiak, M. Kalberer, V. Ratmeyer, U. Kuller, M. Bleckwehl, G. Fischer, A. Zimmermann, H. Buschhoff, W. Balzer)

For sampling in the water column, a multiple closing net (multinet), in-situ pumps, GoFlo bottles and a Photosea under-water camera system were used. From the ships' membrane pump which is installed in 3.5 m water depth, 1-2 L of seawater were filtrated three times daily for subsequent chlorophyll (Chl a) analysis. For the sampling of sediment with undisturbed surface, a multi-corer was used at five stations.

The primary goal during the cruise was the recovery and/or the deployment of moorings containing sediment traps and current meters; Fig. 9a, b show the positions in the Atlantic where moorings were deployed during M23/1 or previous cruises dealing with the same objectives.

Details for the individual sampling devices are given in the following paragraphs 5.1.2-5.1.9. A summary of the occupied stations including the list of equipment used is given in the station list (see chapter 7.1.1).

5.1.2 Particle flux with sediment traps

(G. Fischer, M. Kalberer, V. Ratmeyer, U. Rosiak, U. Kuller, M. Bleckwehl)

Deployment and recovery data for all moorings as well as the sampling data of the traps are listed in Ch. 7.1.2. North of Gran Canaria (CI2), south of Cabo Verde (CV1), in the eastern (EA9) and in the western equatorial upwelling area (WA1 and WA2) mooring arrays with 2-4 multisample sediment traps and current meters were deployed.

The mooring "Canary Islands No.1" (CI1) deployed during M20/1 was completely recovered on September 9. Both traps had worked perfectly providing 40 samples in total. 20m underneath the upper traps a special current meter instrument developed by the group of Prof. Krause (AWI) recorded current speed, direction, temperature and conductivity as well as backscattering and fluorescence. At the same site, we redeployed the mooring (CI2) which will be recovered during M23/3.

A new mooring ("Cabo Verde No.1", CV1) with two traps and one RCM8 was installed at about 11˚30 N and 21˚W close to the divergence of the North Equatorial Current and the North Equatorial Counter Current. It is intended to recover and re-deploy these instruments during M23/3.

Between October 9 and October 12 we successfully recovered the moorings EA6, EA7 and EA8 located on a north-south transect in the eastern equatorial upwelling area. Except for one trap from the EA8 site, all other traps (7) had sampled continuously; Fig.10a-c gives a first impression of the seasonal sedimentation of particles in 598m, 1833m and in 2890m water depth between Dec.12, 1991 and Oct.6, 1992 (see Ch. 7.1.2). The trap in 1255m did not sample properly. At the EA7 site, we redeployed an array with 3 traps and one current meter (EA9) on October 10. All instruments will be recovered in April 1993 (M23/3).

We finally installed two mooring systems with five traps and two current meters in the western equatorial Atlantic at approximately 25˚W and 4˚ and 7˚S. They are part of a SW-NE transect over the western equatorial upwelling area which will be completed with a third mooring further north during M23/3.

5.1.3 In-situ Particle Camera System (V. Ratmeyer, U. Rosiak)

For the determination of the particle concentration, its size distribution and the aggregate composition in the upper 600m of the water column, a high-resolution fotocamera system was employed. It was designed and improved according to experience with similar systems as described by Honjo et al. (1984), Asper (1987) and Lampitt (1985). This method provides in-situ information on the origin and the abundance of particles and aggregates (marine snow). In addition to the use of sediment traps, particle flux can be measured with this method even at sites with high lateral transport.

We used a 70mm deep-sea camera (model PHOTOSEA 70) with 45.7m film capacity providing an acceptable optical resolution. Two 150 Ws strobelights (model PHOTOSEA 1500S) were installed as light sources. The illuminating beam was collimated by a pair of highly refractive fresnel-lenses mounted inside a steelframe at focal distance in front of the strobes. Camera and light sources were installed in orthogonal position thus avoiding backscattering by water molecules and highly hydrated particles. The system is fixed inside a collapsible frame 200 x 80 x 80 cm, which is made of 48 mm (o.d.) galvanized steel pipe. The weight of the complete system is approximately 130 kg in air. The camera and the strobe-collimator unit can be slided to any position inside the frame (see Figure 11).

The whole system was testet during the M22/1 cruise for the first time. During its descend to 600m water depth the camera was triggered continuously by a computer on deck of the ship. Typically every 5 m one picture was shot while lowering the system with a speed of 0.3m/sec. The flash duration of < 1/10.000 second was short enough to get sharp pictures of particles down to a size of 100m using Kodak Tri X Pan Film. The pictures show variant particle and plankton concentrations through 500m water depth, with maximal concentrations in the upper 30m.

5.1.4 CTD-O_2-transparency probe (G. Fischer, V. Ratmeyer)

For continuous records of seawater properties, a CTD-profiler (SEABIRD SBE 19) was equipped with an oxygen sensor and a 25 cm side view transmissometer (SEATECH). This unit was attached to the wire 20 m above the multicorer in most cases. At ten stations the raw data were immediately transfered from the self-contained instrument to a computer. Downcast standard plots were produced which subsequently served for the selection of sampling depths for the deployment of in-situ pumps and GoFlo-bottles. Measured oxygen values were compared to those of the WINKLER titration: while the shape of both oxygen profiles was almost identical, the in-situ oxygen concentrations were generally lower by 0.5-0.7ml/L than the discrete bottle values. This may be due to the alterations of the three years old O_2-membrane.

A typical profile obtained with the self-contained probe is depicted in Fig. 12. Most instructive for the positioning of other devices was the O_2-profile: its concentration reaching down to almost 1ml/L shows two distinct minima at 100m and 500m water depth; the concentration increased rapidly downwards to approximately 5ml/L in the North Atlantic Deep Water. Just below the deeper O_2-minimum the core of the Antarctic Intermediate Water can be recognized by its salinity minimum. Except for the top 50m the light beam attenuation (LBA) was generally very low.

5.1.5 Plankton Sampling Using the Multinet

(M. Kalberer, U. Kuller, V. Ratmeyer, G. Fischer)

Plankton was sampled with a multiple closing net (multi-net, Fa. HYDROBIOS) with 0.25m opening and 64 micrometer mesh size. It was used for vertical holes at seven sites. At each site, 2-3 holes with different depth-intervals were conducted (see: 7.1.1). The standard depths were:

1) to 1000 m water depth with the intervals 1000-500m, 500-300m, 300-100m, 100-50m, 50-0m.
2) to 400 m water depth with the intervals 400-200m, 200-100m, 100-40 m, 40-20m, 20-40m.
3) to 250 m water depths with the intervals 250-100m, 100-75m, 75-50m, 50-25m, 25-0m.

The samples containing mostly zooplankton and only small amounts of phytoplankton were carefully rinsed with seawater and transferred to KAUTEX bottles. After fixation with mercury chloride to reduce bacterial action the samples were stored at 4˚C.

5.1.6 Continuous Chlorophyll a Measurements

(M. Kalberer, V. Ratmeyer, G. Fischer)

For the determination of chlorophyll concentrations of surface waters, 1-2L seawater taken 3 times a day from the membrane pump (inlet in 3.5m water depth) were filtrated onto glass fibre filters and deep frozen at -20˚C. Chla measurements will be done in the home laboratory. Up to now, chla data are available from several Meteor cruises in the Atlantic Ocean (M6/6, M9/4, M12/1/2, M16/1/2, M20/1/2). These data will be compared to values derived from fluorescence measurements of an in-situ probe (Prof. Krause, AWI).

5.1.7 In-situ Filtration of Suspended Particles

(W.Balzer, H.Buschhoff, F.Gonzales Palma, D.Schneider, A.Zimmermann)

Within the German JGOFS project "Vertical transport of particulate trace elements in the equatorial upwelling region" the distribution of dissolved trace elements has to be compared with their concentration in suspended particulate material (SPM), in particles caught with sediment traps and in sediments. The main objectives are

(i) the deepening of our general knowledge about the control of trace element distribution by interaction with biogenic and abiotic particles and
(ii) to investigate how particle sedimentation in a high-productivity region affects the vertical trace element distribution.

Within the 3 main classes of elements (according to their vertical distribution grooped into: "conservative", "nutrient-type", "scavenged") as many elements as possible at acceptable accuracy will be determined in different matrices (see also: Research Programme). Three particulate phases were sampled using different techniques:

(i) the SPM to be filtered using in-situ pumps is supposed to consist of slowly sinking biogenic and terrestrial detritus exhibiting a large surface area for sorptive processes,
(ii) the material caught with intercepting sediment traps consists of larger, faster sinking particles which incorporated trace elements during their formation in the ocean's top layer and by scavenging of SPM,
(iii) the sediment represents in that respect the ultimate result of all water column processes and early diagenetic modifications near the sediment/water interface.

In addition to the determination of trace element concentrations, emphasis will be put to the analysis of carrier phases such as carbonate, organic carbon, opal and lithogenics. Therefore aliquots of the trap material (see chapter 7.1.2) will be analyzed at home for trace and major components after digestion with nitric and hydrofluoric acid.

Due to the low concentration of SPM larger volumes of seawater have to be filtered, if trace elements are to be analyzed in SPM. Between 200 L and 800 L seawater from depths down to 5400 m were filtered through acid cleaned 293 mm Nuclepore filter using an in-situ pump (see chapter 7.1.4). To reduce contamination risks non-metallic wire was used and all handling of the filters was performed under a clean bench. Because in-situ pumping is very time-consuming pumps were combined with bottle casts whenever possible. From pump deployments a total of 39 filters were obtained, 6 of which, however, being torn.

5.1.8 Water Sampling

(W.Balzer, H.Buschhoff, F.Gonzales Palma, D.Schneider, A.Zimmermann)

At all 7 stations where sediment traps were recovered/deployed 2 casts of 6 GoFlo bottles were taken to analyze the vertical distribution of trace elements in the water column; at stations 466 and 468 only the top 600-800m were sampled in accordance with the respective pump deployments yielding a total of 90 trace element samples. For the trace metal studies precautions had to be taken against the risks of contamination: before use the GoFlo bottles were acid cleaned thoroughly, at stations the bottles were attached to a non-metallic wire, during handling on deck both opening ends were covered with plastic bags, all manipulations after subsampling were performed under a clean bench.

When the filled bottles were brought to the lab, dissolved oxygen was subsampled first, followed by a flask for stable isotope analysis that was filled without air-bubbles, poisoned and secured with paraffin; then two plastic containers were filled for trace elements and acidified thereafter using subboiled HNO_3; finally sub-samples for nutrient analysis were taken and deep-frozen.

When brought back to the home laboratories, selected trace elements (primarily: Ba, Cd, Co, Cr, Cu, Mn, Ni, Pb) will be analyzed, and the vertical and horizontal distribution will be compared with results from the particle analysis.

The only component that was determined directly on board was oxygen (by conventional Winkler titration) serving to check the calibration of the in-situ probe. A first evalution provided evidence for a systematic deviation between both sets of oxygen determinations.

5.1.9 Sediment Sampling with the Multicorer

(U. Rosiak, G. Fischer, M. Kalberer, V. Ratmeyer, D. Schneider, F. Gonzales Palma)

At the five mooring sites CI1/2, CV1, EA7/8, WA1 and WA2, multicorer samples were retrieved from the seafloor. Near-bottom water samples (100 cm^3 and 250 cm^3) for stable oxygen and carbon isotope analysis were taken from the cores approximately 10cm above the sediment surface. The samples for 13-C analysis were poisoned with mercury chloride; the bottles were sealed with wax and stored at 4˚C. About 20ml near-bottom water was taken for nutrient analysis and stored at -20˚, too.

For benthic foraminifera, two cores (each 10 cm in diameter) were cut into 1 cm segments, stained with bengalrose/ethanol and held cool at 4˚C. Samples were also taken for organic compound analysis (frozen at -20˚), as well as for the analysis of diatoms, radiolarians and magnetic bacteria assemblages. Two small-sized cores of 6 cm in diameter were used by the marine chemistry group for trace element analysis (see chapter 7.1.4).

5.2 Physical Oceangraphy M 22/2

5.2.1 CTD Measurements and Oxygen Calibration (L. Stramma, J. Waniek)

The CTD (Neil Brown Mark III) was well operating during the entire leg two of METEOR cruise M22. In total 65 profile were gained (see Fig. 1b). On most stations reversing thermometers were used to check temperature and pressure and water probes were taken from the bottles to calibrate the salinity and oxygen sensors of the CTD. As the CTD measurements went on until the evening before reaching Recife and as the conductivity and the oxygen sensors showed some time dependence no final data set could be produced before the end of the cruise. Therefore, only a preliminary data set was made from the data with full data rate.

Water probes were collected from rosette sampler for measurements of the concentration of dissolved oxygen in seawater. A calibration of the oxygen sensor with the results of the titrated oxygen measurements will be done. The water samples for titration were taken from 10 l bottles directly after collecting samples for Freon measurements. They were filled in 100 ml glass bottles without bubbles and 1 ml of KOH and KJ were immediately added with a dispenser. The titration of the samples was done directly afterwards, using the standard Winkler-method. It was done in the sampling glass-bottles which were made especially for this use, therefore errors arising from filling the samples into other bottles and cleaning bottles were eliminated. The volume of each bottle had been determined in Kiel, where also the reagents had been weighted in portions for 200 ml of distilled water. Afterwards they were packed hermetically. So it was possible to use reagents on board when needed and run all standards and blanks in distilled water. The blank was determined to be 0.06 ml/l and has been taken into account at the determination of oxygen in seawater samples. After every ten CTD stations samples were taken for estimating the repeatability of titrated oxygen, which was found to be 0.016 ml/l. In total 700 oxygen samples from 40 CTD stations were taken. After the first 15 stations (section 44˚W) a first estimate was made to calibrate the oxygen sensor. It showed that there was a time-dependent drift of the sensor which vanished during the further cruise. The oxygen sensor normally shows a strong dependence on pressure whereas the oxygen distribution is dependent on temperature. Therefore the calibration of the oxygen sensor has to be made after the final calibration of the temperature and pressure sensors.

Figure 13 shows the salinity distribution from the preliminary data set along the 35˚W section from the surface to 1000m depth. At about 100m depth two salinity maxima are present. The maximum at 4˚ to 5˚S near the Brazilian coast with values higher than 37 shows the core of the North Brazil Current which shows its velocity maximum at 35˚ W in the ADCP measurements in 100 to 150m depth. The salinity maximum between 1˚S and 1˚N shows the location of the Equatorial Undercurrent. The maximum in salinity with values higher than 36.8 is not found at the equator but at almost 1˚S. The probable cause is the adding of salinity-rich water from the North Brazil Current into the southern side of the Equatorial Undercurrent.

The Antarctic Intermediate Water (AAIW) can be seen with salinity values less than 34.5 south of 2˚N in Figure 13. In the corresponding TS-diagrams (Fig. 14) two jumps in salinity are found in the salinity minimum at about 5˚C. The lowest salinities of about 34.44 are situated between the coast and two degrees south, where the strongest westward transport of AAIW is expected. The middle part with salinities of about 34.5 is located between two degrees south and 1˚30'N. North of 1˚30'N the salinity rises to about 34.53.

The shift of the TS-curves towards lower salinities in Fig. 14 below 2˚C is the typical sign for the influence of the bottom water, which is known in literature as the two degree discontinuity. A clear difference compared to METEOR cruise 14 (see HINZ et al., 1991) can be seen on the 44˚W section. While in October 1990 low surface salinity was found north of 4˚N decreasing to salinities of 32.6 at 6˚ 40'N, which shows the presence of Amazon Water being carried to the east by the retroflection of the North Brazil Current into the North Equatorial Counter Current, there was no indication on Amazon Water in October 1992 at 44˚W south of 6˚ 40'N. Further comparisons of the CTD values from the different METEOR cruises will be done after the final calibration.

5.2.2 Freon Analysis F11, F12 (M. Rhein, M. Elbrächter)

During the cruise, the CFM system worked continuously and about 1400 samples including gas standards measurements have been analysed. At Oct.26, a short circuit destroyed the interface and the electric actuators of 4 valves. Two of them could be repaired, contrary to the interface, so that in the following, the valves had to be switched manually.

About 100ml water are transferred from the precleaned Niskin bottles to a purge and trap system with the help of a ground glass syringe. The CFMs are separated on a Gaschromatograph containing a packed stainless steel column filled with Porasil C and detected by electron capture detection (ECD). Calibration is done with a gas standard kindly provided by R. Weiss, Scripps Institution of Oceanography, San Diego.

The F11 analysis could be carried out successfully during the cruise, and exhibited a small blank of 0.003pmol/kg, decreasing to 0.001pmol/kg and a reproducibility of ±0.004pmol/kg was obtained. But south of 3˚ 09'S, 35˚W and afterwards the F12 analysis was hindered by an unknown substance with similar retention time as F12, thus making the availability of reliable F12 data more sporadic.

As known from the two previous cruises, the CFM maxima in the upper (1800m) and lower deepwater (3800m) are characteristic for the tropical boundary current (Fig. 15). At 35˚W and at 5˚ S the F11 concentrations of both water masses have increased, and at 44˚ W the regions with F11 values higher than 0.12 pmol/kg are more extended than in Oct.1990. For the first time we sampled the region north of the Ceara Rise and found high F11 concentrations in the lower deep water, supporting the view, that part of that water mass flows on the northern side of the ridge.

The splitting of the upper deep water at the equator is evident in the F11 distributions as well as the confinement of the lower F11 core to south of the equator. Measurements at the 5˚S section found the lower F11 core between 34˚W and 31˚W, so that on the previous cruises, where the section ended at 32˚W, we presumably have missed part of the flow. Striking is the increase in F11 concentrations in the Antarctic Bottom Water (AABW) below 4000 m, where it starts with values near the detection limit and increases with depth to concentrations comparable to the lower F11 core, which originates in the Northern Atlantic.

At 10˚S, the F11-concentrations in AABW exceeds those for the lower deep water from northern origin, but the upper deep water remains the most prominent signal with values >0.05pmol/kg east of 34˚W. Its F11 signal has decreased by a factor of two from 5˚S to 10˚S reflecting its dilution with less ventilated water from the ocean's interior and/or the time dependant increase of the CFM signal.

5.2.3 lADCP (J.Fischer,C.Meinke)

At all CTD stations a self-contained lowered Acoustic Doppler Current Profiler (lADCP) was attached to the frame of the water sampling rosette. This application gave good results during previous 'Meteor' cruises M14 and M16 and is now routinely used. During the cruise two different ADCPs, a so called 'narrow-band' and a 'broad-band' ADCP were used. The ADCPs measure short (about 200m range) velocity segments while the instrument is lowered and raised through the water column. Every 8 s to 10 s one of these velocity segments is stored inside the ADCP. After the cast the data are retrieved, and the segments are combined to a velocity profile extending from the surface down to the deepest point of the cast.

For the first time we used a modified rosette specially suited to mount the ADCP in upright position and to protect the transducers. Further modifications of the lower rosette frame were made with the help of the ship's crew. Now the ADCP can be mounted or removed within a few minutes.

After 39 mostly ocean deep profiles one of the tranducers of the 'narrow-band' ADCP broke and water was leaking into the instrument. This instrument could not be used further on the cruise. The deepest profile with the 'narrow-band' ADCP was down to 4670m which is one of the deepest ADCP profiles obtained so far.

The first trials with the 'broad-band' ADCP were less successful. This instrument was produced just in time to be send directly to the Meteor in Recife. We had severe problems getting the ADCP working, and there are still large problems to be solved. First, we made some parameter studies with this ADCP in parallel to CTD stations. For this purpose the ADCP was deployed 7m below the surface by using the small krane at the stern of the ship. Then we had three CTD/ADCP casts on stations where Pegasus casts were available. Later, due to the damaging of the 'narrow-band' ADCP the new ADCP was used routinely after station 519. Unfortunately, all stations deeper than 2000m with the new ADCP had large data gaps during the up-cast. The reason for this instrument failure is still unknown. The data evaluation therefore concentrated on the down-cast and on parameter studies. At shallower stations (1500m depth) the new ADCP had no data gaps, and the data quality was comparable to the 'narrow-band' ADCP.

At the end of the cruise all ADCP data are preliminary processed; comprising the calculation of velocity profiles, velocity sections along the ships track (sections 44˚ W, 35˚ W and partly 5˚ S) and even first estimates of transports for selected current cores. As an example we show the velocity pattern of the upper 1000m across the meridional section at 44˚ W (Fig. 16). Close to the shelf break we observed the North-Brazil Current in the top 500m transporting about 12 Sverdrup (Sv) westwards across the equator. Between 500m and 1000m another 14Sv are flowing westward. Farther to the north we found an eastward flowing undercurrent. The core of this undercurrent lies between 2˚ N and 3˚ N at about 200m depth. About 18Sv are flowing eastwards in the layer between 100 and 500 m, and another 9Sv in the 500-1000m layer. At the northern end of the section the highest velocities (up to 150cm/s) associated with the eastward flowing North-Equatorial Counter Current are found. At 5˚ S the northward flowing North-Brazil Current shows velocities up to 90 cm/s (Fig. 17). Transport estimates for the upper 500m (14Sv) were of the same magnitude than those observed at 44˚ W.

5.2.4 **Mooring Deployments** (J.Fischer, U.Papenburg)

A significant contribution to this cruise was the deployment of three current meter moorings in the western boundary current region along the 44˚W meridian. The aim of this investigation is to measure the mean circulation in the western boundary current region and fluctuations of the currents and transports on time scales from weeks to seasonal. In combination with two earlier deployments which were partly carried out with the 'Meteor' (during M 14) we should get a detailed picture of the boundary current system between the equator and 2˚ 30'N.

The moorings were deployed over the stern of the ship using the A-Frame to lift the instruments. This procedure worked well during the M 14 cruise. Especially at station K359 with variable bottom topography and surface currents of 2 - 3 knots the higher maneuverability of the ship, compared to deploying over the side, was appreciated.

a) u-component,
b) v-component

At all three mooring sites the topography was surveyed and the ships drift was determined prior to the deployment. Thereafter, the moorings were laid out at the surface, and finally the anchor was dropped after the mooring was towed into position (K359 and K360). The final mooring positions are 00˚ 14.6' N, 44˚ 18.6' W (K359 -2880m depth), 00˚ 37' N, 44˚ 10' W (K360 - 3660m depth) and 1˚ 11.15' N, 44˚ 02.7' W (K361 - 4110m depth); the water depth was corrected with respect to sound speed.

5.2.5 XBT Programme (L. Stramma, G. Kroll)

During leg M 22/2 in total 190 XBTs were thrown. The distribution of the XBT drops is shown in Fig. 3 and in the list in chapter 7.2.2. The XBT sections were carried out in addition to the CTD sections as well as on the transit to 44˚ W along the Brazilian coast and on the transfer from 44˚ W to 35˚ W.

Fig. 18 shows the highly resolved XBT section for the thermocline of the 35˚ W section. Between 3˚ 30' S and 3˚ N a clear signal of internal waves with maximum amplitudes of more than 30 meters is found in the thermocline. In addition, the equatorial divergence can be seen with the rising of the 25˚ and 26˚ C isotherm between 0˚ 10'S and 1˚ N. This happens where relatively cold water compared to the surrounding water is moving towards the sea surface.

The XBT temperature section between the 44˚ W section and the 35˚ W section is presented in Fig. 19. The distance between two drops was only about 10 miles. The ship ADCP showed in the upper 100 m eastward currents west of 42˚ W, a strong southeastward current between 37˚ 30'W and 42˚ W and a northward component between 35˚ and 37˚ 30'W. From the XBT section it can be seen that the thermocline depths as well as the thermocline thickness decreases in the region of the southeastward flow. Above it water is found which is warmer than in the east and west of this section. In the region of the eastward current at 43˚ W the mixed layer depth reaches almost 100 m and the thermocline shows a smaller temperature gradient than further to the east.

5.2.6 Pegasus Profiling System (U. Send, G. Krahmann)

As on cruises M14 and M16, the free-falling Pegasus probe was used again to obtain high-resolution profiles of horizontal currents. The acoustic transponders that need to be deployed on the sea floor for this system, already existed from previous years on 20 stations along the sections at 44˚ W, 35˚ W, and 5˚ S. The transponders on 44˚ W had been deployed in spring 1990 by K. Leaman (RSMAS, Miami) and of the 7 stations occupied, 6 were still operational (2 transponders per station). This means that those transponders (type Benthos) have a lifetime of 2 1/2 years or more, at least in deep water. This is significantly more than the manufacturer's specifications of 2 years. All other transponders on the remaining sections, which we had deployed on M14 and M16, were still fully operational.

We deployed four new transponder stations on M22, of which two (S14, S15) now extend the 35˚ W section all the way to the coast. Station S11 at 1.5˚ N, which had been planned originally, was not deployed due to time constraints. Instead, towards the end of the cruise, when we were more flexible, two unplanned stations were deployed (S16, S17) in order to extend the 5˚ S section farther offshore. These stations had been added in the hope to find the lower deep water there, which cannot flow along the coast due to topographic constraints.

Also on this cruise, we performed a final test of the Pegasus fins (which make it rotate) versus a "Hula skirt" of several hundred strings of 1m length (to improve the streaming properties). In spite of (or just because of?) the improved skirt (longer, denser) compared to M16, we again observed Hula-type spiraling motions in the Pegasus. As the result, we went back to using the original factory-supplied fins again. The quality of the profiles with these fins is as good (and without spiraling) as with the skirt, as documented in a statistical analysis of the down/up differences (Send, 1993). In that study it was shown that the up/down differences, which had been apparent ever since the M14 cruise, can be explained completely in terms of internal wave variability. One disadvantage of using the fins for the Pegasus was a slower descent rate, which made the profiles take longer than with the skirt. This was improved by doubling the drop weights for the Pegasus, which had no adverse effect on the quality of the profiles. As a result, the Pegasus usually surfaced within 10-30 min of the CTD, which is an ideal time lag to steam back to the starting position.

We could also further improve the deck operations for the Pegasus in terms of speed. For example, a PC was installed on the bridge, which displayed acoustic information about the distance to the Pegasus. This made it possible to navigate the ship close the Pegasus even before it had surfaced. As a consequence, the probe usually was on deck within 12-20 min of surfacing. Also the four transponder surveys were carried out very swiftly - the last two took only 2 1/4 each including their deployment.

For obtaining sections of directly measured currents, we had two complementary and partially redundant systems in use on this cruise - the Pegasus and the ADCP lowered with the CTD rosette. The ADCP provides better horizontal station resolution, since it can be used at any CTD station independent of transponders being present. The Pegasus has better vertical resolution and currently still is the reference system to test and compare the new ADCP method with. Thus the final sections of currents from this cruise will be a combination of ADCP and Pegasus data. For this reason, we are presenting at this point only the section from 5˚ S, where the ADCP had failed and the Pegasus provides the only directly measured currents, and we will show observations of some strongly layered jets of 40-70m vertical scale, observed near the coast and especially at station S6.

Figure 20 shows the section of meridional currents along 5˚ S (the stations at 32˚ W and 31˚ 30'W are new compared to M14 and M16). A marked structure of alternating bands of north/south currents is visible in the entire depth range of the deep water. Close to the coast, there is a large southward transport from about 1200m to 3800m, thus covering all 4 layers of the deep water. A current core is present in the range of the Labrador Sea deep water. Farther from the coast, at 33˚ 13'W, we have northward currents in the upper 3 layers of the deep water, with a strong core in the uppermost (old) deep water. This current reversal had been observed already on M14 and M16, and thus it seems to be a permanent structure in this region, even though during the previous cruises it only included the 2 layers of the upper deep water. A new feature in our section is another southward current region even more to the east, with 15-20cm/s, covering the Labrador Sea upper deep water down to the lowest deep water, with a core at 3700m. This is the typical depth of the Freon maximum in the lower deep water. This southward flow was not present on M14 and M16. Thus in total, a picture emerges of strong meanders and recirculations, with some permanent features but generally high variability.

Another interesting observation is shown in figure 21. At station S6 we measured strong horizontal jets closely layered in the vertical, which had already been noticed in Pegasus profiles during M14 and M16. On the present cruise, we passed station S6 twice and also this time we had continuous ship-board ADCP data even on station. With that, we could obtain a good view of the temporal stability of these structures, as seen in figure 21. Preliminary analysis of ship ADCP data suggests that these jets can partially be found along the entire coast to about 40˚ W. However, they seem to have high spatial variability and strongly changing directions.

5.2.7 Vessel-mounted ADCP (J. Reppin)

The vessel-mounted ADCP is a very valuable instrument for the exploration of the mainly surface intensified currents in this equatorial region, as the earlier cruises (M14 and M16) have shown before.

The data set obtained on this cruise is the first complete data set of this season, because the ADCP installed in the hull of the vessel was defect during the cruise in autumn 1990 (M14). We had to install a SC-ADCP (self-contained) in the ships hydrographic well prior to the 35˚ W section.

During M16 we made very good experiences with a VM-ADCP installed in the hydrographic well. At the beginning of the 35˚ W section we installed another VM-ADCP in the hydrographic well with help of the ship's crew because the VM-ADCP installed in the ship's hull did just reach down to 230 to 300m depth. This Instrument in the well then got ranges between 270 and 400m. Another advantage of this instrument were better data in the top two bins.

The profiles recorded are averages of 5 minutes with a ping ever second. Due to a defect of a synchro converter leading to heading dependent offsets of the heading values fed into the ADCP up to 15 degrees, the profiles had to be corrected with the heading values recorded by the central data data processing and recording system DVS. This worked fine for the ship being underway or on station with a nearly constant heading over the period of an ADCP ensemble (5 min.). The profiles during station arrival, station departure and transponder navigation had to be discarded. The following calibration using the difference between on-station-data versus on cruise-data-still worked well. On this cruise we used an own GPS-receiver (MAGNAVOX MX200) as navigation source for the first time. With the help of the board-electricians the antenna was installed at a very good position in the mast. The receiver obtained very good position data for the referencing of the VM-ADCP profiles as well as for the transponder navigation at the Pegasus transponders deployed during this cruise.

The difference of the surface current system to the spring situation can clearly be seen in the ADCP data. In contrast to the weak retroflection of the North Brazil Current (NBC) during M16, it is visible in this season. Although the NBC retroflects west of 44˚ W the strong North Equatorial Counter Current (NECC) is visible in the northern part of our research area.

The NBC does show in the VM-ADCP data on the transfer between Recife and the 44˚ W section and on the first stations on the southern part of the 5˚ S section already (Fig. 22). The shelf section at the southern end of the 44˚ W section revealed a transport of 2Sv across the shelf. At 44˚ W the equatorward undercurrent is located between 1˚ N and 3˚ N (Figs. 23a, b) with an southeastward maximum at about 225m depth, that seems to feed into the Equatorial Undercurrent (EUC) between about 2˚ S and 2˚ N at 35˚ W (Figs. 23c, d). On the transsect between 44˚ W and 35˚ W the meandering of the retroflected NECC can be seen. The VM-ADCP does not show any inflow of the South Equatorial Current (SEC) into the southern box between 5˚ S and 10˚ S. At 10˚ S the North Brazil Current was observed (NBC?) (Fig. 22) with a maximum between 200 and 300m.

5.2.8 **DVS** (J. Reppin, Th. Mitzka)

A subsample of the DVS data has been recorded every 2 minutes during the entire cruise. Drift and windmaps (Figs. 24 and 25) averaged over 0.1 degree have been calculated and plotted on board. The drift mainly shows the structures of surface currents seen in the vesselmounted ADCP. The echosoundings fed into the DVS were used to extract the bottom topography along the sections and the heading data were used to correct the defect ADCP-heading information.

5.3 **Physical Oceanography M 22/3-4** (W. Zenk, T.J. Müller)

Here we present four selected highlights as they became available already during the cruise or within a few weeks afterwards. They deal with the Brazil

Current as manifested in the hydrography during M 22/3. We further present evidences for a continuous equatorward flow of unmixed bottom water, and give an impression of the finished Eulerean and the freshly started Lagrangean current observation at the southern rim of the Brazil Basin.

Figure 26a shows the position of three hydrographic sections across the Brazil Current between 26˚ S and 29˚ S. They run normal to the main topography from less than 200m to more than 2000m depth. In Figure 26b we display the distribution of potential temperature and salinity in the upper 1000m. The most striking feature is the strong inclination of isotherms near the shelf break. From the isotherms, the core of the current is found between 50m and 500m over the shelf edge. It is most pronounced in the northern section. Also in all three sections a counter current appears on the ocean side of the Brazil Current. Further analysis will show whether this feature is part of a big cyclonic ring. Antarctic Intermediate Water as indicated by a salinity minimum around 900 m to 1000m depth is not fully resolved in these upper ocean sections.

The transect back to Rio allowed the investigation of the northward route of Weddell Sea Deep Water, the coldest water crossing the Vema Sill for greater depths of the Brazil Basin (SPEER and ZENK, 1993). The route of this bottom flow is by no means clear from existing charts. Having discovered a deep trough north of the Vema Channel during the first DBE cruise, METEOR occupied a CTD station within this valley before deploying mooring K3 there. Potential temperature profiles (Fig. 27) show that the coldest water is just 26mK warmer than the coldest water at the sill (-0.131˚C compared to -0.157˚C). This exciting observation suggests that there must be direct deep connection between the sill (ZENK et al., 1993) and its extension at K3 which is hardly affected by any mixing. We suggest calling this hypothetical connecting trough the Vema Canyon.

Next we discuss an example of an Eulerean current observation already read and decoded from data storage units on board. In Figure 28 we show progressive vector diagrams of mooring BE on the offshore edge of the expected position of the Brazil Current at about 3300m water depth. Early in the record, an energetic event displaces all but the deepest trajectory eastward, while after passage of that feature these currents are steady towards the southwest, i.e. parallel to the local bathymetry. Contrarily, the whole record from the near bottom current meter at 3215 m depth, shows northeasterly direction. The mean temperature recorded by this instrument is 1.7 C which indicates the upper level of Antarctic Bottom Water entering the Brazil Basin from the southwest.

Finally we display (Fig. 29) an early version of the first RAFOS float trajectories from the Antarctic Intermediate Water level. The obtained trajectories are not inconsistent with the large-scale circulation in the subtropical South Atlantic suggested by REID (1989). They all show the westward current component indicative for a recirculation of Intermediate Water from mid ocean regions.

Especially the trajectory of float #66 is incompatible with the classical picture of a continuous northward flow of Intermediate Water parallel to the Brazilian continental shelf break (WÜST, 1935).

5.4. Marine Physics M 22/5

(U. Beckmann, C. Duncombe Rae, W. Erasmi, I. Girod, J. Holfort, U. Koy, P. Meyer, R. Onken, A. Welter, N. Zangenberg)

The main objective of the work of the marine physics group was to measure hydrographic parameters by CTD and rosette on every station (see chapter 7.4.1). In order to satisfy the WOCE requirements for high vertical resolution, two successive CTD/rosettes were lowered on stations where the water depth was more than 3500m. By this method, up to 36 water samples were taken on a single station. During the entire leg, currents, sea surface temperature, and sea surface salinity were recorded continuously by the shipborne-ADCP and the thermosalinograph. For better horizontal resolution of temperature measurements, XBT probes were launched mid-way between CTD stations (see chapter 7.4.2) where the distance between stations was greater than 30nm. High resolution XBT sections were conducted in the Brazil and Benguela Currents. On two Brazil Current crossings XBTs were launched at 30 min intervals yielding a resolution between 2 and 3nm. In the Benguela Current XBT drops were done every 10nm. On those stations located in the Brazil or Benguela Current area, an overside-ADCP (see chapter 7.4.6) was used for the first time to give information on the vertical structure of the currents. In order to get a further independent direct current measurement, 15 XCP probes were launched (see chapter 7.4.3). In addition, six surface drifting buoys were launched between 15˚ W and the Greenwich meridian (see chapter 7.4.5) and one RAFOS float in the Vema Channel (see chapter 7.4.4).

Preliminary section plots of potential temperature, salinity, and sigma-T along 30˚S are displayed in Figures 30 - 32. Except to the east of the Greenwich meridian, the main thermocline extends between the surface and 800m. Vertical temperature gradients in this range are 0.02K/m. In the same depth range, the salinity decreases vertically at a rate of 0.002/m. Between 800 and 1200m, temperature gradients are 0.005K/m, whereas the salinity exhibits a minimum value around 900m, and increases again below. This is the core layer of the Antarctic Intermediate Water, the depth of which becomes shallower from west to east by roughly 300m.

Below 1200m, the patterns of temperature and salinity look very different in each basin. Between the Rio-Grande Rise and the Mid-Atlantic Ridge, the temperature gradients are very weak (0.0005K/m) between 1200 and 3000m, and a large thermostad can be found between 2000 and 3000m. The salinity, however, increases with depth. A maximum occurs at about 3000m and below the water becomes fresher again. This is the regime of the North Atlantic Deep Water (NADW) and the Circumpolar Deep Water (CDW). Closer to the bottom, both temperature and salinity gradients become stronger caused by the transition from the Deep Water to the Antarctic Bottom Water (AABW). In general, the isotherms are sloping from west to east indicating northward AABW flow.

For potential temperatures below 2˚C, the temperature and salinity patterns in the Cape Basin are very similar, but in the depth range between 2000 and 3000m, they are very different. This suggests that the histories for the AABW in the Brazil and Cape Basin are similar, but they are different for the deep water. A completely different structure can be seen in the Angola Basin. The bottom water is warmer than in the other basins, there is no water colder than 1.8˚C. This is surely due to the fact that the AABW has mixed with the deep water above along its long way from the southern sources through the Argentine and Brazil Basin and the Romanche Fracture Zone.

To the west of the Rio Grande Rise, i.e. in the Vema Channel and over the Lower Santos Plateau, the transition between the AABW and the NADW is characterized by strong vertical gradients of temperature and salinity below 3000m. The AABW seems to move northward in two deep western boundary currents leaning against the western shoulder of the Vema Channel and the continental shelf. The closed contours in temperature distribution suggest the NADW deep western boundary current to be located in the depth range between about 1500 and 2500m.

During the entire leg no serious organizational or technical problems arose. Only two CTD/rosette casts had to be repeated partially or completely because of a malfunction of the rosette trigger release. Initial stability problems with one salinometer could be solved quickly. At the beginning of the leg, some difficulties arose in receiving the XCP signals, but this problem could be solved by turning the antenna to a vertically polarized direction. The lADCP which was used for the first time by the group worked well. Rotation of the device about the vertical axis was diagnosed on the test station, and was remedied by fixing an Aanderaa vane laterally. Unfortunately the lADCP failed close to the end of the cruise at station no. 96. Obviously water had penetrated into one of the transducers.

5.5 Marine Chemistry

(H. Johannsen, K. Johnson, U. Karbach, A. Korves, L. Mintrop, A. Morak, J. Morlang, B. Schneider)

During the cruise no. M 22/5 the chemical oceanography group investigated the oceanic carbonate system and its response to the exchange of CO_2 between the atmosphere and the ocean and determined nutrient and oxygen concentrations. In the following an overview of the measurement program and a preliminary evaluation of the data is given.

5.5.1 The Partial Pressure of CO_2 (pCO_2)

The pCO_2 of surface waters was measured continuously with a spatial resolution of about 1 nautical mile over the whole cruise track. For this work the ship's kreiselpump system was utilized to continually pump water from a depth of approximately 5m to an equilibrator onboard connected to an Infrared (IR) analyser for CO_2 detection. While on station, the atmospheric CO_2 concentration was measured and the IR analyser was calibrated. Figure 33 shows the distribution of the pCO_2 in the surface water as well as the partial pressure of CO_2 in the atmosphere along the 30˚ S parallel. Because large areas in this region have heretofore not been studied or had not been recently studied no comparisons with the M 22 data are given. Especially noteworthy is the strong oversaturation of CO_2 across wide stretches of the area of study.

5.5.2 Total Carbon Dioxide (TCO_2)

The analyses of TCO_2 were made in cooperation with the Brookhaven National Laboratory. This allowed the deployment of two SOMMA-Coulometer analytical systems so that every second hydrographic station could be completely sampled for CO_2. This means that a CO_2 measurement was made on every sample which was also analyzed for alkalinity and tracer (freon) concentrations. Despite problems with the analytical systems, probably due to power fluctuations, the determination of TCO_2 in reference samples was accurate to $\pm$ 2 umol/kg.

5.5.3 Alkalinity

At 28 stations samples from all depths were taken for the potentiometric determination of alkalinity, total carbonate and pH. The titrations were carried out using two systems in parallel. Aim of the investigations was on one hand the determination of the parameter alkalinity for the calculation of the anthropogenic CO_2-signal, using coulometer-determined total carbonate values as well as nutrient and oxygen data. On the other hand, the reported discrepancy between potentiometrically obtained TCO_2 values and those coming from other analytical methods was to be investigated in detail. This is necessary for the evaluation of the numerous literature data (e.g. GEOSECS) which are older than about five years, as well as to account for possible effects on alkalinity data.

The alkalinity profiles obtained show the expected shape. Especially obvious is the strong correlation with salinity. The final calculation of the values, however, was not possible yet on board since, above all, the adjustment of the electrode characteristics for the two different systems requires the recalculation and comparison of all data. The same holds true for the calculation of delta-TCO_2, the anthropogenic CO_2-signal.

5.5.4 Nutrients and Oxygen

For all depth sampled, the oxygen and nutrient concentrations were determined. Oxygen was determined by the Winkler method, and the nutrients (nitrite/nitrate, phosphate and silicate) were determined by a continuous-flow method with an auto-analyzer. For the oxygen determination 100ml bottles with wide stoppers were used so that it was possible to perform the Winkler titrations in the sample bottle. This eliminated several manual manipulations required to transfer samples to titration vessels, and as a consequence significantly reduced the sources of errors. To determine the standard deviation, 10 parallel samples from water at different stations with high and low concentrations of O_2 were periodically analyzed. The standard deviation was better than 0.4%. In the case of the automated photometric determination of the nutrients, there are fundamental problems especially at low concentrations (surface water) and likewise at high concentrations (deep water). In order to measure high concentrations, the sensitivity of the method may have to be lowered, but this makes it difficult to measure the lower concentrations. For the determination of precision at high concentrations, 24 samples were taken from a depth of 3400 meters and analyzed. The precision for the analyses follows:

Silicate	1.3%
Phosphate	1.5%
Nitrite/Nitrate	1.1%

5.6 Biological Oceanography and Marine Taxonomy (C. Zelck)

The zonal transect along 30˚ S was occupied across the southern-central part of the South Atlantic subtropical gyre. The zoogeography of this region consists of a largely subtropical fauna (PARIN, 1970). Although the first 19 hauls (from the coast of Brazil to 40˚ W) were a replicate of a section taken by cruise METEOR no. 15 (1991; ANDRES et al., 1992), the other samples provide new information. This survey continues the long-term study of the Atlantic ichthyoplankton (and some invertebrate) conducted by Dr. H.-Ch. JOHN from the taxonomic working group.

The plankton at the marine surface (neuston) were taken by the standard method with a neuston sampler, with mesh size (of both the upper and lower nets) of 335mm. A total of 73 catches were taken, in approximately alternating day and night sequence. Stations near the coast were taken closer together than in the central part of the gyre, because of the smaller-scale biological differences at the shelf and continental slope. Catching time was 15 min at a mean towing speed of the catamaran of 2.5 m/s (s = 0.3, N = 61) giving a mean sampled surface of 708 m^2 (s = 67, N = 61). The sample condition was in general good. The plankton concentration was small as anticipated, except for two high salt-content samples, as the zonal section runs through a biological minimum area (HENTSCHEL, 1933). All samples were checked macroscopically on board and conspicuous species were noted. All fish larvae and some invertebrate plankton of 31 upper net samples were sorted under a stereomicroscope. Most of the samples came from the western stations. From a total of 365 ichthyoplankton individuals 32 taxa were identified.

The hydrographical and biological conditions at the sea surface from Brazil to 40˚ W are shown in Figure 34. Maximum temperature and salinity were observed at the coastal stations (A). East of 25˚ W the temperature rose again to the same level as before. This elevated surface temperature was 1 to 3˚ C above the mean temperature for January (DHI 1971). The mean ichthyoplankton concentration was 16.2 n/1000 m2 (s = 12.9, N = 31). Night- and dawn/dusk catches showed just slightly greater numbers of fish larvae up to x = 18.6 n/1000 m2 (s = 16.0, N = 15). Day samples yielded only 14.0 n/1000 m2 (s = 7.5, N = 16). The total ichthyoplankton abundance and composition (Fig. 34b) was almost the same as on METROR cruise no. 15 (ANDRES et al., 1992). Diurnal catch differences are also seen in the species composition. For example Cyclothone larvae and micronektonic nyctoepipelagic Myctophidae (such as Gonichthys barnesi, Hygophum hygomii, Myctophum nitidulum and M. phengodes) were regularly found in the night and dawn/dusk catches, while the flying fishes (such as Exocoetus spp. and Cypselurinae) as well as the Gempylidae are in general photopositive.

The zoogeographical classification of the taxa resulted in four different groups, as was observed on METEOR cruise no. 15 (ANDRES, op. cit.). The neritic indicator species of the shelf and continental slope were found at stations closest to the coast (see Fig. 34c). This group consisted of Mugilidae, Trachurus sp., Balistidae, Coryphaena hippurus, Dactylopterus volitans, Makaira nigricans and a large leptocephalus of over 20cm length. Tropical indicator species (Fig. 34d) such as M. nitidulum and Oxyporhamphus micropterus became more abundant further offshore, but still within the region of the Brazil Current and Return Current (ZEMBA, 1991). The subtropical ichthyoplankton (E) such as Nanichthys simulans, M. phengodes and H. hygomii slowly replaced the above mentioned western groups and became dominant east of 41˚ W. Only the subtropical convergence species G. barnesi (after HULLEY, 1981) is present over the section even though in small numbers and frequency (Fig. 34d with *).

Of the invertebrate plankton the Gammaridae genus Synopia (F) and the marine insect Halobates micans (G) was observed. Once again Synopia were frequent and abundant at dawn/dusk and night stations, but it also occurred in warmer saline water (ANDRES, op. cit.). H. micans was only found at temperatures over 22˚ C, and only west of 6˚ W. Anthropogenic influences such as tarballs and bits of plastic (occasionally with Bryozoa and Lepas attached to them) were found at almost every station. While the frequency and numbers of tarballs were once again higher in the Brazil Current region (METEOR criuse no. 15), the fishery twine and other types of plastic were more often found in the central part of the section.

5.7 Tracer Oceanography (K. Bulsiewicz, G. Fraas, A. Putzka, J. Weyland)

The investigated tracers are Helium, Tritium and the chlorofluorocarbons (CFC) F-11, F-12, F-113 and carbon tetrachloride CCl_4. The main part of Tritium, the unstable hydrogen isotope which decays to ^3He, and the CFCs are man-made. Their time dependent input at the ocean surface is well known. The tracer concentration is altered by mixing processes and by radioactive decay (in the case of Tritium) while the water descends to deeper levels of the ocean. Measuring the concentration of the tracers delivers information on time scales of transport and mixing processes.

The atmospheric F-11 and F-12 contents increased monotonously with different rates since the forties. CCl4 increased since 1920 while F-113 started in 1970. Hence the concentration ratios of the different tracers vary over a wide range and could be used to indicate the 'age' of water masses (age since leaving the surface). If mixing processes are negligible, 'younger' water is tagged to higher CFC concentration compared with 'older' water. The comparison of concentration- versus ratio-'age' delivers information on mixing processes.

Samples were taken according the WOCE scheme as follows:

CFCs:	glass syringes, 1400 samples, measurements on board.
Helium:	glass pipets for on board extraction, 340 samples; copper tubes for on shore extraction, 720 samples.
Tritium:	glass bottles, 700 samples.
^{14}C-AMS:	glass bulbs for the Institut für Umweltpyhsik Heidelberg, 100 samples Helium-, Tritium- and 14C-Samples to be measured on shore.

On 78 stations a total of 1400 water samples was analyzed. In addition to former expeditions the device used during this cruise was not only equipped to measure F-11 and F-12, but also F-113 and CCl_4.

Results:
In the following only CFC measurements are shown since these measurements are done on board while the Helium and Tritium measurements are to be measured later on shore.

As one result we show the F-11 section Figure 35 basing on preliminary data. Some of the main characteristics are mentioned below.

The isoline for 0.5pmol/kg is found about 500m lower at 1000-1100m compared to the WOCE-WHP A9 19˚ S section of M 15/3. This is an indication for the Antarctic intermediate water (AIW) which is found much younger on 30˚ S. The western boundary current of the North Atlantic deep water is only seen as a slight increase of F-11 concentration at 43˚ W in the range of 2000-2500m. Antarctic Bottom Water is indicated by an F-11 maximum at the bottom. As expected the highest F-11 content is found in the Vema Channel, the main entrance for bottom water to the Brazil Basin. But also in the area of the lower Santos Plateau rather high F-11 values are found. Within the whole deep Brazil Basin between 20-30˚W the F-11 concentration is above detection limit. Beyond that there is no F-11 greater than 0.015pmol/kg found in the deep water below 1800m within the Brazil, the Angola and the Cape Basin.

5.8 Atmospheric Physics (J. Brinkmann, M. Krämer, S. Matthias-Maser)

5.8.1 Size Distibution of Marine-borne Aerosol Particles - Spectral Recording of the Biological and the Water Soluble Fraction, Total Amount of Particulate Carbon

5.8.1.1Size Distribution and Water Soluble Fraction of Atmospheric Aerosol Particles

Atmospheric aerosol particles (APs) vary in size over a broad range and differ in their chemical composition. This is dependent on the region where they are found, above towns, the country, or the ocean. The size and the solubility of APs play an important role during the formation of clouds or fog because their ability to adsorb water vapor is closely connected with these properties. Therefore it is necessary to obtain knowledge of these parameters in different regions, also in marine air. The results can be used in numerical models simulating the microphysics of the development of clouds or fog.

During the M 22/5 cruise the size distribution of the APs was measured in the range of 0.005 µm up to 50 µm. two optical particle counters and the impactors mentioned below were used for this purpose.

Preliminary results show that the marine size distribution used up to now for numerical simulations has to be corrected because there are clearly less particles in the coarse mode than previously assumed. To determine the size fractionated water soluble part of the APs, particles were sampled on filters. These samples could not be evaluated on board.

5.8.1.2 The Biological Fraction of the Atmospheric Aerosol Particles

The biological particles are one component of the atmospheric aerosol particles. Among other effects their direct influence on humans is known (they cause allergies and other diseases of the respirator tract). They also play an important role in cloud physics. Pollen is able to accumulate water and decomposition products of vegetation may act as sources for atmospheric ice nuclei (IN). Besides plankton and some fungi, bacteria can work as atmospheric IN and help in forming clouds. Biological APs are ubiquitous and occur in all size classes. One important source for micro-organisms (i.e. bacteria, algae etc.) is the ocean. The "bubble-burst-mechanism" put microbes together with sea salt particles into the atmosphere. Up to now little has been known about the amount of that intake.

During cruise M 22/5 impactor measurements were done daily. Particles with r > 10 mm were measured with a so called wing impactor, particles with 0.2 mm < r < 2 mm were collected by a two stage slit impactor. Identification and evaluation of the latter will be done ashore by use of a scanning electron microscope equipped with an energy dispersive X-ray spectrometer. The larger particles were evaluated using a light microscope. The biological particles were marked with a protein dye. Since the dye takes two to three weeks to saturate the particles only the samples from the first half of the cruise could be analyzed on board. It could be seen that the biological fraction of the particles with r > 2 mm was remarkably high: It is about 25%. In comparison, the fraction of biological particles in Mainz/Germany is 30%. In addition, the biologically contaminated particles were evaluated. This fraction is about 10%. Final conclusions will be drawn when the whole analysis will be done.

5.8.1.3 Total Amount of Particulate Carbon

In the atmosphere carbon is present in gaseous as well as in particulate phase. The latter consists of elemental carbon (EC) and organic constituents. As mentioned above biological particles act well as cloud condensation nuclei (CCN) whereas freshly generated EC is very hydrophobic. Two mechanisms seem to compensate the poor ability to act as CCN. First, aging improves the hygroscopy; moreover, soot (EC) is a product of combustion both of anthropogenic and natural origin. APs generated in this way have the maximum of their number size spectra at exactly the size suited best for acting as CCN. Furthermore, the concentration of particulate carbon is of interest because of the high absorption of soot and the resulting influence on the radiation balance. The amount of particulate carbon above the ocean, a relatively unpolluted area, is poorly known. On this cruise two sets of filter measurements were obtained. In one case the air was sucked through a nuclepore filter. The absorption of the deposit will be measured and thus the fraction of EC determined. The other filters are "ash-free" membrane filters which will be analyzed by use of pyrolytic methods. This gives the amount of total carbon in the air sampled. Neither analytical determination of carbon could be done on the vessel. First qualitative evaluations (optical estimation of the amount of deposit sampled) show evident variations in filter burden. In some regions the concentration of carbon seems to be much higher than expected before the cruise.

5.8.2 Precipitation Analysis

The concentrations of noxious substances in precipitation in anthropogenically influenced regions has increased in recent decades. In comparison to studies concerning the chemical composition of rainwater carried out recently in Mainz/Germany, it is now interesting to investigate rainwater in unpolluted regions. The acidity, electrical conductivity, total concentration and the major ions will be analyzed. With a "wet-only" rainwater sampler, four samples were collected during the M 22/5 cruise. The acidity of the samples is clearly less than in rainwater of anthropogenically polluted areas, whereas the total concentration of soluble mass is higher dues to the dominance of large sea salt particles in marine air.

6 Ship's Meteorological Station

6.1 M 22/1 (Dr. Tiesel, W.-T. Ochsenhirt)

A strong wide-range low pressure complex dominated all the way from Hamburg to the Iberian peninsula. The weather, therefore, was cool with winds blowing mostly from westerly directions. At Sept. 24, a cold front with 8 Bft from SW crossed RV Meteor in the English Channel followed at Sept. 26 in the Biscaya by a strong low pressure wave (later developed as a hurricane over France) with squalls of with up to 10 Bft. Aftermaths of the hurricane "Charly" controlled the weather on the way of the Meteor along the Portuguese coast.

On the way from Portugal to the Canary Islands - between the wide-ranging pressure high of the Azores Islands and the heat lows over NW Africa - friendly, dry and warm weather prevailed with steady trade winds blowing from NE with 6 Bft.

From Oct. 4 to Oct. 9 the Meteor crossed the equatorial low pressure zone of the Intertropical Convergence (ITC): within the hot and wet ITC zone bringing about surface water temperatures of 29.5˚ C and nearly permanent rain the Meteor passed the east side of a low at the Cabo Verde Islands on Oct. 5. Off Liberia a westbound developing low ("easterly wave") with storms and strong squalls controlled the weather for the Meteor at Oct. 8. After passing the Equator at Oct. 10 RV Meteor reached the stable Passat zone of the southern hemisphere with steady SE winds of 6 Bft. Until Oct. 14 dense inversion clowding prevailed along with rain showers. While crossing the equatorial Atlantic from east to west, RV Meteor moved more and more into warm, friendly weather under the influence of the subtropical high of the South Atlantic.

6.2 M 22/2 (R. Tiesel)

In the first week, the weather was warm and fair under the influence of the strong south Atlantic subtropical high. Only in the neighborhood of the Brazilian coast strong convection clouds with precipitation could be observed with east to northeast winds exceeding 6Bft. From Oct.31-Nov.2 the southern part of the ITCZ (Intertropical Convergence Zone) was situated between 5˚ N and 6˚ N and it was clouded and some precipitation occurred. After leaving the influence of the ITCZ, the weather became fair again with constant southeast trade winds. At and south of the equator, the subtropical high with its center east of Rio de

Janeiro provided an almost cloudless sky and southeast trade winds up to 6 Bft. No rainfall occurred till Nov.15, where we arrived in Recife. The air and water temperatures during the cruise varied from 25.0 to 27.5˚ C.

6.3 **M 22/3-5** (E. Röd)

On November 18, METEOR left Recife. During most of the time of all 3 legs the subtropical high remained stationary in the eastern part of the South Atlantic. However, with maximum pressure only about 1020hPa this subtropical anticyclone was not very strong. The resulting southeasterly trade winds therefore were very weak and unstable. Most lows of the temperate zone, which moved in a quite northerly track between 35˚ S and 45˚ S influenced also the areas north of 30˚ S with their frontal systems. The first cold front passed METEOR on November 23, (leg 3), south of Recife near 23˚ S with strong rainfall and gusty winds near Bft 6 average speed. The next low passed the vessel near Santos on December 1; its waving cold front caused rainfall for about 18 hours and very low temperatures near 15˚ C. A small-ranged, but heavy low developed on December 12, in the frontal zone east of Mar del Plata. It passed METEOR in the evening hours little north with easterly winds Bft 7 to 8, veering south to southwest increasing Bft 10 to 12 during the night hours. The minimum pressure was registrated 982hPa at the weather station onboard and the temperature went down to 15˚ C, caused by strong cold air convection. Cyclonic activity continued also during the following days; on December 18 a low with minimum pressure near 1000hPa was analyzed east of Rio del Plata. At its preside northerly winds up to Bft 10 were registrated on METEOR next day. Further lows crossed the working area of the research vessel but without extreme weather activity. However, in the time period December 18 to January 8, 1993 more then 10 cold fronts crossed METEOR, causing precipitation at 18 days, sometimes even very heavy rainfall with thunderstorms. Temperatures therefore were below normal with maxima only between 15 and 19˚C.

During leg 5 weather conditions changed when the vessel left South America with easterly course; the subtropical high took more and more influence with fair conditions. Sometimes a high swell from south, caused by sub-antarctic lows, was noticed onboard with characteristic wave heights near 5m. Approaching South Africa the wind increased slowly from southeasterly directions near Bft. 5 to 6 but without reducing vessel speed. On 31 January METEOR finished its voyage at Cape Town.

7 Lists

7.1 Leg M22/1

7.1.1 List of Stations

Station No.	GeoB No.	Date 1992	Device	Time bottom contact (UTC)	Latitude	Longitude	Water-depth (m)	Remarks
Celtic Shelf								
462-92	-	25.09.	HS/PS	14:15 -16:42	48˚09.0 N -48˚00.0 N	07˚00.0 W -07˚39.0 W	171	Test HS/PS
463-92	-	25.09. -26.09.	HS/PS	16:42 -01:57	48˚00.0 N -46˚45.0 N	07˚39.0 W -08˚58.0 W	3787	Test HS/PS
464-92	1801-1	26.09.	KAM	09:23	45˚24.3 N	09˚32.7 W	4446	Test; to 70m
Canary Islands								
465-92	1802-1	30.09. -01.10	P/GFO	07:02	29˚09.2 N	15˚26.1 W	3638	GFO not successful P:1000m
	1802-2		SFV(CI1)	08:24 -11:21	29˚06.8 N	15˚26.8 W	3603	Recovery of CI1
	1802-3		SFV(CI2)	12:03 -15:24	29˚07.0 N	15˚24.2 W	3604	Deployment of CI2
	1802-4		KAM	15:42	29˚07.1 N	15˚24.2 W	3604	Down to 100m

Station No.	GeoB No.	Date 1992	Device	Time bottom contact (UTC)	Latitude	Longitude	Water-depth (m)	Remarks
	1802-5	30.09. -01.10	MN	16:25	29˚06.9 N	15˚23.9 W	3629	b:400-200,200-100,100-40, 40-20,20-0m;c:250-100, 100-75,75-50,50-25,25-0m
	1802-6		KAM	17:08	29˚06.7 N	15˚24.0 W	3631	Down to 100m
	1802-7		P/GFO	20:05	29˚10.7 N	15˚24.3 W	3651	P:3120m;GFO:3080,2000 empty,1000,800,400,200m
	1802-8		P/GFO	22:25	29˚10.5 N	15˚24.5 W	3651	P:400m; GFO:100,50,25m
	1802-9		KAM	23:08	29˚10.5 N	15˚24.6 W	3605	Down to 250m
	1802-10		MUC/CTD	00:27	29˚10.7 N	15˚24.0 W	3603	2 large tubes empty
Cap Blanc								
466-92	1803-1	03.10.	P/GFO	06:55	20˚35.1 N	20˚50.0 W	4015	P:100,400m;GFO:25,50,100, 200,400,800m
	1803-2		KAM	07:72	20˚35.2 N	20˚50.3 W	4013	Down to 10m
Cabo Verde Islands								
467-92	1804-1	05.10. -06.10.	SFV(CV1)	08:50 -11:50	11˚29.0 N	21˚01.0 W	4968	Deployment of CV1

Station No.	GeoB No.	Date 1992	Device	Time bottom contact (UTC)	Latitude	Longitude	Water-depth (m)	Remarks
	1804-2		KAM	12:05	11˚28.8 N	21˚00.6 W	4970	Down to 100m
	1804-3		P/GFO	15:29	11˚24.5 N	21˚00.5 W	4979	P:1050,4520m;GFO:600, 800,1000,1500,3000,4480m
	1804-4		MN	18:49	11˚24.3 N	20˚59.7 W	5084	1000-500,500-300,300-100, 100-50,50-0m
	1804-5		MN	19:43	11˚24.2 N	20˚59.7 W	5005	250-100,100-75,75-50,50-25, 25-0m
	1804-6		KAM	20:02	11˚24.2 N	20˚59.6 W	5008	Down to 50m
	1804-7		P/GFO	21:37	11˚21.2 N	20˚59.8 W	4982	P:100,410m;GFO:25, 50,100,200,300,390m
	1804-8		MUC/CTD	24:00	11˚21.2 N	20˚59.8 W	4982	35cm in all tubes
Sierra Leone Basin								
468-92	1805-1	07.10.	P/GFO/ CTD	08:30	07˚50.0 N	16˚54.9 W	4680	P:100,400m;GFO:25, 50,100,200,400,600m
	1805-2		KAM	09:47	07˚50.3 N	16˚54.1 W	4676	Down to 100m

Station No.	GeoB No.	Date 1992	Device	Time bottom contact (UTC)	Latitude	Longitude	Water-depth (m)	Remarks
Guinea Basin								
469-92	1806-1	09.10.	P/GFO	02:56	03˚05.8 N	11˚56.7 W	4449	P:900,3930m;GFO:7000, 900,1400,2000,3000,3900m
	1806-2		KAM	05:11	03˚05.7 N	11˚55.5 W	4448	Down to 200m
	1806-3		MN	06:01	03˚05.7 N	11˚55.5 W	4453	1000-500,500-300, 300-100,100-50,50-0m
	1806-4		MN	07:11	03˚03.3 N	11˚53.0 W	4453	250-100,100-75,75-50,50-25, 25-0m
	1806-5		SFV(EA6)	07:25 -11:12	03˚03.2 N	11˚53.1 W	4450	Recovery of EA6
	1806-6		P/GFO	12:31	03˚02.1 N	11˚52.8 W	4497	P:100,350m;GFO:25, 50,100,350,500m
	1806-7		KAM	13:41	03˚01.7 N	11˚52.4 W	4503	Down to 250m
470-92	1807-1	10.10.	SFV(EA7)	08:58	00˚03.3 S	10˚49.3 W	4497	Recovery of EA7

Station No.	GeoB No.	Date 1992	Device	Time bottom contact (UTC)	Latitude	Longitude	Water-depth (m)	Remarks
	1807-2		P/GFO	13:06	00˚00.6 S	10˚47.0 W	4613	P:100,400m;GFO:25,50, 100,200,400,600m
	1807-3		SFV(EA9)	15:19 -18:15	00˚01.0 S	10˚48.4 W	4312	Deployment of EA9
	1807-4		KAM	18:40	00˚00.9 S	10˚47.7 W	4665	Down to 200m
	1807-5		P/GFO	21:13	00˚00.4 S	10˚46.7 W	4682	P:1200,4000m; GFO:750,1000,1200,2000, 3000,3900m empty
	1807-6		KAM	23:44	00˚00.5 S	10˚45.8 W	4673	Down to 200m
	1807-7		MN	00:27	00˚00.7 S	10˚45.5 W	4661	1000-500,500-300, 300-100,100-50,50-0m
	1807-8		MN	01:11	00˚01.0 S	10˚44.6 W	4693	250-100,100-75,75-50, 50-25,25-0m
	1807-9		P	02:22	00˚01.4 S	10˚44.4 W	4711	P:700m

Station No.	GeoB No.	Date 1992	Device	Time bottom contact (UTC)	Latitude	Longitude	Water-depth (m)	Remarks
471-92	1808-1	12.10. -13.10.	SFV(EA8)	13:11 -15.44	05˚47.1 S	09˚25.5 W	3445	Recovery of EA8
	1808-2		P/GFO	17:08	05˚47.1 S	09˚24.2 W	3421	P:700,3050m; GFO:700,900,1200, 1800,2500,2950m
	1808-3		KAM	20:14	05˚46.7 S	09˚24.1 W	3422	Down to 250m
	1808-4		MN	21:03	05˚46.7 S	09˚24.0 W	3414	1000-500,500-300, 300-100,100-50,50-0m
	1808-5		MN	21:53	05˚46.6 S	09˚23.9 W	3414	250-100,100-75,75-50, 50-25,25-0m
	1808-6		P/GFO	23:12	05˚48.3 S	09˚24.0 W	3379	P:100,400m;GFO:25,50,100, 200,400,500m
	1808-7		MUC/CTD	00:44	05˚48.0 S	09˚24.0 W	3364	6-7cm in 2 large and 3 small tubes
	1808-8		KAM	02:00	05˚47.7 S	09˚24.2 W	3410	Down to 200m

Station No.	GeoB No.	Date 1992	Device	Time bottom contact (UTC)	Latitude	Longitude	Water-depth (m)	Remarks
Northern Brazil Basin								
472-92	1809-1	16.10.-17.10	P/GFO	19:52	03˚59.8 S	25˚30.1 W	5533	P:400,5200m; GFO:900,1200,2000, 3000,4000,5000m
	1809-2		MN	22:13	03˚59.4 S	25˚30.3 W	5530	Down to 250m
	1809-3		MN	23:03	03˚59.4 S	25˚30.5 W	5530	1000-500,500-300 300-100,100-50,50-0m
	1809-4		MN	23:32	03˚59.6 S	25˚30.5 W	5530	400-200,200-100, 100-40,40-20,20-0m
	1809-5		KAM	00:04	03˚59.5 S	25˚30.5 W	5530	250-100,100-75,75-50, 50-25,25-0m
	1809-6		P/GFO	01:53	04˚00.0 S	25˚30.0 W	5530	P:700,1200m;GFO:25, 50,100,150,350,600m
	1809-7		KAM	03:47	04˚00.2 S	25˚30.2 W	5531	Down to 500m
	1809-8		P	06:21	04˚00.1 S	25˚29.3 W	5529	P:2000,3000m;

Station No.	GeoB No.	Date 1992	Device	Time bottom contact (UTC)	Latitude	Longitude	Water-depth (m)	Remarks
	1809-9		SFV(WA1)	08:18 -12:27	04˚00.0 S	25˚34.0 W	5528	Deployment of WA1
	1809-10		MUC/CTD	15:28	04˚03.1 S	25˚37.2 W	5517	35-40cm in all tubes
	1809-11		P	17:53	04˚04.0 S	25˚37.4 W	4988	P:100,400m
473-92	1810-1	18.10. -19.10.	P/GFO	20:42	07˚30.0 S	28˚00.0 W	5579	P:5100,5400m;GFO:1000, GFO:1000,1500,2200,1500, 2200,3300,4400,5050m
	1810-2		KAM	00:24	07˚29.5 S	28˚00.0 W	5572	Down to 500m
	1801-3		MN	01:29	07˚29.4 S	28˚00.2 W	5570	1000-500,500-300,300-100, 100-50,50-0m
	1810-4		MN	02:21	07˚29.4 S	28˚00.1 W	5571	400-200,200-100,100-40, 40-20,20-0m
	1810-5		MN	02:52	07˚29.4 S	28˚00.2 W	5571	250-100,100-75,75-50, 50-25,25-0m
	1810-6		P	05:34	07˚29.0 S	28˚00.1 W	5571	P:4400,4800m

Station No.	GeoB No.	Date 1992	Device	Time bottom contact (UTC)	Latitude	Longitude	Water-depth (m)	Remarks
	1810-7		SFV(WA2)	08:12 -12:23	07˚31.3 S	28˚02.5 W	5571	Deployment of WA2
	1810-8		MUC/CTD	12:06	07˚31.3 S	28˚04.0 W	5536	All tubes empty
	1810-9		KAM	16:01	07˚30.7 S	28˚03.8 W	5591	Down to 500m
	1810-10		P/GFO	18:22	07˚31.5 S	28˚05.3 W	5558	P:700,2000m;GFO:25,50, 100,200,400m,650m

Acronyms

CTD	Probe for Conductivity/Temperature/Depth/Oxygen/Transparency
GFO	GoFlo-Bottles
HS	Hydrosweep
KAM	In-situ-Camera
MN	Multi-Net
MUC	Multi-Corer
P	In-situ-Pump
PS	Parasound
SFV	Mooring with sediment traps

7.1.2 List of Moored Sediment Traps

Mooring	Position	Water depth (m)	Sampling-interval	Instr.	Depth (m)	Intervals
Mooring recoveries during M22-1:						
CI1	29˚06.8 N	3605	25.11.91	HDW	1000	20x15.25 days
	15˚26.8 W		25.9.92	HDW	3078	20x15.25 days
				STKr7	1023	
EA6	03˚03.2 N	4453	03.12.91	HDW	901	20x15.25 days
	11˚53.1 W		06.10.92	HDW	3911	20x15.25 days
				ST8	924	
EA7	00˚03.3 S	4255	05.12.91	HDW	949	1x14.4.19x15.4d
	10˚49.3 W		06.10.92	HDW	4029	1x14.4.19x15.4d
				ST8	972	
EA8	05˚47.1 S	3450	15.12.91	HDW	598	1x3.4;19x15.4d
	09˚25.5 W		06.10.92	HDW	1255	1x3.4;19x15.4d
				HDW	1833	1x3.4;19x15.4d
				HDW	2890	1x3.4;19x15.4d
				ST8	1278	
				ST5	2913	
Mooring deployments during M22-1:						
CI2	29˚07.0 N	3606	1.10.92-	HDWn	1036	20x9.5 days
	15˚24.2 W		9.4.93	HDWn	3067	20x9.5 days
				ST7Kr	1059	
CV1	11˚29.0 N	4968	5.10.92	HDW	1003	20x9.5 days
	21˚01.0 W		4.4.93	HDW	4523	20x9.5 days
				ST8	1026	
EA9	00˚01.0 N	4563	11.10.92	HDW	646	19x9.5 days
	10˚48.4 W		01.04.93	HDW	1226	19x9.5 days
				HDW	3786	19x9.5 days
				ST8	669	
WA1	04˚00.0 S	5530	17.10.92	HDW	652	20x7.75 days
	25˚34.0 W		21.03.93	HDW	1232	20x7.75 days
				HDW	4991	20x7.75 days
				ST8	675	

Mooring	Position	Water depth (m)	Sampling-interval	Instr.	Depth (m)	Intervals
Mooring deployments during M22-1:						
WA2	07˚31.3 S	5570	19.10.92	HDW	591	20x7.75 days
	28˚02.5 W		21.03.93	HDW	5031	20x7.75 days
				ST8	614	

Instruments used:

HDW =3D Sediment trap Type Howald Electronics (now Hagenuk)
HDWn=3D Sediment trap Type Howald Electronics (new version)
ST8 =3D current meter Aanderaa, RCM 8
ST5 =3D current meter Aanderaa, RCM 5
STKr =3D current meter with special sensors (Krause, AWI)

7.1.3 Chlorophyll a Samples

(MP: membrane pump; RP: rotating pump)

No.	Date 1992	Time UTC	Longitude	Latitude	Water depth	Salin. psu	Temp. ˚C	Vol L	Remarks
1	29.09.	09:30	14˚04.0 W	36˚59.0 N	5046	36.52	20.89	1	MP
2	28.09.	14:45	13˚04.0 W	36˚03.0 N	4812	36.46	21.09	1	MP
3	28.09.	22:45	13˚34.0 W	34˚37.0 N	4049	36.53	21.61	1	MP
4	29.09.	08:00	14˚08.0 W	33.01.0 N	4309	36.58	21.93	1	MP
5	29.09.	15:30	14˚35.0 W	31˚41.0 N	4329	36.57	22.61	1	MP
6	29.09.	22:30	15˚00.0 W	30˚25.0 N	3260	36.56	22.75	1	MP
7	30.09.	09:30	15˚27.0 W	29˚07.0 N	3606	36.55	22.77	1	MP
8	30.09.	21:00	15˚24.5 W	29˚10.5 N	3603	36.54	22.80	1	MP
9	01.10.	11:00	16˚30.0 W	27˚31.0 N	3526	36.67	23.02	1	MP
10	01.10.	16:30	17˚03.0 W	26˚37.9 N	3631	36.59	23.01	1	MP
11	01.10.	22:00	17˚37.0 W	25˚45.0 N	3397	36.60	23.15	1	MP
12	02.10.	07:15	18˚35.4 W	24˚12.4 N	2794	36.69	23.43	2	MP
13	02.10.	14:45	19˚18.8 W	23˚02.3 N	3519	36.22	22.37	2	MP
14	02.10.	23:30	20˚12.0 W	21˚37.0 N	4043	35.91	23.58	1	MP
15	03.10.	08:15	20˚50.0 W	20˚33.0 N	3958	35.98	23.30	1	MP
16	03.10.	14:45	20˚51.0 W	19˚18.0 N	3408	36.07	24.58	1	MP
17	03.10.	23:00	20˚53.1 W	17˚44.8 N	3161	36.10	25.99	1	MP
18	04.10.	08:00	20˚54.9 W	16˚07.6 N	3803	35.94	26.70	1	MP
19	04.10.	17:15	20˚56.8 W	14˚19.7 N	4297	35.51	26.90	1	MP
20	04.10.	22:15	20˚58.0 N	13˚25.0 N	4538	34.67	28.10	1	MP
21	05.10.	15:00	21˚00.0 W	11˚24.0 N	4980	35.45	27.80	1	MP
22	05.10.	22:45	21˚00.0 W	11˚21.0 N	4981	35.38	27.90	1	MP
23	06.10.	10:45	19˚41.6 W	10˚14.1 N	4649	34.76	28.01	1	MP
24	06.10.	14:45	19˚10.8 W	09˚47.6 N	4048	34.97	28.50	1	MP
25	07.10.	06:45	17˚00.6 W	07˚54.9 N	4697	34.64	27.86	2	MP
26	07.10.	15:00	16˚13.3 W	07˚10.6 N	4686	34.29	27.78	1	MP
27	08.10.	07:30	14˚04.6 W	05˚08.2 N	4759	34.22	27.04	1	MP
28	08.10.	22:30	12˚13.3 W	03˚22.4 N	4459	34.77	26.68	1	MP
29	09.10.	08:00	11˚53.1 W	03˚03.5 N	4453	34.64	26.74	1	MP
30	09.10.	15:05	11˚48.0 W	02˚48.9 N	4662	34.74	26.92	1	MP
31	09.10.	22:00	11˚25.7 W	01˚43.2 N	4363	35.71	25.74	1	MP
32	10.10.	08:00	10˚51.8 W	00˚03.8 N	4397	35.80	24.07	1	MP
33	10.10.	18:00	10˚47.8 W	00˚00.8 N	4665	35.77	24.07	1	MP
34	10.10.	22:30	10˚46.7 W	00˚00.3 N	4685	35.85	23.91	1	MP

No.	Date 1992	Time UTC	Longitude	Latitude	Water depth	Salin. psu	Temp. ˚C	Vol L	Remarks
35	11.10.	08:30	10˚30.8 W	00˚56.7 S	3833	35.72	23.71	1	MP
36	11.10.	15:00	10˚16.5 W	02˚00.3 S	3727	35.74	23.94	1	MP
37	11.10.	22:05	09˚60.0 W	03˚13.9 S	4173	35.77	23.66	1	MP
38	12.10.	08:00	09˚37.1 W	04˚55.8 S	3803	35.41	22.94	1	MP
39	12.10.	17:00	09˚24.3 W	05˚47.0 S	3422	35.64	22.70	1	MP
40	12.10.	23:00	09˚24.0 W	05˚48.2 S	3394	35.60	22.61	1	MP
41	15.10.	09:30	20˚00.4 W	04˚36.9 S	4789	35.61	23.90	1	RP
42	15.10.	22:00	22˚30.7 W	04˚20.1 S	4797	35.78	24.61	1	RP
43	16.10.	08.00	24˚26.4 W	04˚07.0 S	5153	35.65	24.50	1	RP
44	16.10.	15:10	25˚30.3 W	03˚59.8 S	5530	35.81	24.98	1	RP
45	17.10.	01:00	25˚30.1 W	04˚00.1 S	5537	35.90	24.78	2	RP
46	18.10.	08:30	27˚16.3 W	06˚26.9 S	5638	36.06	24.80	2	RP
47	18.10.	15:15	27˚59.1 W	07˚28.5 S	5577	35.92	24.69	2	RP
48	18.10.	22:15	28˚00.3 W	07˚29.3 S	5571	35.89	24.51	2	RP
49	19.10.	09:30	28˚03.3 W	07˚30.8 S	5571	35.87	24.55	2	RP
50	19.10.	15:00	28˚05.4 W	07˚31.4 S	5557	35.95	24.63	2	RP

7.1.4 Particle Filtration

Station No.	Water depth (m)	Date 1992	Time start (UTC)	Volume pumped L	Pumping speed L/h	Remarks
465-92	(1000)	30.09.	05.55	412	618	Torn at edge
	3135		18.00	469	562	
	400		20.28	304	608	
466-92	400	03.10.	06.02	369	553	
	100		06.12	296	444	
467-92	4520	05.10.	12.40	573	573	
	1000		12.50	526	526	
	(410)		20.41	375	562	Torn
	(100)		20.41	474	711	Torn
468-92	100	07.10.	07.42	236	472	
	400		07.42	298	596	
469-92	900	09.10.	01.00	500	500	
	(3930)		01.00	552	552	Torn
	350		11.45	278	556	
	100		11.45	289	578	
470-92	100	10.10.	13.10	262	524	
	400		13.10	273	546	
	1200		19.10	552	552	
	4000		19.10	544	544	
	200	11.10.	01.23	368	552	
	700		01.23	374	561	
471-92	700	12.10.	16.16	499	499	
	3050		16.16	560	560	
	100		22.25	256	512	
	400		22.25	286	572	
472-92	4000	16.10.	14.15	767	511	Started at 3280 m
	5200		14.15	766	510	Started at 4580 m
	675		22.31	430	430	
	1175		22.31	581	581	
	2000	17.10.	02.31	705	528	
	3000		02.31	632	474	
	100		15.09	245	367	
	400		15.09	370	555	

Station No.	Water depth (m)	Date 1992	Time start (UTC)	Volume pumped L	Pumping speed L/h	Remarks
473-92	(5400)	18.10.	15.32	810	540	Torn
	(5100)		15.32	650	433	Torn
	4800	19.10.	01.04	770	513	
	4400		01.04	787	524	Evtl. not tight
	2000		14.50	570	570	
	700		14.50	503	503	

7.2 Leg M 22/2

7.2.1 List of Stations

METEOR 22/2 Station List											
Stat No.	CTD Prof.	ADCP Prof.	Peg Stat	Peg Prof	Day 1992	Time UTC	Latitude λ	Longitude φ	Water Depth [m]	Profile Depth [db]	Comment
474	1	A01	S07	1	24.10.	04:34	5˚34.1'S	34˚36.2'W	3339	3422	
475	2	A02	S06	2	24.10.	10:44	5˚37.9'S	34˚54.3'W	1378	1204	
476	3	A03			27.10.	00:15	0˚08.9'N	44˚22.8'W	1125	1067	
477	4	A04			27.10.	02:53	0˚23.0'N	44˚15.8'W	3278	3283	
478	-				27.10.	14:00	0˚14.6'N	44˚17.9'W	2880	-	K-359
479	5	A05			27.10.	23:13	0˚36.5'N	44˚10.9'W	3629	3663	K-360
480	6	A06	N27	3	28.10.	04:59	0˚17.6'N	44˚20.8'W	3058	3048	
481	7	A07			28.10.	18:17	1˚10.0'N	44˚03.6'W	4098	4148	K-361
482	8	A08			29.10.	00:06	1˚35.5'N	44˚00.1'W	4110	4145	
483	9	A09	N03	4	29.10.	05:56	1˚58.0'N	44˚01.4'W	4130	4174	
484	10	A10			29.10.	13:52	2˚30.3'N	44˚01.6'W	4166	4212	
485	11	A11	N04	5	29.10.	21:46	3˚18.2'N	43˚59.9'W	4200	4250	
486	12	A12			30.10.	04:31	3˚46.3'N	44˚02.1'W	4210	4258	
487	13	A13	N26	6	30.10.	10:25	4˚13.8N	44˚01.9'W	4170	4220	
488	14	A14			30.10.	18:04	4˚50.9'N	44˚01.5'W	3341	3410	
489	15	A15			31.10.	01:10	5˚42.4'N	44˚00.9'W	4030	4073	
490	16	A16			31.10.	06:37	6˚04.6'N	44˚00.3'W	4148	4262	
491	17	A17	N6	7	31.16.	13:48	6˚39.1’N	44˚00.3'W	4634	4700	
492	18	A18			02.11.	20:01	4˚00.2'N	35˚01.6'W	3511	2515	
493	19	A19			03.11.	03:20	3˚10.3'N	35˚01.8'W	3520	2505	
494	20	A20			03.11.	10:43	2˚20.1’N	35˚01.8'W	4142	2513	
495	21	A21			03.11.	18:03	1˚30.3'N	35˚02.0'W	4034	2501	
496	22	A22	S10	8	04.11.	02:07	0˚38.9'N	34˚59.5'W	4528	4584	

METEOR 22/2 Station List											
Stat No.	**CTD Prof.**	**ADCP Prof.**	**Peg Stat**	**Peg Prof**	**Day 1992**	**Time UTC**	**Latitude λ**	**Longitude φ**	**Water Depth [m]**	**Profile Depth [db]**	**Comment**
497	23	A23		9	04.11.	10:27	0˚01.6'S	34˚59.5'W	4420	4580	
498	24	B24	S2	10	04.11.	19:13	0˚46.8'S	34˚59.5'W	4441	4455	BBADCP
499	25	A25			05.11.	00:51	1˚03.7'S	34˚59.4'W	4376	4426	
500	26	A26			05.11.	05:24	1˚16.0'S	34˚59.7'W	4349	4700	
501	27	A27	S3	11	05.11.	09:41	1˚28.3'S	34˚59.7'W	4280	4321	
502	28	A28			05.11.	15:28	1˚44.4'S	34˚59.4'W	4100	4139	
503	29	A29	S4	12	05.11.	21:45	2˚16.6'S	34˚59.4'W	3967	4005	
504	30	A30	S5	13	06.11.	06:50	3˚09.4'S	34˚52.7'W	3809	3850	
505	31	A31			06.11.	12:48	3˚29.4'S	35˚13.7'W	3451	3474	
506	32	B32	S14	14	06.11.	23:25	3˚58.7'S	34˚56.9'W	3525	3545	BBADCP
507	33	A33			07.11.	04:44	4˚19.2'S	35˚02.3'W	3385	3416	
508	34	A34	S15	15	07.11.	12:58	4˚29.8'S	35˚04.9'W	3160	3162	
509	35	A35			07.11.	18:38	4˚55.4'S	34˚53.1'W	877	877	
510	36	A36			07.11.	20:41	5˚01.4'S	35˚00.0'W	539	532	
511	37	A37			08.11.	01:16	5˚37.0'S	34˚56.9'W	505	497	
512	38	B38	S6	16	08.11.	02:46	5˚37.7'S	34˚54.5'W	1249	1142	BBADCP
512	382	A38			08.11.	04:24	5˚38.1'S	34˚54.2'W	-	251	
513	39	A39			08.11.	08:12	5˚35.4'S	34˚47.2'W	2685	2665	
514	40	A40	S7	17	08.11.	11:57	5˚33.8'S	34˚36.2'W	3435	3448	
515	41	A41	S12	18	08.11.	17:18	5˚32.7'S	34˚19.9'W	3948	3977	
516	42	A42	S8	19	08.11.	23:20	5˚31.6'S	34˚00.9'W	4204	4214	
517	43				09.11.	05:50	5˚29.6'S	33˚38.6'W	4396	4449	
518	44		S13	20	09.11.	12:16	5˚25.4'S	33˚10.5'W	4524	4581	
519	45	A45			09.11.	17:40	5˚20.1'S	32˚59.6'W	4547	4607	BBADCP
520	46	B46	S9	21	10.11.	00:15	5˚20.0'S	32˚27.4'W	4610	4672	BBADCP
521	47	B47	S16	22	10.11.	09:51	5˚14.7'S	31˚59.2'W	4661	4726	BBADCP
522	48	B48	S17	23	10.11.	19:48	5˚09.7'S	31˚29.4'W	4722	4785	BBADCP

METEOR 22/2 Station List											
Stat No.	**CTD Prof.**	**ADCP Prof.**	**Peg Stat**	**Peg Prof**	**Day 1992**	**Time UTC**	**Latitude λ**	**Longitude φ**	**Water Depth [m]**	**Profile Depth [db]**	**Comment**
523	49	B49			11.11.	03:20	5˚07.7'S	30˚59.2'W	4874	4952	BBADCP
524	50	B50			11.11.	10:10	5˚03.3'S	30˚29.3'W	4970	5054	BBADCP
525	51	B51			11.11.	16:58	4˚59.6'S	29˚59.6'W	4985	5061	BBADCP
526	52	B52			12.11.	02:04	5˚59.6'S	30˚34.7'W	5132	1500	BBADCP
527	53	B53			12.11.	08:19	6˚59.8'S	31˚04.8'W	5168	1504	BBADCP
528	54	B54			12.11.	16:22	8˚00.0'S	31˚29.8'W	5231	1501	BBADCP
529	55	B55			12.11.	23:34	8˚59.9'S	31˚59.8'W	5028	1500	BBADCP
530	56	B56			13.11.	07:46	9˚59.7'S	32˚29.6'W	4922	4999	BBADCP
531	57	B57			13.11.	14:54	9˚59.2'S	33˚09.9'W	4821	4893	BBADCP
532	58	B58			13.11.	22:22	9˚59.7'S	33˚50.2'W	4681	4749	BBADCP
533	59	B59			14.11.	04:08	9˚59.6'S	34˚15.4'W	4197	4317	BBADCP
534	60	B60			14.11.	08:25	9˚59.6'S	34˚30.1'W	3223	3232	BBADCP
535	61	B61			14.11.	12:37	9˚59.3'S	34˚44.6'W	3774	3801	BBADCP
536	62	B62			14.11.	16:50	9˚59.6'S	35˚04.9'W	3379	3396	BBADCP
537	63	B63			14.11.	20:21	9˚59.2'S	35˚14.3'W	2325	2325	BBADCP
538	64	B64			14.11.	23:21	9˚59.1'S	35˚24.5'W	1552	1552	BBADCP
539	65	B65			15.11.	01.31	9˚59.0'S	35˚29.7'W	1049	1060	BBADCP

TM22/2

7.2.2 List of XBT Drops

METEOR 22-2 XBT Stations									
XBT	Stat	Day	Start Time		Latitude	Longitude	Water Depth	XBT Depth	Comment
001	---	23.10.92	20:04		34°39.1'W	06°52.9'S	30m	760m	test
002	---	24.10.92	00:51		34°37.2'W	05°58.1'S	2158m	760m	
003	---	24.10.92	02:12		34°36.3'W	05°41.8'S	3324m	300m	
004	---	24.10.92	18:41		35°33.6'W	04°35.1'S	2210m	760m	
005	---	24.10.92	20:04		35°48.5'W	04°27.3'S	2584m	760m	
006	---	24.10.92	23:23		36°25.9'W	04°07.4'S	2549m	760m	
007	---	25.10.92	01:16		36°47.5'W	03°56.1'S	2532m	760m	
008	---	25.10.92	06:07		37°41.8'W	03°27.0'S	1595m	760m	
009	---	25.10.92	10:05		38°29.0'W	03°02.8'S	1385m	760m	
010	---	25.10.92	11:04		38°40.7'W	02°56.8'S	1495m	760m	
011	---	25.10.92	12:02		38°52.2'W	02°50.3'S	983m	760m	
012	---	25.10.92	13:01		39°03.8'W	02°44.2'S	200m	214m	shallow water
013	---	25.10.92	23:29		41°04.5'W	02°02.3'S	1080m	760m	
014	---	26.10.92	02:04		41°36.1'W	01°52.5'S	2393m	760m	
015	---	26.10.92	04:01		42°01.0'W	01°44.7'S	2589m	760m	
016	---	26.10.92	06:06		42°26.0'W	01°36.8'S	2550m	760m	
017	---	26.10.92	08:14		42°48.9'W	01°28.6'S	2379m	760m	
018	---	26.10.92	08:19		42°53.2'W	01°28.1'S	2270m	760m	
019	---	26.10.92	08:24		42°54.4'W	01°27.7'S	2270m	760m	
020	---	26.10.92	10:08		43°14.3'W	01°21.5'S	883m	760m	
021	---	27.10.92	15:54		44°15.8'W	00°21.8'N	3252m	760m	
022	---	27.10.92	16:27		44°14.6'W	00°27.0'N	3370m	760m	
023	---	27.10.92	17:08		44°11.5'W	00°33.0'N	3548m	480m	
024	---	27.10.92	20:22		44°03.8'W	01°11.0'N	4095m	760m	
025	---	28.10.92	21:30		44°02.2'W	01°23.2'N	4100m	710m	
026	482	29.10.92	02:20		44°00.7'W	01°36.1'N	4105m	760m	
027	---	29.10.92	03:32		44°01.1'W	01°49.7'N	4124m	760m	
028	---	29.10.92	09:24		44°03.3'W	01°57.8'N	4124m	760m	
029	484	29.10.92	11:17		44°02.2'W	02°17.3'N	4153m	620m	2 trials
030	485	29.10.92	16:00		44°01.5'W	02°31.0'N	4168m	760m	
031	---	29.10.92	17:12		44°01.9'W	02°45.9'N	4185m	600m	
032	---	29.10.92	18:34		44°02.0'W	03°02.0'N	4195m	760m	
033	---	30.10.92	00:45		44°00.1'W	03°18.0'N	4199m	760m	
034	---	30.10.92	01:59		44°01.9'W	03°33.0'N	4212m	760m	
035	486	30.10.92	06:40		44°01.7'W	03°48.4'N	4213m	760m	
036	---	30.10.92	08:06		44°02.4'W	04°05.3'N	4207m	760m	
037	487	30.10.92	13:23		44°02.5'W	04°13.5'N	4177m	760m	
038	---	30.10.92	14:46		44°00.2'W	04°30.1'N	3382m	760m	
039	---	30.10.92	16:07		44°02.1'W	04°45.3'N	3395m	760m	
040	488	30.10.92	19:39		44°00.6'W	04°53.3'N	3323m	760m	
041	---	30.10.92	23:02		44°01.6'W	05°34.0'N	3781m	760m	
042	489	31.10.92	03:28		44°00.3'W	05°44.9'N	4088m	760m	
043	---	31.10.92	04:45		44°01.8'W	06°00.2'N	4105m	760m	
044	---	31.10.92	10:15		43°59.4'W	06°20.5'N	4507m	710m	
045	---	31.10.92	11:06		43°59.5'W	06°31.0'N	4637m	125m	

METEOR 22-2 XBT Stations

XBT	Stat	Day	Start Time		Latitude	Longitude	Water Depth	XBT Depth	Comment
046	---	31.10.92	17:21		43˚58.5'W	06˚39.8'N	4635m	760m	
047	---	31.10.92	18:14		43˚48.9'W	06˚36.9'N	4617m	700m	
048	---	31.10.92	19:01		43˚40.4'W	06˚34.7'N	4686m	760m	
049	---	31.10.92	20:01		43˚29.8'W	06˚31.1'N	4520m	760m	
050	---	31.10.92	20:57		43˚19.5'W	06˚28.0'N	4533m	760m	
051	---	31.10.92	21:57		43˚08.4'W	06˚24.8'N	4555m	760m	
052	---	31.10.92	22:58		42˚57.0'W	06˚22.0'N	4676m	760m	
053	---	31.10.92	23:59		42˚42.2'W	06˚18.5'N	4598m	760m	
054	---	01.11.92	00:55		42˚36.0'W	06˚15.5'N	4678m	760m	
055	---	01.11.92	01:58		42˚25.0'W	06˚12.2'N	4687m	760m	
056	---	01.11.92	03:03		42˚13.4'W	06˚08.9'N	4688m	760m	
057	---	01.11.92	04:02		42˚03.0'W	06˚05.9'N	4685m	760m	
058	---	01.11.92	05:04		41˚51.6'W	06˚02.3'N	4684m	760m	
059	---	01.11.92	06:03		41˚40.8'W	05˚59.2'N	4684m	760m	
060	---	01.11.92	06:59		41˚31.0'W	05˚56.3'N	4675m	760m	
061	---	01.11.92	07:59		41˚19.0'W	05˚52.8'N	4683m	760m	
062	---	01.11.92	09:01		41˚07.5'W	05˚49.4'N	4652m	760m	
063	---	01.11.92	10:01		40˚56.8'W	05˚45.8'N	4676m	760m	
064	---	01.11.92	10:57		40˚46.5'W	05˚43.1'N	4674m	760m	
065	---	01.11.92	11:58		40˚36.4'W	05˚38.2'N	4678m	760m	
066	---	01.11.92	13:15		40˚21.8'W	05˚34.2'N	4742m	760m	
067	---	01.11.92	13:57		40˚13.7'W	05˚31.8'N	4513m	760m	
068	---	01.11.92	15:04		40˚01.0'W	05˚27.9'N	4650m	760m	
069	---	01.11.92	16:02		39˚50.5'W	05˚25.3'N	4290m	760m	
070	---	01.11.92	17:01		39˚38.7'W	05˚22.3'N	4581m	760m	
071	---	01.11.92	17:56		39˚28.3'W	05˚19.6'N	4651m	0m	corrupted data
072	---	01.11.92	19:14		39˚13.3'W	05˚15.4'N	4656m	760m	
073	---	01.11.92	20:00		39˚04.6'W	05˚12.8'N	4517m	760m	
074	---	01.11.92	21:10		38˚50.9'W	05˚10.1'N	4506m	760m	
075	---	01.11.92	21:58		38˚40.8'W	05˚06.1'N	4682m	760m	
076	---	01.11.92	22:56		38˚30.5'W	05˚02.6'N	4671m	760m	
077	---	01.11.92	23:56		38˚19.3'W	04˚59.3'N	4513m	760m	
078	---	02.11.92	00:55		38˚08.1'W	04˚56.0'N	4256m	640m	
079	---	02.11.92	01:54		37˚57.0'W	04˚52.6'N	4538m	760m	
080	---	02.11.92	03:05		37˚43.3'W	04˚48.8'N	4571m	680m	
081	---	02.11.92	04:01		37˚32.7'W	04˚45.6'N	4437m	760m	
082	---	02.11.92	05:08		37˚20.0'W	04˚41.8'N	4617m	760m	
083	---	02.11.92	06:01		37˚10.0'W	04˚38.8'N	4231m	760m	
084	---	02.11.92	06:57		37˚00.0'W	04˚35.7'N	4050m	760m	
085	---	02.11.92	07:59		36˚48.9'W	04˚32.4'N	4038m	700m	
086	---	02.11.92	08:59		36˚38.4'W	04˚29.3'N	3960m	760m	
087	---	02.11.92	10:00		36˚27.5'W	04˚25.8'N	4351m	760m	
088	---	02.11.92	10:56		36˚18.0'W	04˚23.3'N	4160m	720m	
089	---	02.11.92	11:55		36˚08.5'W	04˚20.4'N	4151m	760m	
090	---	02.11.92	12:55		35˚59.2'W	04˚17.6'N	3942m	760m	
091	---	02.11.92	13:54		35˚50.0'W	04˚14.8'N	3818m	760m	
092	---	02.11.92	15:03		35˚39.1'W	04˚11.7'N	3561m	760m	

METEOR 22-2 XBT Stations									
XBT	Stat	Day	Start Time		Latitude	Longitude	Water Depth	XBT Depth	Comment
093	---	02.11.92	15:59		35˚30.3'W	04˚09.0'N	3786m	760m	
094	---	02.11.92	17:10		35˚19.8'W	04˚06.0'N	3819m	760m	
095	---	02.11.92	18:02		35˚11.9'W	04˚03.6'N	3445m	760m	
096	---	02.11.92	21:19		35˚01.4'W	04˚00.1'N	3510m	760m	
097	---	02.11.92	23:18		35˚02.0'W	04˚00.0'N	3692m	760m	
098	---	03.11.92	01:19		35˚01.9'W	03˚20.0'N	3586m	760m	
099	---	03.11.92	05:37		35˚02.0'W	03˚00.0'N	3638m	720m	
100	---	03.11.92	07:42		35˚01.7'W	02˚40.0'N	3657m	760m	
101	---	03.11.92	12:01		35˚01.8'W	02˚20.1'N	4162m	760m	
102	---	03.11.92	14:09		35˚01.9'W	02˚00.0'N	4211m	760m	
103	---	03.11.92	16:07		35˚02.0'W	01˚40.0'N	4010m	760m	
104	---	03.11.92	20:09		35˚01.8'W	01˚20.7'N	4030m	760m	
105	---	03.11.92	22:09		35˚00.8'W	01˚00.0'N	3581m	760m	
106	---	03.11.92	23:36		35˚00.2'W	00˚45.0'N	4522m	760m	
107	---	04.11.92	05:37		34˚59.9'W	00˚30.0'N	4525m	760m	
108	---	04.11.92	07:02		34˚59.8'W	00˚15.0'N	4523m	760m	
109	---	04.11.92	08:38		34˚59.7'W	00˚00.0'N	4521m	760m	
110	---	04.11.92	13:13		35˚00.3'W	00˚03.2'S	4465m	760m	
111	---	04.11.92	14:56		34˚59.8'W	00˚20.8'S	4493m	760m	
112	---	04.11.92	16:44		35˚00.3'W	00˚40.0'S	4448m	760m	
113	---	04.11.92	23:01		34˚59.9'W	01˚06.0'S	4367m	760m	
114	---	05.11.92	07:17		34˚59.8'W	01˚20.0'S	4031m	760m	
115	---	05.11.92	13:18		35˚00.1'W	01˚40.0'S	4064m	760m	
116	501	05.11.92	18:33		35˚00.1'W	02˚00.0'S	4561m	760m	
117	---	06.11.92	01:24		34˚58.2'W	02˚30.0'S		760m	no depth
118	---	06.11.92	04:14		34˚54.3'W	03˚00.0'S	3830m	760m	
119	505	06.11.92	14:35		35˚13.2'W	03˚30.3'S	3444m	760m	
120	506	07.11.92	01:30		34˚57.9'W	03˚59.6'S	3516m	760m	
121	---	07.11.92	06:59		35˚02.1'W	04˚29.0'S	3159m	760m	
122	---	07.11.92	16:46		34˚58.6'W	04˚45.0'S	916m	760m	
123	---	07.11.92	21:33		34˚59.6'W	05˚03.7'S	540m	760m	
124	---	08.11.92	06:11		34˚54.5'W	05˚37.3'S	891m	760m	
125	---	08.11.92	10:12		34˚40.0'W	05˚34.8'S	3142m	760m	
126	---	08.11.92	19:45		34˚20.3'W	05˚33.4'S	3915m	760m	
127	516	09.11.92	01:59		34˚01.3'W	05˚33.0'S	4164m	760m	
128	---	09.11.92	03:37		33˚45.0'W	05˚30.7'S	4349m	760m	
129	---	09.11.92	08:34		33˚30.0'W	05˚27.8'S	4450m	760m	
130	518	09.11.92	14:52		33˚10.6'W	05˚25.4'S	4523m	760m	
131	519	09.11.92	19:24		32˚58.4'W	05˚19.8'S	4548m	760m	
132	520	10.11.92	03:11		32˚27.5'W	05˚20.7'S	4611m	760m	
133	---	10.11.92	04:25		32˚15.0'W	05˚18.1'S	4545m	760m	
134	521	10.11.92	12:43		32˚00.0'W	05˚15.3'S	4623m	760m	
135	---	10.11.92	14:35		31˚41.3'W	05˚12.6'S	4646m	760m	
136	---	10.11.92	22:40		31˚29.2'W	05˚09.8'S	4726m	760m	
137	---	10.11.92	00:04		31˚15.0'W	05˚09.1'S	4842m	760m	
138	523	11.11.92	05:36		30˚58.1'W	05˚07.0'S	4872m	760m	
139	---	11.11.92	06:48		30˚45.9'W	05˚06.2'S	4918m	760m	

METEOR 22-2 XBT Stations									
XBT	Stat	Day	Start Time		Latitude	Longitude	Water Depth	XBT Depth	Comment
140	525	11.11.92	12:14		30˚28.4'W	05˚03.2'S	4921m	760m	
141	---	11.11.92	13:56		30˚11.2'W	05˚01.4'S	4946m	760m	
142	---	11.11.92	19:24		29˚59.9'W	05˚00.5'S	4980m	760m	
143	---	11.11.92	20:24		30˚06.3'W	05˚10.0'S	5010m	760m	
144	---	11.11.92	21:21		30˚11.6'W	05˚20.0'S	5030m	760m	
145	---	11.11.92	22:19		30˚17.3'W	05˚30.0'S	5065m	760m	
146	---	11.11.92	23:23		30˚23.3'W	05˚40.0'S	5089m	760m	
147	---	12.11.92	00:22		30˚29.1'W	05˚50.0'S	5114m	760m	
148	526	12.11.92	02:46		30˚34.8'W	06˚00.0'S	5135m	760m	
149	---	12.11.92	03:43		30˚40.0'W	06˚10.0'S	5140m	760m	
150	---	12.11.92	04:42		30˚44.9'W	06˚19.9'S	5040m	760m	
151	---	12.11.92	05:42		30˚49.8'W	06˚29.9'S	5160m	760m	
152	---	12.11.92	06:42		30˚54.9'W	40˚00.0'S	5167m	760m	
153	---	12.11.92	07:51		31˚00.0'W	06˚51.0'S	5180m	760m	
154	---	12.11.92	09:55		31˚04.9'W	07˚00.1'S	5170m	760m	
155	---	12.11.92	11:00		31˚09.5'W	07˚10.9'S	5221m	760m	
156	---	12.11.92	11:50		31˚13.2'W	07˚20.0'S	5225m	760m	
157	---	12.11.92	12:49		31˚17.4'W	07˚30.0'S	5256m	760m	
158	---	12.11.92	13:51		31˚21.5'W	07˚40.0'S	5225m	760m	
159	---	12.11.92	14:46		31˚25.7'W	07˚50.0'S	5228m	760m	
160	528	12.11.92	17:04		31˚30.1'W	08˚00.9'S	5227m	760m	
161	---	12.11.92	17:59		31˚34.5'W	08˚10.0'S	5196m	760m	
162	---	12.11.92	18:57		31˚39.9'W	08˚20.0'S	5198m	760m	
163	---	12.11.92	19:55		31˚44.9'W	08˚30.0'S	5075m	760m	
164	---	12.11.92	20:56		31˚49.6'W	08˚40.0'S	2935m	760m	
165	---	13.11.92	00:11		31˚59.7'W	08˚59.8'S	5022m	760m	
166	---	13.11.92	01:12		32˚05.1'W	09˚10.4'S	4997m	760m	
167	---	13.11.92	02:04		32˚09.8'W	09˚20.0'S	4982m	760m	
168	---	13.11.92	03:01		32˚14.6'W	09˚30.0'S	4963m	760m	
169	---	13.11.92	04:00		32˚20.0'W	09˚40.0'S	4949m	760m	
170	---	13.11.92	04:56		32˚25.0'W	09˚50.0'S	4928m	760m	
171	---	13.11.92	09:48		32˚30.0'W	10˚00.0'S	4920m	760m	
172	---	13.11.92	10:52		32˚42.8'W	10˚00.0'S	4896m	760m	
173	---	13.11.92	11:33		32˚50.8'W	09˚60.0'S	4872m	760m	
174	---	13.11.92	12:19		32˚50.0'W	10˚00.0'S	4850m	760m	
175	531	13.11.92	17:11		33˚10.0'W	09˚58.6'S	4818m	760m	
176	---	13.11.92	18:00		33˚20.0'W	09˚59.2'S	4798m	760m	
177	---	13.11.92	18:52		33˚29.9'W	10˚00.0'S	4755m	760m	
178	---	13.11.92	19:45		33˚40.0'W	10˚00.0'S	4717m	760m	
179	532	14.11.92	00:20		33˚50.9'W	09˚59.1'S	4680m	760m	
180	---	14.11.92	01:08		33˚60.0'W	09˚59.7'S	4674m	760m	
181	---	14.11.92	01:59		34˚10.0'W	10˚00.1'S	4638m	760m	
182	---	14.11.92	06:14		34˚20.0'W	09˚59.6'S	4053m	760m	
183	---	14.11.92	10:00		34˚30.0'W	10˚00.0'S	2926m	760m	
184	---	14.11.92	10:48		34˚40.0'W	09˚59.7'S	3855m	760m	
185	535	14.11.92	14:22		34˚50.1'W	09˚59.4'S	3703m	760m	
186	---	14.11.92	15:11		35˚00.0'W	10˚00.0'S	3485m	760m	

METEOR 22-2 XBT Stations										
XBT	Stat	Day	Start Time		Latitude	Longitude	Water Depth	XBT Depth	Comment
187	---	14.11.92	18:49		35˚10.0'W	09˚59.5'S	2389m	760m	
188	---	14.11.92	22:06		35˚20.0'W	09˚59.6'S	1960m	760m	
189	---	14.11.92	23:55		35˚24.1'W	09˚58.5'S	1439m	760m	
190	---	15.11.92	02:02		35˚28.7'W	09˚57.2'S	963m	760m	2 trials

7.3 Leg M 22/3-4

7.3.1 CTD Stations

Stat./ Profile	Date 1992	Time UTC	Latitude	Longitude	Depth (m)
540/1	11/20	10:15	13˚57.4 S	36˚16.6 W	4343
542/2	11/22	14:50	19˚39.86 S	39˚11.14 W	920
543/3	11/22	23:58	21˚09.98 S	38˚46.78 W	2623
544/4	11/23	9:06	22˚09.88 S	37˚52.00 W	3523
545/5	11/24	20:23	26˚27.10 S	42˚02.06 W	2587
547/6	11/25	20:27	28˚50.15 S	44˚25.66 W	3697
548/7	11/26	2:18	28˚20.11 S	44˚50.23 W	3445
549/8	11/26	8:57	28˚15.20 S	45˚13.94 W	3208
551/9	11/26	16:10	28˚10.07 S	45˚27.92 W	2857
552/10	11/26	19:49	28˚05.99 S	45˚45.04 W	2754
553/11	11/26	23:03	28˚03.09 S	46˚04.06 W	2461
554/12	11/27	1:42	28˚01.18 S	46˚16.08 W	2305
555/13	11/27	4:29	27˚57.97 S	46˚25.76 W	1901
556/14	11/27	7:07	27˚54.92 S	46˚37.05 W	1354
559/15	11/27	19:41	27˚50.02 S	46˚53.03 W	700
560/16	11/27	22:10	27˚47.12 S	47˚05.22 W	494
561/17	11/28	0:13	27˚43.06 S	47˚17.97 W	221
562/18	11/28	2:33	27˚39.75 S	47˚30.02 W	142
563/19	11/28	8:21	26˚55.06 S	46˚59.90 W	155
564/20	11/28	12:02	26˚55.06 S	46˚25.08 W	442
565/21	11/28	15:30	27˚06.95 S	45˚56.94 W	1805
566/22	11/28	19:21	27˚15.07 S	45˚34.24 W	2231
567/23	11/28	23:44	27˚26.88 S	45˚07.00 W	2599
568/24	11/29	5:46	26˚54.96 S	44˚34.99 W	2682
569/25	11/29	9:50	26˚40.11 S	44˚53.15 W	2499
570/26	11/29	13:31	26˚29.11 S	45˚09.72 W	2130
571/27	11/29	16:42	26˚18.96 S	45˚25.09 W	1646
572/28	11/29	19:58	26˚05.85 S	45˚40.60 W	491
573/29	11/29	21:49	25˚58.02 S	45˚52.97 W	328
574/30	11/29	23:48	25˚46.99 S	46˚05.09 W	157
575/31	12/3	21:25	28˚27.11 S	44˚27.47 W	3620
576/32	12/4	5:46	28˚59.82 S	43˚34.00 W	3919
577/33	12/4	20:13	29˚31.07 S	42˚42.23 W	4013

Stat./ Profile	Date 1992	Time UTC	Latitude	Longitude	Depth (m)
578/34	12/5	2:10	29˚48.06 S	42˚12.05 W	4022
579/35	12/5	7:17	30˚01.83 S	41˚49.35 W	3913
580/36	12/5	21:11	30˚34.79 S	40˚46.10 W	3727
581/37	12/6	2:47	30˚53.05 S	40˚21.57 W	4033
582/38	12/6	8:34	31˚10.82 S	39˚50.90 W	3796
586/39	12/7	0:11	31˚11.80 S	39˚31.66 W	4354
587/40	12/7	3:15	31˚12.07 S	39˚28.25 W	4166
588/41	12/7	6:10	31˚11.92 S	39˚26.39 W	4561
589/42	12/7	9:24	31˚12.27 S	39˚24.68 W	4601
594/43	12/8	2:30	31˚12.27 S	39˚20.99 W	4567
596/44	12/8	17:03	31˚11.86 S	39˚16.34 W	4063
601/45	12/10	23:25	33˚51.61 S	30˚54.41 W	5147
603/46	12/11	23:51	34˚18.18 S	28˚29.96 W	4031
607/47	12/15	0:38	34˚36.33 S	27˚02.96 W	4301
608/48	12/15	6:14	34˚29.97 S	27˚18.27 W	4319
609/49	12/15	19:20	34˚31.54 S	26˚59.39 W	4326
612/50	12/16	20:59	31˚37.84 S	28˚47.37 W	3806
613/51	12/17	13:02	30˚10.18 S	31˚15.70 W	4067
615/52	12/18	13:45	27˚23.42 S	34˚13.60 W	4201
616/53	12/19	0:33	26˚53.20 S	34˚47.53 W	4762

7.3.2 List of XBT Drops

Profile No.	Date 1992	Time UTC	Latitude	Longitude	Depth (m)
1	11/22	13:38	19˚39.80 S	39˚11.50 W	
2	11/22	14:57	19˚43.30 S	39˚10.20 W	1227
3	11/22	14:32	19˚49.10 S	39˚08.40 W	1629
4	11/22	15:00	19˚54.70 S	39˚07.10 W	1654
5	11/22	15:29	20˚01.00 S	39˚05.50 W	1922
6	11/22	15:56	20˚06.00 S	39˚04.00 W	1922
7	11/22	16:28	20˚12.20 S	39˚02.40 W	1963
8	11/22	14:58	20˚17.80 S	39˚00.90 W	2129
9	11/22	17:28	20˚23.70 S	38˚59.30 W	2262
10	11/22	17:54	20˚28.60 S	38˚58.00 W	2300
11	11/22	18:25	20˚34.60 S	38˚56.40 W	2440
12	11/22	18:56	20˚40.40 S	38˚54.70 W	2476
13	11/22	19:34	20˚47.30 S	38˚54.00 W	2525
14	11/22	19:58	20˚51.80 S	38˚52.40 W	2481
15	11/22	20:27	20˚57.10 S	38˚51.20 W	2645
16	11/22	21:04	21˚02.40 S	38˚49.30 W	2581
17	11/22	21:28	21˚07.80 S	38˚47.50 W	2568
18	11/22	23:38	21˚10.00 S	38˚47.60 W	
19	11/22	23:59	21˚12.70 S	38˚44.80 W	
20	11/23	0:29	21˚16.80 S	38˚40.70 W	
21	11/23	0:57	21˚20.80 S	38˚37.00 W	
22	11/23	1:24	21˚24.70 S	38˚33.50 W	
23	11/23	1:57	21˚28.60 S	38˚29.80 W	
24	11/23	2:27	21˚33.40 S	38˚25.50 W	3434
25	11/23	3:05	21˚38.70 S	38˚20.70 W	3477
26	11/23	3:31	21˚42.30 S	38˚17.40 W	3511
27	11/23	3:58	21˚45.90 S	38˚14.20 W	3523
28	11/23	4:26	21˚50.30 S	38˚10.30 W	3509
29	11/23	4:56	21˚54.40 S	38˚06.50 W	3515
30	11/23	5:29	21˚58.80 S	38˚02.30 W	3509
31	11/23	5:59	22˚02.80 S	37˚58.70 W	3526
32	11/23	6:29	22˚07.40 S	37˚54.40 W	3533
33	11/23	10:59	22˚22.00 S	38˚03.40 W	3439
34	11/23	12:59	22˚38.80 S	38˚19.50 W	
35	11/23	15:00	22˚55.70 S	38˚35.90 W	3128

Profile No.	Date 1992	Time UTC	Latitude	Longitude	Depth (m)
36	11/23	16:57	23˚11.60 S	38˚51.30 W	3229
37	11/23	18:57	23˚27.70 S	39˚06.50 W	3062
38	11/23	20:58	23˚43.50 S	39˚22.00 W	3358
39	11/23	22:59	23˚58.60 S	39˚36.60 W	3128
40	11/24	1:06	24˚14.50 S	39˚51.90 W	3075
41	11/24	3:37	24˚35.80 S	40˚12.80 W	3038
42	11/24	4:55	24˚46.10 S	40˚22.70 W	2970
43	11/24	6:57	25˚02.00 S	40˚38.30 W	3080
44	11/24	8:58	25˚17.60 S	40˚53.50 W	2684
45	11/24	11:09	25˚34.20 S	41˚10.40 W	2596
46	11/24	12:57	25˚47.80 S	41˚23.20 W	2760
47	11/24	14:57	26˚02.50 S	41˚37.70 W	2689
48	11/24	16:58	26˚17.50 S	41˚52.60 W	2505
49	11/24	20:58	26˚37.40 S	42˚12.30 W	2542
50	11/24	22:56	26˚53.10 S	42˚27.80 W	2440
51	11/25	0:56	27˚08.90 S	42˚43.60 W	2373
52	11/25	2:58	27˚25.70 S	42˚59.80 W	2495
53	11/25	4:55	27˚42.80 S	43˚16.10 W	2983
54	11/25	6:57	27˚58.70 S	43˚33.30 W	3366
55	11/25	8:57	28˚15.80 S	43˚50.50 W	3570
56	11/25	11:04	28˚32.00 S	44˚06.90 W	3660
57	11/25	12:58	28˚42.40 S	44˚17.40 W	3673
58	12/16	21:28	31˚36.90 S	28˚49.70 W	3698
59	12/16	21:57	31˚34.20 S	28˚54.40 W	3442
60	12/16	23:55	31˚22.40 S	29˚14.40 W	2811
61	12/17	1:55	31˚08.50 S	29˚37.20 W	3046
62	12/17	3:52	30˚55.70 S	29˚58.70 W	3286
63	12/17	6:08	30˚40.20 S	30˚25.30 W	3838
64	12/17	7:51	30˚28.80 S	30˚44.60 W	4042
65	12/17	9:53	30˚15.50 S	31˚06.90 W	4065
66	12/17	13:23	30˚10.10 S	31˚15.50 W	4066
67	12/17	13:56	30˚07.30 S	31˚19.30 W	4065
68	12/17	15:50	29˚53.40 S	31˚36.10 W	4053
69	12/17	17:50	29˚39.00 S	31˚53.40 W	3720
70	12/17	19:48	29˚24.70 S	32˚10.40 W	3762
71	12/17	21:52	29˚09.30 S	32˚28.80 W	2409

Profile No.	Date 1992	Time UTC	Latitude	Longitude	Depth (m)
72	12/17	23:52	28˚55.20 S	32˚45.70 W	2279
73	12/18	1:51	28˚40.80 S	33˚02.90 W	4348
74	12/18	3:52	28˚26.20 S	33˚20.10 W	4100
75	12/18	5:49	28˚12.40 S	33˚34.50 W	4259
76	12/18	8:04	27˚52.10 S	33˚50.90 W	4473
77	12/18	9:55	27˚36.00 S	34˚03.70 W	4497
78	12/18	14:13	27˚22.60 S	34˚14.80 W	4254
79	12/18	14:53	27˚18.10 S	34˚19.90 W	4197
80	12/18	16:58	27˚02.40 S	34˚37.40 W	3873
81	12/19	1:24	26˚53.20 S	34˚47.90 W	4776
82	12/19	2:52	26˚43.80 S	34˚55.40 W	4639
83	12/19	4:51	26˚31.20 S	35˚05.60 W	4438
84	12/19	6:52	26˚19.60 S	35˚15.30 W	4342
85	12/19	8:51	26˚08.70 S	35˚24.10 W	4226
86	12/19	11:00	25˚58.50 S	35˚32.20 W	4189
87	12/19	12:51	25˚50.70 S	35˚38.60 W	4167
88	12/19	14:50	25˚46.20 S	35˚59.70 W	4184
89	12/19	16:52	25˚40.90 S	36˚03.50 W	4183
90	12/19	18:50	25˚35.20 S	36˚18.60 W	4248
91	12/19	20:50	25˚29.00 S	36˚34.80 W	4232
92	12/20	0:56	25˚15.90 S	37˚09.40 W	4151
93	12/20	2:50	25˚08.50 S	37˚29.40 W	4113
94	12/20	4:53	25˚00.40 S	37˚51.10 W	3968
95	12/20	6:52	24˚52.70 S	38˚11.80 W	3867
96	12/20	9:02	24˚45.60 S	38˚31.10 W	3785
97	12/20	10:59	24˚38.50 S	38˚50.20 W	3636
98	12/20	13:04	24˚31.80 S	39˚08.00 W	3475
99	12/20	15:49	24˚24.90 S	39˚26.70 W	3327
100	12/20	18:55	24˚17.10 S	39˚47.80 W	3090
101	12/20	21:13	24˚10.90 S	40˚03.90 W	3034
102	12/20	23:30	24˚05.50 S	40˚19.00 W	2955
103	12/21	2:19	23˚59.20 S	40˚36.20 W	2755
104	12/21	5:27	23˚52.90 S	40˚53.30 W	2228
105	12/21	6:52	23˚49.30 S	41˚02.00 W	1860
106	12/21	8:28	23˚46.30 S	41˚11.20 W	1355

7.3.3 Mooring Activities

7.3.3.1 Sound Source Moorings

Sta. No.	Ext No.	Int No.	Date 1992	Latitude	Longitude	Depth (m)	Nr. of Instr.	Remarks
556	K1	351	11/25	28˚49.7 S	44˚26.3 W	3705	SoSo 79 MAFOS 11	launched window 1.30 UTC watch dog 5509, CB
583	K2	350	12/6	31˚07.5 S	39˚54.1 W	3807	SoSo 49 MAFOS 12	launched window 0.30 UTC watch dog 5514, CB
603	K0	352	12/11	34˚18.9 S	28˚30.0 W	4054	SoSo 71	launched window 1.30 UTC watch dog 5510, CB
616	K3	349	12/18	26˚52.0 S	34˚47.2 W	4864	SoSo 68 3ACM	launched window 1.00 UTC watch dog 5508,CB,fl

7.3.3.2 Current Meter Moorings

Sta. No.	Ext No.	Int No.	Date	Latitude	Longitude	Depth (m)	Nr. of Instr.	Remarks
*1	BW	333	1/1/91	27˚54.1 S	46˚42.4 W	1179	1ADCP 4ACM	watch dog 15171
558			11/27/92					100% recovered
*8	BM	334	1/2/91	27˚59.2 S	46˚20.5 W	2187	5ACM	
557			11/27/92					100% recovered
*12	BE	335	1/3/91	28˚16.2 W	45˚13.8 W	3258	1ADCP 6ACM	watch dog 15172
550			11/26/92					100% recovered
*16	DB1	906	1/4/91	28˚28.0 S	44˚27.8 W	3633	5VACM 1XPonder	watch dog +CB ok
575			12/3/92					100% recovered
*20	DB2	907	1/5/91	29˚02.6 S	43˚29.0 W	3953	5VACM 1XPonder	watch dog +CB ok
576			12/4/92					100% recovered
*24	DB3	908	1/6/91	29˚32.0 S	42˚42.2 W	4017	2VACM 1XPonder	CB def.
577			12/4/92					100% recovered
*28	DB4	909	1/7/91	30˚05.2 S	41˚44.2 W	3798	5VACM 1XPonder	watch dog + CB ok
579			12/5/92					100% recovered
*32	DB5	910	1/8/91	30˚35.3 S	40˚47.3 W	3720	2VACM 1XPonder	CB
580			12/5/92					not recovered
*36	VW	336	1/9/91	31˚12.3 S	39˚46.0 W	3965	5ACM	CB ok
584			12/6/92					100% recovered
*37	VM	337	1/9/91	31˚09.8 S	39˚26.5 W	4637	3ACM	CB no response
590			12/7/92					lost

Sta. No.	Ext No.	Int No.	Date	Latitude	Longitude	Depth (m)	Nr. of Instr.	Remarks
*40	VE	338	1/11/91	31˚08.4 S	39˚26.0 W	4646	7ACM	CB dual release
585			12/6/92					100% recovered
*39	DB6	912	1/11/91	31˚05.1 S	39˚09.1 W	4140	3VACM 1XPonder	CB
591			12/7/92					100% recovered
*44	DBK	343	1/12/91	31˚09.3 S	38˚49.6 W	3652	5ACM 1XPonder	CB ok
592			12/7/92					100% recovered
*38	DBK'343' 911		1/10/91	31˚06.5 S	38˚47.5 W	3599	1VACM 1release	lost during deployment
593			12/7/92					confirmed
602	H1	353	12/11/92	34˚15.5 S	28˚52.3 W	4112	6ACM 1MAFOS	launched 10 CB
604	H2	354	12/12/92	34˚25.5 S	27˚51.6 W	4292	2ACM	launched CB
605	H3	355	12/12- 14/92	appr 1500 m SSW of (34˚22.4 S	27˚42.3 W)	(4436)	5ACM	launch interrupt. by unexpected storm, no CB, dual release
606	H4	356	12/14/92	34˚30.8 S	27˚19.2 W	4336	2ACM 200mThCh	launched CB
607	H5	357	12/14/92	34˚35.1 S	27˚03.4 W	4836	2ACM 200mThCh	launched CB, flash
609	H6	358	12/15/92	34˚32.3 S	26˚58.5 W	4303	ADCP 5ACM	launched watch dog 5506, CB dual release
612	R	363	12/16/92	31˚37.1 S	28˚48.6 W	3719 (-3750)	2ACM	launched CB

* = M 15/1 (siehe: Siedler, G. und W. Zenk (1992): WOCE Südatlantik 1991, Reise Nr. 15, 30. Dezember 1990 - 23. März 1991. METEOR-Berichte, Universität Hamburg, 92-1, 126 S.)

Acronyms:

ADCP	Acoustic Doppler Current Profiler
ACM	Aanderaa current meter
CB	bouy radio transmitter (CB radio)
VACM	Vector averaging current meter
ThCh	Thermistor chain
XPonder	transponder

7.3.4 RAFOS Floats and MAFOS Activities

7.3.4.1 RAFOS Floats

Sta No.	Float IfM	Date 1992	Time UTC	Latitude	Longitude	Depth (m)	ARGOS (DecNr)	Duration (month)	Remarks
540	63	11/20	13:07	13˚56.91 S	36˚16.44 W	4343 (6837)	6AD7A	9	trop. ocean
545	65	11/24	19:36	26˚28.57 S	42˚03.32 W	2587 (6839)	6ADDC	9	BrasC
575	67	12/03	21:28	28˚27.08 S	44˚27.68 W	3627 (6841)	6AE5B	9	DB1
577	66	12/04	20:28	29˚30.87 S	42˚42.14 W	4017 (6840)	6AE08	3	DB3
580	68	12/05 12/11	21:25	30˚34.92 S	40˚42.14 W	3728	6AEAE (6842)	[12] surfaced	DB5
595	70	12/08	13:51	31˚12.0 S	39˚21.0 W	4558 (12627)	C54F1	6	Vema 1
595	71	12/08	13:55	31˚11.8 S	39˚21.1 W	4557 (6844)	6AF17	9	Vema 2
597	72	12/09	6:20	31˚40.0 S	37˚45.2 W	4035 (6845)	6AF44	3	RioG W
598	74	12/09	18:20	32˚13.9 S	35˚50.0 W	2667 (6847)	6AFE2	12	RioG M
599	75	12/10	4:39	32˚46.0 S	33˚54.9 W	4000 (6848)	6B00E	6	RioG E
600	77	12/10	14:11	33˚19.0 S	31˚59.9 W	4152 (7461)	74966	9	RioG/Hunt
601	76	12/10	1:09	33˚51.0 S	30˚53.6 W	5152 (6849)	6B05D	3	Deep VlyS
607	80	12/15	2:00	34˚36.78 S	27˚01.28 W	4249	74A14 (7464)	12	Hunter

Sta No.	Float IfM	Date 1992	Time UTC	Latitude	Longitude	Depth (m)	ARGOS (DecNr)	Duration (month)	Remarks
610	81	12/16	2:14	33˚39.71 S	27˚32.01 W	4080 (7465)	74A47	6	Hunter N
611	82	12/16	9:30	32˚30.22 S	28˚17.30 W	4026 (7466)	74AB2	9	Hunter-R
612	84	12/16	21:12	31˚38.06 S	28˚47.61 W	3828 (7468)	74B0B	3	RioGrRise
613	86	12/17	13:18	30˚10.55 S	31˚15.02 W	4070 (7470)	74BAD	12	DeepVlyN
614	87	12/18	5:11	28˚17.80 S	33˚30.10 W	3590 (12616)	C5215	6	RioGrR N
615	88	12/18	14:03	27˚22.93 S	34˚14.35 W	4220 (12617)	C5246	9	DeepBasE
616	89	12/18	1:09	26˚53.0 S	34˚47.4 W	4772 (12618)	C52B3	3	Vema Ext
617	91	12/19	13:19	25˚49.8 S	35˚40.1 W	4169 (12620)	C530A	12	DeepBasM
618	90	12/19	23:12	25˚21.49 S	36˚54.49 W	4191	C52E0 (12619)	6	DeepBasW

7.3.4.2 MAFOS Monitors

Sta No.	No. IfM	Date 1992	Time UTC	Latitude	Longitude	Deployment Depth (m)	Mooring	Duration (days)
K1	M11	11/25	15:13	28˚43.7 S	44˚26.3 W	900	SoSo79	650
K2	M12	12/06	10:11	31˚07.5 S	39˚54.1 W	900	SoSo49	650
H1	M10	12/11	13:50	34˚15.5 S	28˚52.3 W	850	CM Mooring	650

7.3.5 Drifter Activities M 22/3-4

Stat No.	Drifter (ARGOS)	Date 1992	Time UTC	Latitude	Longitude	Temp (˚C)	Depth (m)	Remarks
575	15182	12/ 3	21:38	28˚27.0 S	44˚27.6 W	21.7	3636	close to DB1
577	15186	12/ 4	20:35	29˚30.7 S	42˚42.1 W	21.1	4017	close to DB3
580	15178	12/ 5	21:34	30˚34.7 S	40˚45.8 W	20.9	3706	close to DB5
585	15181	12/ 6	20:50	31˚06.4 S	39˚25.0 S	19.9	4638	1Vema Channel
595	11331	12/ 8	13:59	31˚11.6 S	39˚21.1 W	19.7	4568	2Vema Channel
597	11303	12/ 9	6:33	31˚39.7 S	37˚45.4 W	19.5	4036	Rio Gr R West
600	11326	12/10	14:18	33˚18.9 S	31˚59.9 W	18.5	4152	Rio Gr R/Hunt
601	11327	12/10	1:15	33˚51.1 S	30˚53.5 W	18.4	5146	Deep Valley
603	11319	12/11	0:19	34˚17.5 W	28˚30.2 W	19.0	4045	Hunter K0
604	11301	12/12	13:40	34˚25.5 S	27˚51.3 W	18.8	4300	Hunter H3
607	11333	12/15	2:00	34˚36.8 S	27˚01.2 W	17.7	4305	Hunter H5
609	11318	12/15	20:10	34˚32.1 S	26˚58.5 W	17.9	4310	Hunter H6
616	15184	12/18	1:14	26˚52.0 S	34˚47.5 W	22.9	4770	K3
617	15185	12/19	13:30	25˚49.9 S	35˚39.9 W	23.8	4167	DeepB M E
618	11316	12/19	23:17	25˚21.5 S	36˚54.5 W	24.3	4190	DeepB M W
619	12269	12/20	7:43	24˚50.4 S	38˚15.2 W	24.0	3873	DeepB W

7.3.6 List of XCP Launches

Sta. No.	XCP No.	XCP S/N	Date 1992	Time UTC	Latitude	Longitude	Depth (m)
618	1	92061006	12/19	23:40	25˚20.7 S	36˚56.6 W	4202
619	2	92061013	12/20	7:44	24˚50.3 S	38˚18.5 W	3866
-	3	92071017	12/20	11:25	24˚37.7 S	38˚52.5 W	3629
-	4	92071018	12/20	15:45	24˚24.9 S	39˚20.0 W	3400
-	5	92041007	12/20	21:30	24˚10.0 S	40˚02.0 W	3033
-	6	92061008	12/20	23:10	24˚05.4 S	40˚18.9 W	2966
-	7	92061017	12/21	2:14	23˚59.0 S	40˚36.0 W	2793
-	8	92061015	12/21	5:12	23˚52.8 S	40˚53.0 W	2232
-	9	92061014	12/21	8:18	23˚46.1 S	41˚11.0 W	1468

7.4 Leg M 22/5

7.4.1 List of CTD Stations

Station No.	Date 1992/ 1993	Start UTC	End UTC	Latitude	Logitude	Depth (m)	NS	F	He	O_2	Nut	CO_2	Alk	Tr	S	C14	pH
620	12/28	14:10	16:13	25˚39.0 S	42˚10.5 W	2299	X	X	X	X	X	X	X		X		
621		19:04	23:07	25˚58.9 S	42˚35.5 W	2420		X	X	X	X				X		
622	12/30	6:14	7:48	27˚43.5 S	47˚23.0 W	179	X			X	X	X			X		
623		8:55	10:02	27˚46.2 S	47˚12.2 W	327	X	X	X	X	X	X	X		X		
624		11:13	12:20	27˚45.6 S	47˚13.0 W	535	X			X	X	X			X		
625		13:32	16:20	27˚51.6 S	46˚50.7 W	758	X	X	X	X	X	X			X		
626		17:20	20:36	27˚54.5 S	46˚40.0 W	1257	X			X	X				X		
627		21:40	0:08	27˚57.1 S	46˚29.1 W	1699	X	X	X	X	X	X	X	X	X		
628	12/31	1:47	5:10	27˚59.9 S	46˚18.4 W	2226	X			X	X	X			X		
629		6:08	10:00	28˚02.6 S	46˚07.6 W	2422	X	X		X	X	X			X		
630		10:57	15:10	28˚05.4 S	45˚56.7 W	2603	X			X	X				X		
631		16:30	20:27	28˚09.4 S	45˚40.6 W	2793	X	X	X	X	X	X	X	X	X		
632		21:53	0:02	28˚13.6 S	45˚24.5 W	2970		X		X	X				X		
001	1/01	6:00	8:44	28˚24.7 S	44˚48.1 W	3482	X	X		X	X	X			X		
002		12:15	15:00	28˚37.0 S	44˚13.0 W	3699	X			X	X	X			X		
003		18:46	22:42	28˚50.0 S	43˚35.0 W	3892	X	X	X	X	X	X	X	X	X		
004	1/02	2:35	6:00	29˚01.8 S	42˚55.9 W	4003	X			X	X				X		
005		9:30	13:30	29˚13.2 S	42˚21.7 W	4002	X	X		X	X	X			X		
006		16:50	20:05	29˚24.9 S	41˚46.0 W	3925	X			X	X	X			X		
007		23:30	3:15	29˚36.4 S	41˚11.0 W	3902	X	X	X	X	X	X	X	X	X	X	
008	1/03	6:48	10:28	29˚47.9 S	40˚36.4 W	3779	X	X	X	X	X				X		

Station No.	Date 1992/ 1993	Start UTC	End	Latitude	Logitude	Depth (m)	NS	F	He	O_2	Nut	CO_2	Alk	Tr	S	C14	pH
009		13:38	15:55	29˚59.5 S	40˚01.5 W	3193	X	X		X	X	X			X		
010		18:50	22:27	30˚00.1 S	39˚31.8 W	3962		X	X	X	X			X	X		
011	1/4	0:00	4:25	30˚00.2 S	39˚21.0 W	4896	X	X	X	X	X	X	X	X	X	X	
012		6:54	11:02	30˚00.0 S	38˚55.0 W	4275		X		X	X				X		
013		13:00	16:25	30˚00.0 S	38˚31.3 W	4227	X	X	X	X	X	X		X	X		
014		19:03	22:22	30˚00.1 S	38˚00.2 W	3850		X	X	X	X				X		
015	1/5	0:55	3:20	30˚00.0 S	37˚31.4 W	3348	X	X	X	X	X	X	X	X	X		
016		5:10	7:14	30˚00.0 S	37˚10.1 W	2341				X	X				X		
017		8:53	10:53	29˚59.9 S	36˚51.4 W	1698	X	X		X	X	X			X		
018		12:30	13:55	30˚00.1 S	36˚29.8 W	1788				X	X				X		
019		15:30	16:25	30˚00.0 S	36˚11.5 W	788	X			X	X				X		
020		18:00	21:52	30˚00.1 S	35˚58.5 W	2400		X	X	X	X	X		X	X		
021		22:31	0:45	30˚00.0 S	35˚31.0 W	2514	X			X	X				X		
022	1/6	2:25	4:15	30˚00.0 S	35˚10.0 W	2153				X	X				X		
023		5:45	8:04	30˚00.0 S	34˚51.6 W	1655	X			X	X				X		
024		9:50	11:17	30˚00.0 S	34˚30.0 W	1432		X	X	X	X	X	X	X	X		
025		13:40	15:35	30˚00.0 S	34˚01.5 W	1960	X			X	X				X		
026		18:20	20:45	29˚59.9 S	33˚30.0 W	3158		X	X	X	X	X		X	X		
027		23:23	2:30	29˚59.9 S	33˚01.5 W	3517	X			X	X				X		
028	1/7	5:30	9:00	30˚00.0 S	32˚30.0 W	3750		X		X	X	X	X		X		
029		11:38	14:50	29˚59.9 S	32˚01.5 W	3823	X			X	X				X		
030		17:37	20:53	30˚00.0 S	31˚30.1 W	3867		X	X	X	X	X		X	X		
031		23:15	2:30	30˚00.0 S	31˚01.2 W	4073	X	X	X	X	X	X		X	X	X	
032	1/8	5:14	8:23	30˚00.0 S	30˚30.0 W	3943		X		X	X	X	X		X		
033		10:56	14:10	30˚00.0 S	30˚00.9 W	3320	X			X	X				X		

Station No.	Date 1992/ 1993	Start UTC	End UTC	Latitude	Logitude	Depth (m)	NS	F	He	O_2	Nut	CO_2	Alk	Tr	S	C14	pH
034		17:20	19:14	30°00.0 S	29°30.0 W	2260		X	X	X	X	X		X	X		
035	1/9	4:45	7:23	29°59.3 S	29°02.0 W	3199	X			X	X				X		
036		10:12	13:10	29°59.8 S	28°25.1 W	3770		X	X	X	X	X	X		X		
037		17:20	21:25	29°59.9 S	27°35.7 W	4882	X	X		X	X				X		
038	1/10	1:40	5:12	30°00.0 S	26°43.0 W	5317		X	X	X	X	X		X	X		
039		9:22	13:00	29°59.9 S	25°53.3 W	4402	X			X	X				X		
040		17:00	23:29	30°00.0 S	25°01.0 W	5525		X	X	X	X	X	X	X	X		
041	1/11	3:40	7:26	30°00.0 S	24°11.7 W	5038	X			X	X				X		
042		11:44	14:45	30°00.0 S	23°18.9 W	4612		X	X	X	X	X		X	X	X	
043		18:54	22:48	29°59.9 S	22°30.6 W	4586	X			X	X				X		
044	1/12	3:15	6:43	30°00.0 S	21°37.0 W	4845		X	X	X	X	X	X	X	X		
045		11:11	14:52	30°00.0 S	20°47.6 W	4897	X			X	X				X		
046		19:08	22:40	29°59.9 S	19°55.0 W	4803		X	X	X	X	X		X	X		
047	1/13	2:40	8:20	29°59.7 S	19°05.5 W	4105	X	X		X	X				X		
048		11:42	15:00	30°00.1 S	18°22.9 W	4182		X		X	X	X	X		X		
049	1/14	4:00	7:33	30°00.0 S	17°43.6 W	3996	X			X	X				X		
050		10:52	13:25	30°00.0 S	17°01.0 W	3672		X	X	X	X	X		X	X		
051		16:32	19:55	30°00.0 S	16°21.7 W	3519	X			X	X				X		
052		23:13	1:12	30°00.1 S	15°40.0 W	3280		X	X	X	X	X	X		X		
053	1/15	4:31	8:15	30°00.0 S	15°01.6 W	3821	X			X	X				X		
054		11:48	13:55	30°00.0 S	14°19.9 W	2883		X	X	X	X	X		X	X		
055		17:12	19:23	30°00.2 S	13°42.1 W	2291	X			X	X				X		
056		22:40	0:50	30°00.0 S	12°59.6 W	3101		X		X	X	X	X		X		
057	1/16	4:12	7:27	30°00.0 S	12°21.9 W	3266	X	X		X	X				X		
058		11:07	12:55	30°00.0 S	11°40.5 W	3479		X	X	X	X	X		X	X		

Station No.	Date 1992/ 1993	Start	End	Latitude	Logitude	Depth (m)	NS	F	He	O_2	Nut	CO_2	Alk	Tr	S	C14	pH
		UTC															
059		16:53	20:07	30°00.0 S	11°01.8 W	3550	X	X		X	X				X		
060		23:18	1:55	30°00.0 S	10°19.8 W	3784		X		X	X	X	X		X		
061	1/17	5:05	8:25	30°00.0 S	09°42.0 W	3935	X	X		X	X				X		
062		11:42	14:25	30°00.0 S	08°59.9 W	3970		X	X	X	X	X		X	X		
063		18:13	21:37	30°00.0 S	08°11.9 W	3940	X	X		X	X				X		
064	1/18	1:30	5:00	30°00.0 S	07°20.0 W	4167		X	X	X	X		X		X		
065		8:48	14:50	30°00.0 S	06°31.5 W	4279	X	X	X	X	X				X		
066		19:01	22:16	30°00.0 S	05°40.0 W	4386		X	X	X	X	X		X	X		
067	1/19	2:00	5:48	30°00.0 S	04°51.7 W	4277	X	X	X	X	X				X		
068		9:54	12:30	29°59.8 S	04°00.0 W	3986		X	X	X	X	X	X		X		
069		16:32	20:25	30°00.0 S	03°12.0 W	4440	X		X	X	X			X	X		
070	1/20	00:15	03:50	30°00.0 S	02°21.7 W	4403	X	X	X	X	X	X		X	X	X	
071		07:51	11:40	30°00.0 S	01°31.5 W	4481	X	X	X	X	X			X	X		
072		16:05	19:36	30°00.9 S	00°43.9 W	4852		X	X	X	X	X	X	X	X		
073		23:00	2:15	30°00.0 S	00°02.0 W	4130	X	X	X	X	X				X		
074	1/21	5:25	7:41	29°51.9 S	00°34.0 E	3319		X	X	X	X	X		X	X		
075		10:28	13:25	29°44.3 S	01°06.4 E	3686	X	X		X	X				X		
076		16:30	19:13	29°36.1 S	01°42.0 E	3650		X	X	X	X	X		X	X		
077		21:55	0:00	29°28.3 S	02°14.8 E	2727	X			X	X				X		
078	1/22	3:16	6:42	29°20.0 S	02°50.0 E	4252		X	X	X	X	X	X	X	X		X
079		9:03	12:40	29°28.1 S	03°16.7 E	4707	X	X		X	X				X		
080		15:16	18:55	29°36.7 S	03°46.7 E	4926		X	X	X	X			X	X		
081	1/23	7:00	10:33	29°44.4 S	04°13.1 E	4952	X	X	X	X	X	X	X	X	X	X	X
082		15:04	19:00	29°45.0 S	05°06.0 E	5134		X		X	X				X		
083		23:00	3:18	29°45.0 S	05°54.0 E	5133	X	X		X	X	X			X		X

Station No.	Date 1992/ 1993	Start UTC	End UTC	Latitude	Logitude	Depth (m)	NS	F	He	O_2	Nut	CO_2	Alk	Tr	S	C14	pH
084	1/24	8:01	11:30	29°45.2 S	06°46.8 E	5185		X		X	X				X		
085		15:38	19:53	29°45.0 S	07°35.2 E	5178	X	X	X	X	X	X	X	X	X		X
086	1/25	0:45	4:26	29°45.0 S	08°28.0 E	5059		X		X	X				X		X
087		10:00	13:55	29°44.7 S	09°16.6 E	5023	X	X	X	X	X	X		X	X		
088		19:12	0:10	29°44.9 S	10°08.7 E	4884	X	X	X	X	X				X		X
089	1/26	4:48	8:29	29°45.0 S	10°56.8 E	4293	X	X	X	X	X	X	X	X	X		
090		13:00	18:06	29°45.0 S	11°47.3 E	4011	X	X		X	X				X		X
091		19:55	0:20	29°37.8 S	12°08.6 E	3840	X	X	X	X	X	X		X	X		
092	1/27	2:13	7:34	29°30.6 S	12°26.3 E	3677	X			X	X				X		
093		9:12	13:23	29°23.2 S	12°46.0 E	3398	X	X	X	X	X	X	X	X	X		
094		15:07	18:58	29°15.7 S	13°04.2 E	3135	X			X	X				X		X
095		20:36	23:55	29°08.1 S	13°23.5 E	2711	X	X	X	X	X	X		X	X		
096	1/28	1:40	03:56	29°00.7 S	13°42.1 E	2223	X			X	X				X		
097		5:57	07:32	28°53.3 S	14°01.2 E	1607	X	X	X	X	X	X	X	X	X		
098		9:34	10:25	28°45.6 S	14°20.4 E	531	X			X	X				X		X
099		12:05	12:55	28°38.1 S	14°39.5 E	160	X			X	X	X			X		
100		14:27	15:20	28°30.7 S	14°58.2 E	177	X										

NS : Neustron net
F : Freon
He : Helium
O_2 : Oxygen
Nut: Nutreon
CO_2: CO_2
Alk: Alkalinity
Tr : Tritium
S : Salinity
C14: C14
pH : pH

7.4.2 List of XBT Drops

Profile No.	Date 1992	Time UTC	Latitude	Longitude	Depth (m)
107	12/28	1:05	23˚38.1 S	42˚50.5 W	122m
108	12/28	1:30	23˚42.5 S	42˚48.4 W	144m
109	12/28	2:00	23˚47.2 S	42˚46.2 W	210m
110	12/28	2:30	23˚52.6 S	42˚43.9 W	756m
111	12/28	3:00	23˚57.2 S	42˚41.9 W	825m
112	12/28	3:30	24˚01.9 S	42˚39.7 W	902m
113	12/28	4:00	24˚07.0 S	42˚37.5 W	937m
114	12/28	4:30	24˚11.4 S	42˚35.6 W	854m
115	12/28	5:00	24˚15.9 S	42˚33.5 W	910m
116	12/28	5:30	24˚20.5 S	42˚31.4 W	915m
117	12/28	6:00	24˚25.2 S	42˚29.3 W	1592m
118	12/28	6:30	24˚20.0 S	42˚27.2 W	1674m
119	12/28	7:00	24˚34.5 S	42˚25.2 W	1973m
120	12/28	7:30	24˚39.2 S	42˚23.0 W	2019m
121	12/28	8:00	24˚43.7 S	42˚21.1 W	2094m
122	12/28	8:30	24˚48.5 S	42˚18.9 W	2135m
123	12/28	9:00	24˚53.4 S	42˚16.9 W	2328m
124	12/28	9:30	24˚58.0 S	42˚14.6 W	2216m
125	12/28	10:00	25˚02.9 S	42˚12.6 W	2235m
126	12/28	10:30	25˚07.6 S	42˚10.4 W	2168m
127	12/28	11:00	25˚12.4 S	42˚08.0 W	2187m
128	12/28	11:30	25˚17.2 S	42˚05.7 W	2237m
129	12/28	12:00	25˚22.2 S	42˚03.5 W	2293m
130	12/28	12:30	25˚26.4 S	42˚01.6 W	2593m
131	12/28	13:00	25˚31.5 S	42˚01.6 W	2328m
132	12/28	13:30	25˚35.1 S	42˚05.8 W	2333m
133	12/28	14:00	25˚38.8 S	42˚10.2 W	2284m
134	12/29	17:30	28˚15.9 S	45˚15.3 W	3135m
135	12/29	18:00	28˚14.5 S	45˚20.6 W	3083m
136	12/29	18:30	28˚13.0 S	45˚26.6 W	2945m
137	12/29	19:00	28˚11.6 S	45˚31.7 W	2859m
138	12/29	19:30	28˚10.3 S	45˚37.5 W	2824m
139	12/29	20:00	28˚08.8 S	45˚42.8 W	2778m
140	12/29	20:30	28˚07.3 S	45˚48.8 W	2727m
141	12/29	21:00	28˚06.1 S	45˚53.9 W	2649m

Profile No.	Date 1992	Time UTC	Latitude	Longitude	Depth (m)
142	12/29	21:30	28˚04.6 S	45˚59.8 W	2556m
143	12/29	22:00	28˚03.2 S	46˚05.8 W	2456m
144	12/29	22:30	28˚01.7 S	46˚11.5 W	2364m
145	12/29	23:00	28˚00.3 S	46˚17.2 W	2267m
146	12/29	23:30	27˚58.9 S	46˚23.0 W	2053m
147	12/29	24:00	27˚57.4 S	46˚28.9 W	1715m
148	12/30	0:30	27˚56.1 S	46˚34.3 W	1457m
149	12/30	1:00	27˚54.5 S	46˚40.4 W	1239m
150	12/30	1:30	27˚53.1 S	46˚46.3 W	986m
151	12/30	2:00	27˚51.7 S	46˚51.7 W	721m
152	12/30	2:30	27˚50.1 S	46˚57.9 W	595m
153	12/30	3:00	47˚03.6 S	47˚03.6 W	513m
154	12/30	3:30	27˚47.3 S	47˚09.1 W	400m
155	12/30	4:00	27˚45.8 S	47˚14.8 W	271m
156	12/30	4:30	27˚44.4 S	47˚20.3 W	200m
157	12/30	5:00	27˚42.9 S	47˚26.3 W	157m
159	12/30	5:30	27˚41.6 S	47˚29.9 W	146m
159	1/09	15:23	30˚00.0 S	28˚00.0 W	4529m
160	1/09	23:33	30˚00.0 S	27˚09.2 W	4727m
39	1/10	7:25	29˚59.9 S	26˚10.1 W	-
162	1/10	15:00	30˚00.0 S	25˚27.0 W	4555m
163	1/11	1:41	30˚00.0 S	24˚36.0 W	4775m
164	1/11	9:35	30˚00.0 S	23˚44.9 W	4746m
165	1/11	17:07	29˚59.8 S	22˚53.2 W	-
166	1/12	1:00	30˚00.0 S	22˚03.0 W	4646m
167	1/12	9:05	30˚00.2 S	21˚11.9 W	4789m
168	1/12	17:00	30˚00.0 S	20˚21.0 W	-
169	1/13	0:45	30˚00.0 S	19˚30.0 W	4538m
170	1/13	9:54	30˚00.0 S	18˚44.2 W	3800m
171	1/13	20:36	30˚00.0 S	18˚01.3 W	4206m
172	1/14	9:12	30˚00.0 S	17˚20.8 W	3973m
173	1/14	15:05	30˚00.0 S	16˚40.0 W	3466m
174	1/14	21:34	30˚00.0 S	16˚00.0 W	3828m
175	1/15	3:00	30˚00.0 S	15˚20.0 W	3142m
176	1/15	10:05	30˚00.0 S	14˚39.8 W	3426m
177	1/15	15:45	30˚00.0 S	14˚00.0 W	2480m

Profile No.	Date 1992	Time UTC	Latitude	Longitude	Depth (m)
178	1/15	20:59	30˚00.0 S	13˚19.8 W	2843m
179	1/16	2:45	30˚00.0 S	12˚40.0 W	3152m
180	1/16	9:24	30˚00.0 S	11˚59.9 W	3552m
181	1/16	15:30	30˚00.0 S	11˚20.0 W	3452m
182	1/16	21:37	30˚00.0 S	10˚39.9 W	3741m
183	1/17	3:40	30˚00.0 S	10˚00.0 W	3830m
184	1/17	10:00	30˚00.0 S	09˚19.8 W	3850m
185	1/17	16:30	30˚00.0 S	08˚34.1 W	4002m
186	1/17	23:33	30˚00.0 S	07˚43.6 W	4069m
187	1/18	6:58	30˚00.0 S	06˚55.0 W	-
188	1/18	17:05	30˚00.0 S	06˚05.0 W	4384m
189	1/19	0:15	30˚00.0 S	05˚15.0 W	4541m
190	1/19	7:47	30˚00.0 S	04˚24.9 W	4382m
191	1/19	14:40	30˚00.0 S	03˚35.0 W	4310m
192	1/19	22:28	30˚00.1 S	02˚44.5 W	4560m
193	1/20	4:52	29˚59.6 S	02˚06.0 W	4439m
194	1/20	5:52	30˚00.0 S	01˚54.0 W	4665m
195	1/20	6:50	30˚00.0 S	01˚43.4 W	4755m
196	1/20	13:40	30˚00.0 S	01˚05.0 W	4602m
197	1/20	21:30	30˚00.6 S	00˚19.8 W	4407m
198	1/21	3:49	29˚56.0 S	00˚17.0 E	3323m
199	1/21	09:08	29˚47.9 W	00˚51.0 E	3266m
200	1/21	14:55	29˚40.0 S	01˚25.0 E	3743m
201	1/21	20:38	29˚32.0 S	01˚59.3 E	2306m
202	1/22	1:45	29˚24.0 S	02˚33.0 E	1962m
203	1/23	12:53	29˚45.0 S	04˚41.0 E	4891m
204	1/23	21:07	29˚45.0 S	05˚32.3 E	5113m
205	1/24	5:43	29˚45.0 S	06˚22.0 E	5187m
206	1/24	13:50	29˚45.0 S	07˚13.0 E	5182m
208	1/24	22:14	29˚45.0 S	08˚03.3 E	5131m
209	1/25	7:24	29˚45.0 S	08˚54.2 E	5044m
210	1/25	16:32	29˚45.0 S	09˚44.0 E	4942m
211	1/26	2:20	29˚45.0 S	10˚34.0 E	4580m
212	1/26	2:25	29˚45.0 s	10˚34.8 E	
213	1/26	10:54	29˚45.0 S	11˚24.5 E	4129m

Profile No.	Date 1992	Time UTC	Latitude	Longitude	Depth (m)
214	1/26	18:21	29˚45.0 S	11˚53.0 S	3981m
215	1/26	18:34	29˚44.1 S	11˚54.3 E	3983m
216	1/26	19:01	29˚41.2 S	11˚59.8 E	3914m
217	1/27	0:50	29˚36.3 S	12˚12.3 E	3811m
218	1/27	1:00	29˚36.7 S	12˚13.1 E	3800m
219	1/27	1:30	29˚33.8 S	12˚18.5 E	3749m
220	1/27	7:49	29˚28.8 S	12˚30.6 E	3691m
221	1/27	7:56	29˚28.4 S	12˚31.5 E	3724m
222	1/27	8:28	29˚26.3 S	12˚37.7 E	3536m
223	1/27	13:48	29˚21.2 S	12˚50.1 E	3330m
224	1/27	14:00	29˚20.7 S	12˚51.0 E	3320m
225	1/27	14:25	29˚18.8 S	12˚56.5 E	3230m
226	1/27	19:12	29˚13.2 S	13˚08.2 E	3080m
227	1/27	19:22	29˚12.8 S	13˚09.2 E	3052m
228	1/27	19:55	29˚11.3 S	13˚15.7 E	2711m
229	1/8	0:15	29˚06.8 S	13˚27.0 E	2629m
230	1/8	0:25	29˚06.3 S	13˚28.0 E	2607m
231	1/8	1:00	29˚03.8 S	13˚34.5 E	2390m
232	1/8	4:15	29˚00.1 S	13˚44.0 E	2154m
233	1/8	4:24	28˚59.6 S	13˚44.9 E	2128m
234	1/8	5:12	28˚56.2 S	13˚53.7 E	1929m
235	1/8	7:45	28˚53.0 S	14˚03.3 E	1402m
236	1/8	7:50	28˚52.9 S	14˚03.6 E	1400m
237	1/8	8:42	28˚48.8 S	14˚12.7 E	1410m
238	1/8	11:22	28˚41.3 S	14˚31.5 E	185m

7.4.3 List of XCP Launches

Station No.	XCP No.	Date 1993	Time UTC	Latitude	Longitude	Depth (m)
625	10	12/30	16:10	27˚51.0 S	46˚50.0 W	772
626	11	12/30	20:30	27˚54.7 S	46˚38.6 W	1306
627	12	12/31	0:35	27˚56.9 S	46˚27.4 W	1789
629	13	12/31	9:56	28˚01.7 S	46˚05.9 W	2430
630	14	12/31	15:05	28˚05.3 S	45˚52.2 W	2650
631	15	12/31	20:19	28˚08.1 S	45˚37.2 W	2807
090	16	1/26	18:11	29˚45.1 S	11˚52.5 E	3982
091	17	1/27	0:35	29˚37.1 S	12˚12.3 E	3811
092	18	1/27	7:37	29˚29.1 S	12˚29.7 E	3659
093	19	1/27	13:30	29˚21.6 S	12˚50.3 E	3331
094	20	1/27	19:01	29˚13.5 S	13˚07.7 E	3091
095	21	1/28	0:00	29˚07.4 S	13˚26.9 E	2639
096	22	1/28	4:02	29˚00.3 S	13˚44.2 E	2150
097	23	1/28	7:36	28˚53.1 S	14˚02.9 E	1435

7.4.4 RAFOS Floats

Station No.	Float IfM	Date 1993	Time UTC	Latitude	Longitude	Depth (m)	ARGOS (DecNr)	Duration (month)	Remarks
12	93	1/04	11:02	30˚01.10 S	38˚54.70 W	4269	C53FF (12623)	[12] surfaced	

7.4.5 Drifter activities

Station No.	Drifter (ARGOS)	Date 1993	Time UTC	Latitude	Longitude	Depth (m)
053	11347	1/15	8:20	30˚00.2 S	15˚00.3 W	3835
057	11304	1/16	7:33	29˚59.3 S	12˚20.8 W	3136
062	11311	1/17	14:30	30˚02.3 S	08˚59.1 W	3987
066	1583	1/18	22:20	30˚00.2 S	05˚38.9 W	4441
069	11317	1/19	20:30	30˚00.8 S	03˚09.7 W	4351
073	15155	1/21	2:20	29˚59.6 S	00˚00.8 E	3902

7.4.6 List of lADCP Profiles

Station No.	Date 1992/ 1993	Time UTC	Wire-length (m)	Longitude	Latitude	Depth (m)
621	12/28	20:34	1200	25˚59.4 S	42˚35.0 W	2390
	12/29	17:22	ADCP section course 286, 11.0 kn	28˚16.0 S	45˚13.8 W	
625	12/30	14:35	550	27˚51.7 S	46˚51.0 W	746
626	12/30	18:52	1038	27˚54.3 S	46˚40.7 W	1232
627	12/30	23:04	1200	27˚56.7 S	46˚29.1 W	1692
628	12/31	03:35	1200	27˚59.1 S	46˚18.5 W	2212
629	12/31	08:14	1300	28˚02.1 S	46˚07.8 W	2418
630	12/31	13:28	1200	28˚05.2 S	45˚55.4 W	2616
631	12/31	18:36	1300	28˚08.6 S	45˚39.9 W	2799
90	1/26	16:53	1300	29˚45.2 S	11˚51.7 E	4000
91	1/26	23:05	1313	29˚37.6 S	12˚11.7 E	3812
92	1/27	06:22	1300	29˚29.4 S	12˚29.2 E	3648
93	1/27	12:20	1300	29˚22.1 S	12˚49.7 E	3342
94	1/27	17:48	1300	29˚14.2 S	13˚07.2 E	3103
95	1/27	22:45	1300	29.07.5 S	13˚26.0 E	2662

29.01. lADCP terminated due to technical problems

8 Concluding Remarks

The successful observations during METEOR cruise no. 22 could not have been achieved without the excellent assistance of the captains Müller and Kull, together with their crews. We also want to thank the members of the Leitstelle METEOR and particularly Embassador Wallau and Dr. Matthes of the German Embassy in Brasilia as well as General Consul Marquardt at the German Consulate in Recife for their most valuable help. The work was funded by the research contracts Si 111/39-1 of the Deutsche Forschungsgemeinschaft and 03F0050D of the Bundesministerium für Forschung und Technologie.

9 References

ANDRES, H.-G., H.-Ch. JOHN and C. ZELCK (1992): Biologische Ozeanographie und marine Taxonomie. In: SIEDLER, G. und W. ZENK: WOCE Südatlantik 1991, Reise Nr. 15,0B30. Dezember 1990 - 23. März 1991. Meteor-Berichte, Univ. Hamburg 92-1, 74-85.

ASPER, V. L. (1987): Measuring the flux and sinking speed of marine snow aggregates. Deep-Sea Res., 34, 1-17.

DHI (1971): Monatskarten für den südatlantischen Ozean. Nr. 2421. III Auflage, DHI, Hamburg.

HENTSCHEL, E. (1933): Allgemeine Biologie des südatlantischen Ozeans. I. Das Pelagial der obersten Wasserschicht. Wiss. Ergebn. dt. atlant. Exped. "Meteor" 1925-1927, 11, 1-168.

HINZ, K., L. HASSE und F. SCHOTT (1991): SUBTROPISCHER & TROPISCHER ATLANTIK, Reise Nr. 14/1-3, Maritime Meteorologie und Physikalische Ozeanographie, 17. September - 30. Dezember 1990. METEOR-Berichte, Universität Hamburg, 91-3, 58 pp.

HONJO, S., K.W. DOHERTY, Y.C. AGRAWAL and V.L. ASPER (1984): Direct optical assessment of large amorphous aggregates (marine snow) in the deep ocean. Deep-Sea Res., 31, 67-76.

HULLEY, P.A. (1981): Results of the research cruises of FRV "Walter Herwig" to South America. LVIII. Family Myctophidae (Osteichthyes, Myctophiformes). Arch. Fisch. Wiss. 31 (Beih. 1), 1-303.

LAMPITT, R.S. (1985): Evidence for seasonal deposition of detritus to the deep sea floor and its subsequent resuspension. Deep-Sea Res., 32, 885-897.

PARIN, N.V. (1970): Ichthyofauna of the epipelagic zone. Israel Program for Scientific Translations, Jerusalem, 1-205.

REID, J.L., (1989): On the total geostrophic circulation of the South Atlantik Ocean: Flow patterns, tracers, and transports. Progr. Oceanogr., 23, 149-244.

SIEDLER, G. und W. ZENK, (1992): WOCE Südatlantik 1991, Reise Nr. 15, 30. Dezember 1990 - 23. März 1991. METEOR-Berichte, Universität Hamburg, 92-1, 126 pp. (engl. translation available at IfMK).

SPEER, K. and W. ZENK (1993): On the flow of Antarctic Bottom Water across the Rio Grande Rise and beyond. Journ. Physical Oceanogr. (in press).

SPEER, K., W. ZENK, G. SIEDLER, J. PÄETZOLD and C. HEIDLAND, (1992): First resolution of flow through the Hunter Channel in the South Atlantic. Earth a. Planet. Sc. Letters, 113, 287-292.

World Meteorological Organization (1988): World Ocean Circulation Experiment Implementation
Plan, Vol. 1, WRCP-11 , WMO/TD No. 242

WÜST, G., (1935): Schichtung und Zirkulation des Atlantischen Ozeans. Die Stratosphäre. In: Wissenschaftliche Ergebnisse der Deutschen Atlantischen Expedition auf dem Forschungs- und Vermessungsschiff "Meteor" 1925 - 1927, 6. Lieferung 1. Teil, 2, 1-288.
(The stratosphere of the Atlantic Ocean, W.J. EMERY (Editor) 1978, Amerind, New Delhi, 1-112).

ZEMBA, J.C. (1991): The structure and transport of the Brazil Current between 27° and 36° South. Ph.D. Thesis MIT & WHOI, Cambridge and Woods Hole, 160 pp.

ZENK, W., K. SPEER and N. HOGG (1993): Bathymetry at the Vema Sill. Deep Sea Res., 40 (9), 1925-1933.

10 Figures

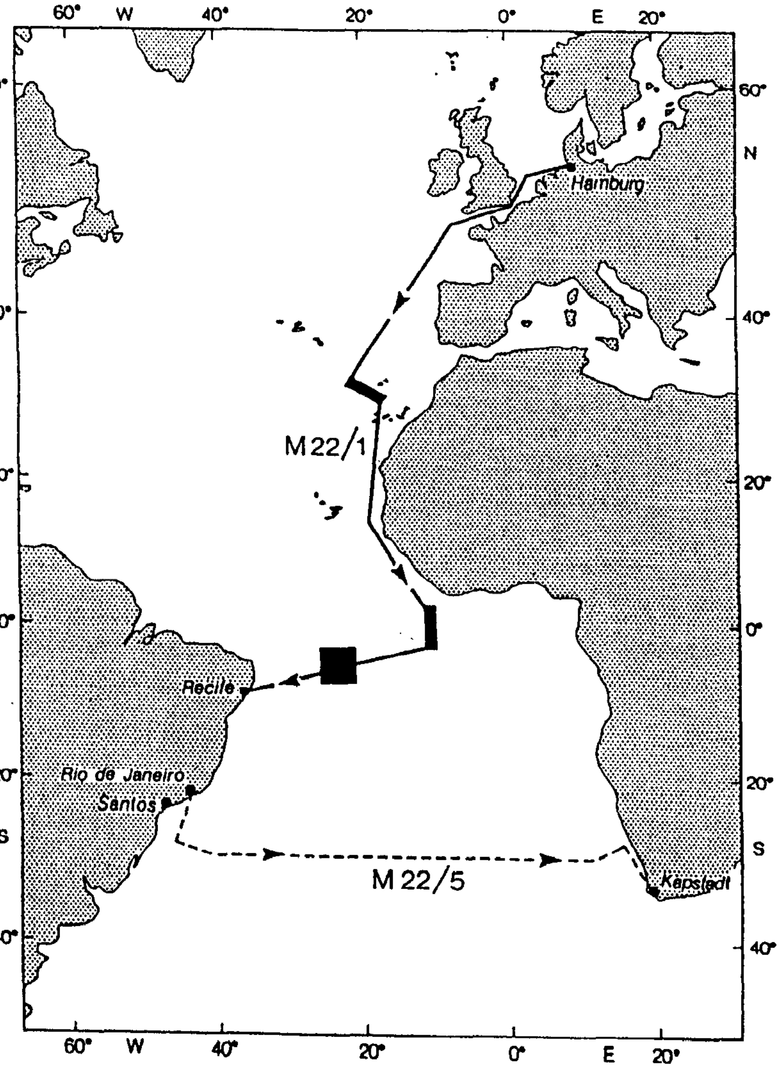

Fig. 1a: Track and working areas of METEOR cruise no. 22, legs 1 and 5

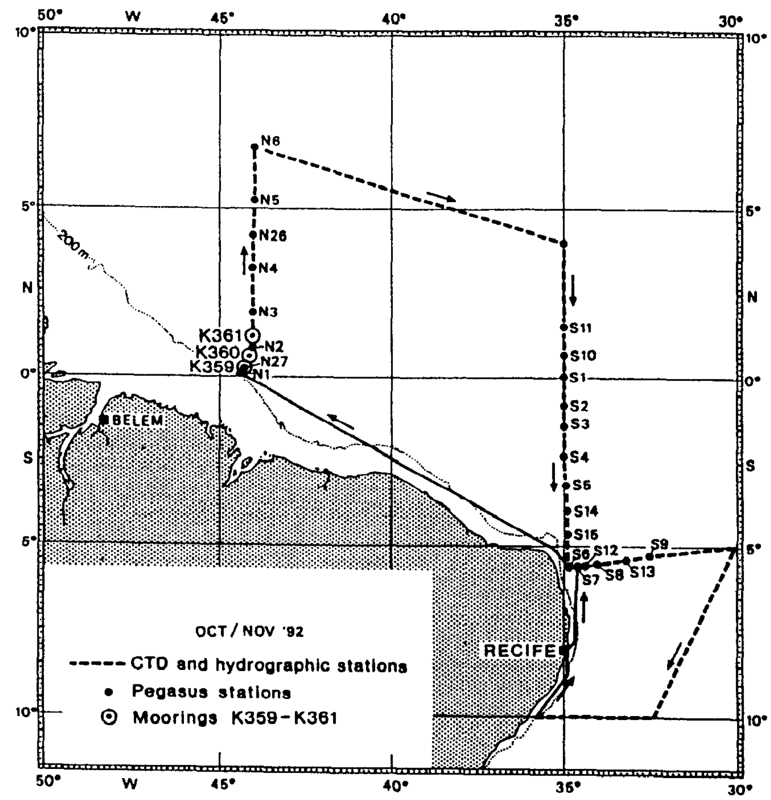

Fig. 1b: Cruise track and oceanographic stations, leg 2

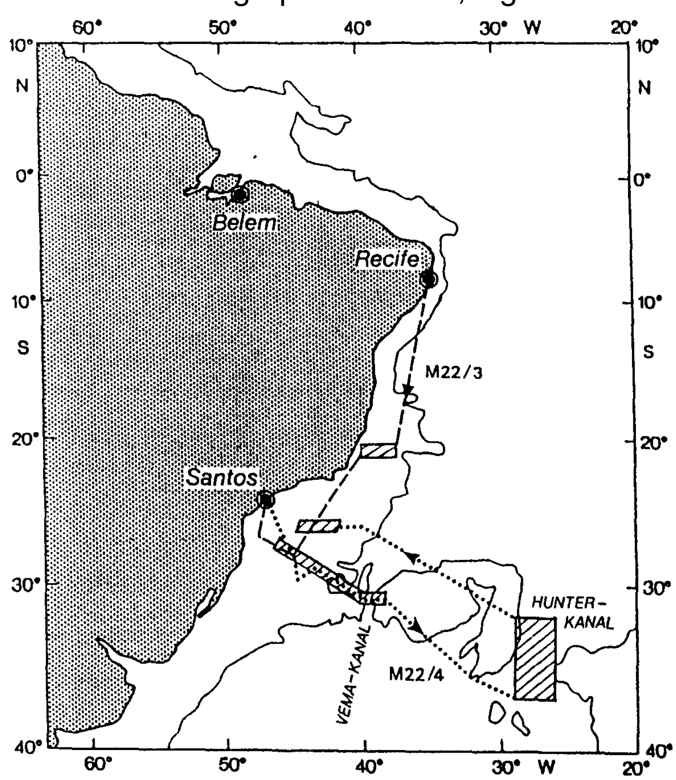

Fig. 1c: Cruise track and working areas, legs 3 and 4

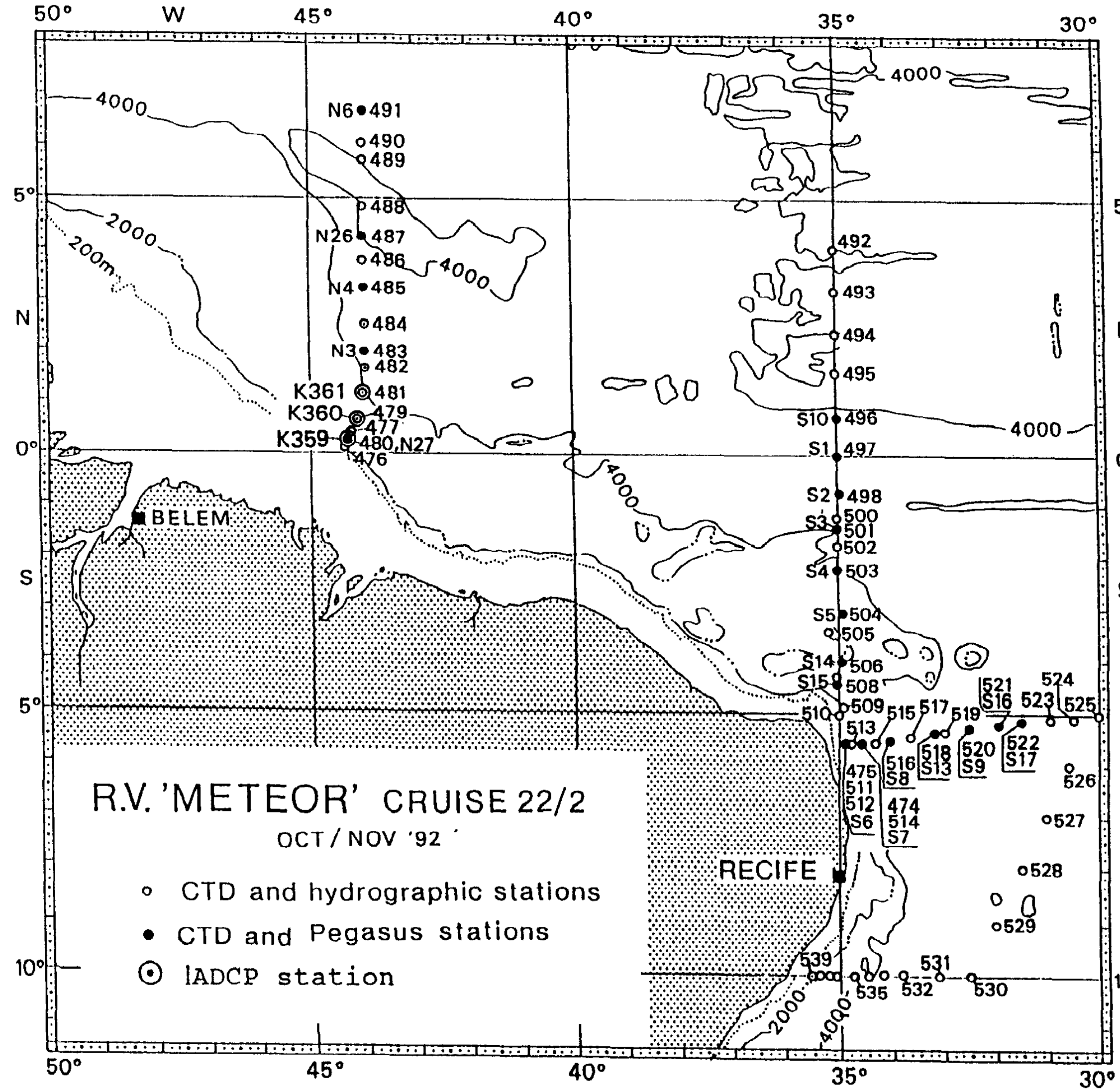

Fig. 1d: Cruise track METEOR 22/2
CTD/IADCP and Pegasus stations, the positions of the moorings are included

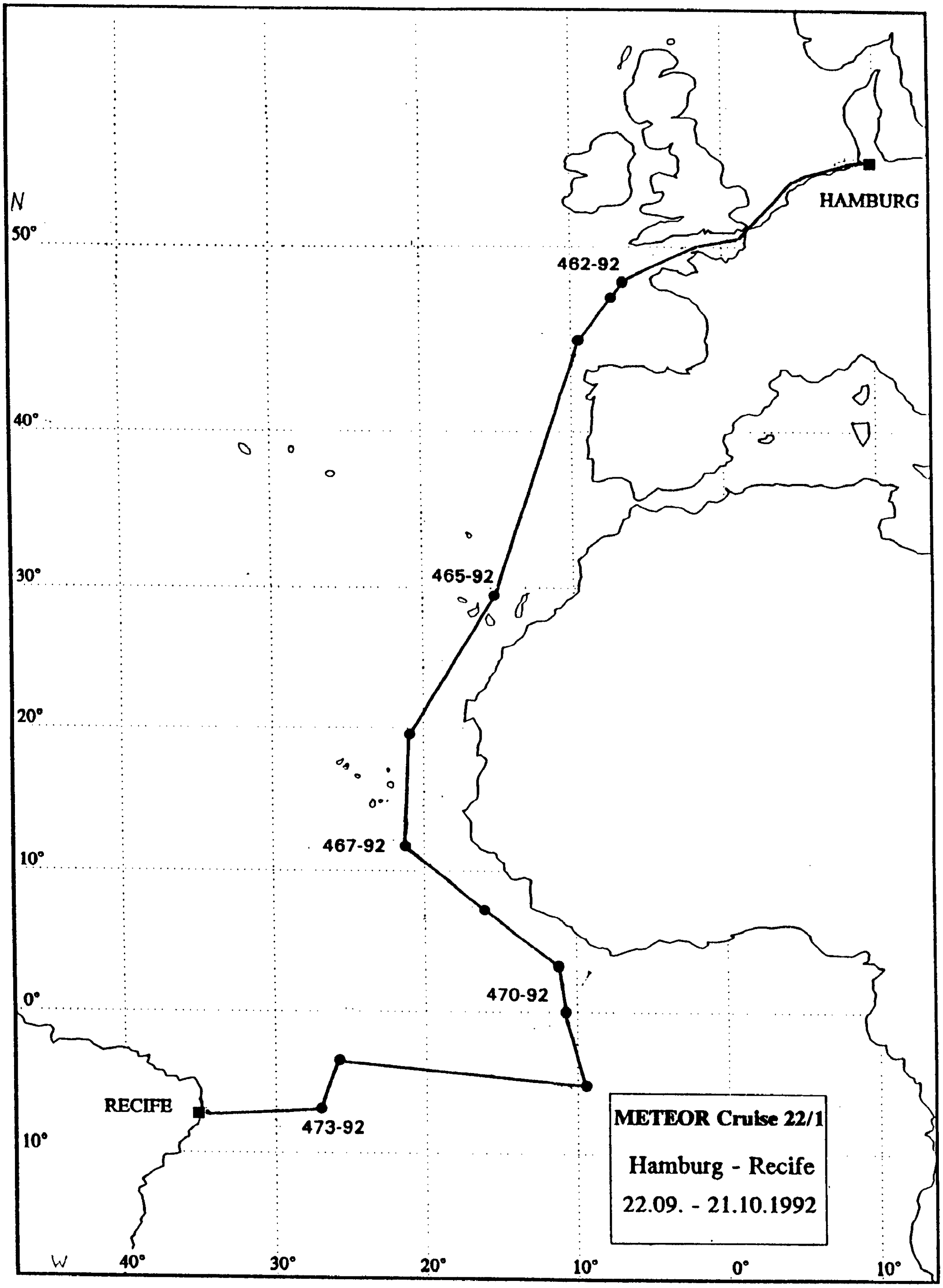

Fig. 2: Cruise track of METEOR cruise no. 22, leg 1

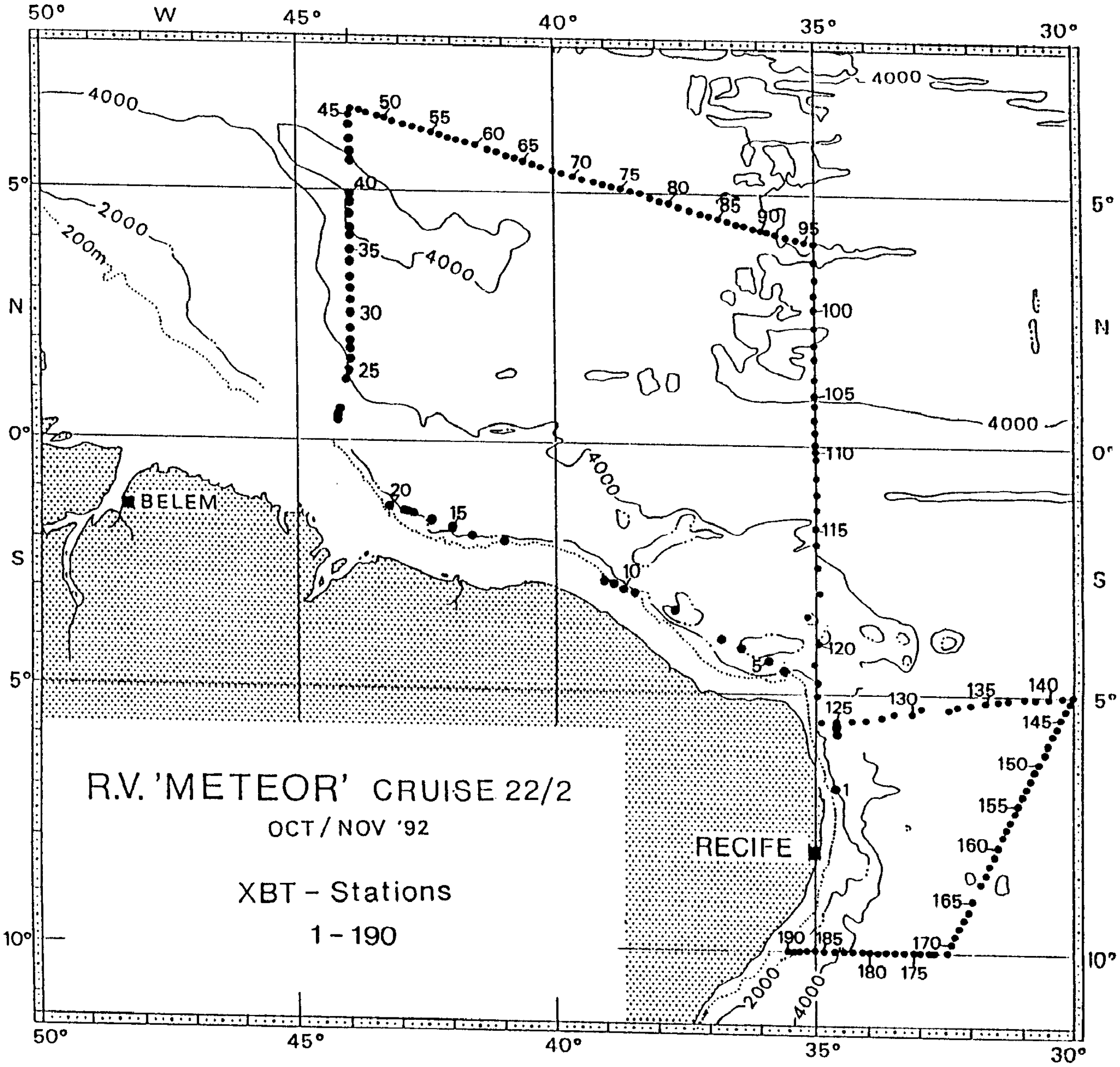

Fig. 3: Cruise track M 22/2. XBT drops during M 22/2

M22/3 Positionen, XBT, CTD, Verankerung

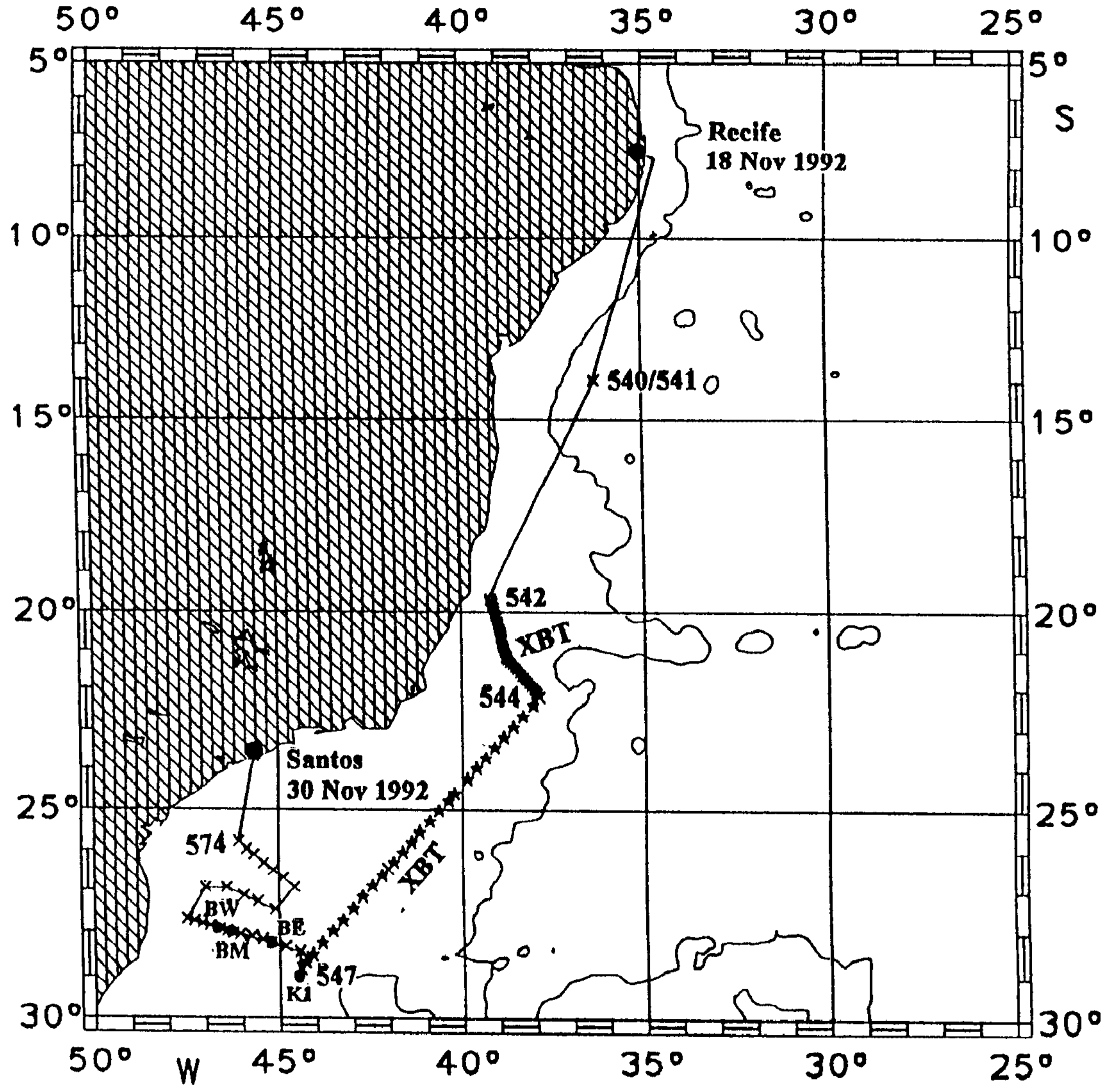

Fig. 4: METEOR M 22/3 cruise track: XBTs (stars), CTD stations (crosses), sound source mooring K1 (deployed) and current meter moorings BE, BM, BW (recovered).

METEOR Cruise 22/4

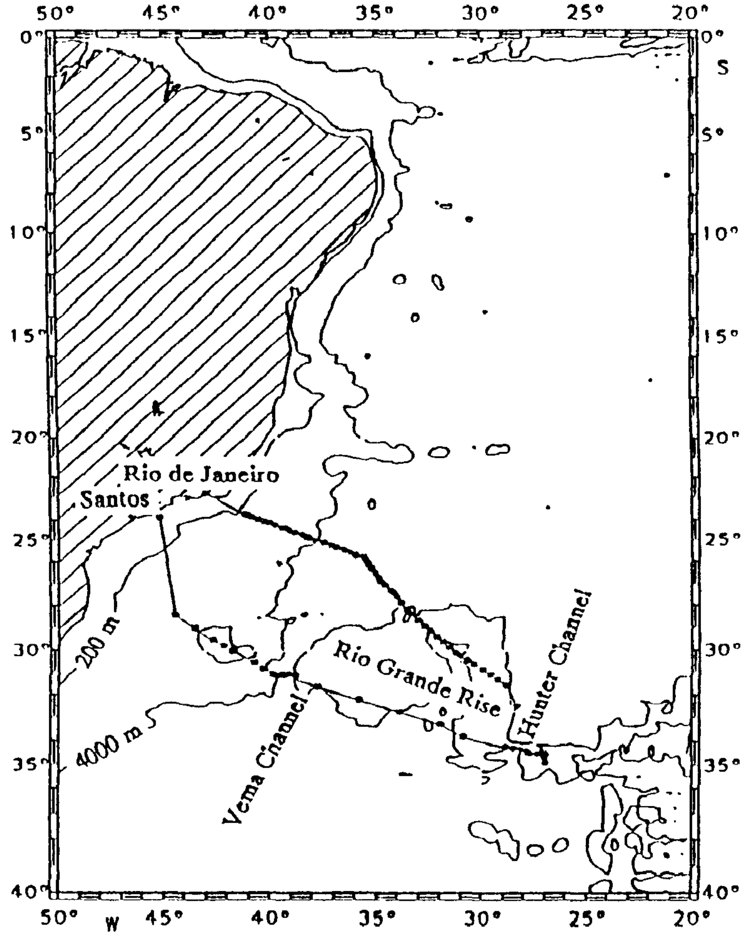

Fig. 5a: Track chart of METEOR cruise 22/4. This leg started in Santos on December 2, 1992 and was terminated in Rio de Janeiro on December 22, 1992.

Fig. 5b: Scientific party of METEOR cruise 22/4. For list of participants see Table 2.

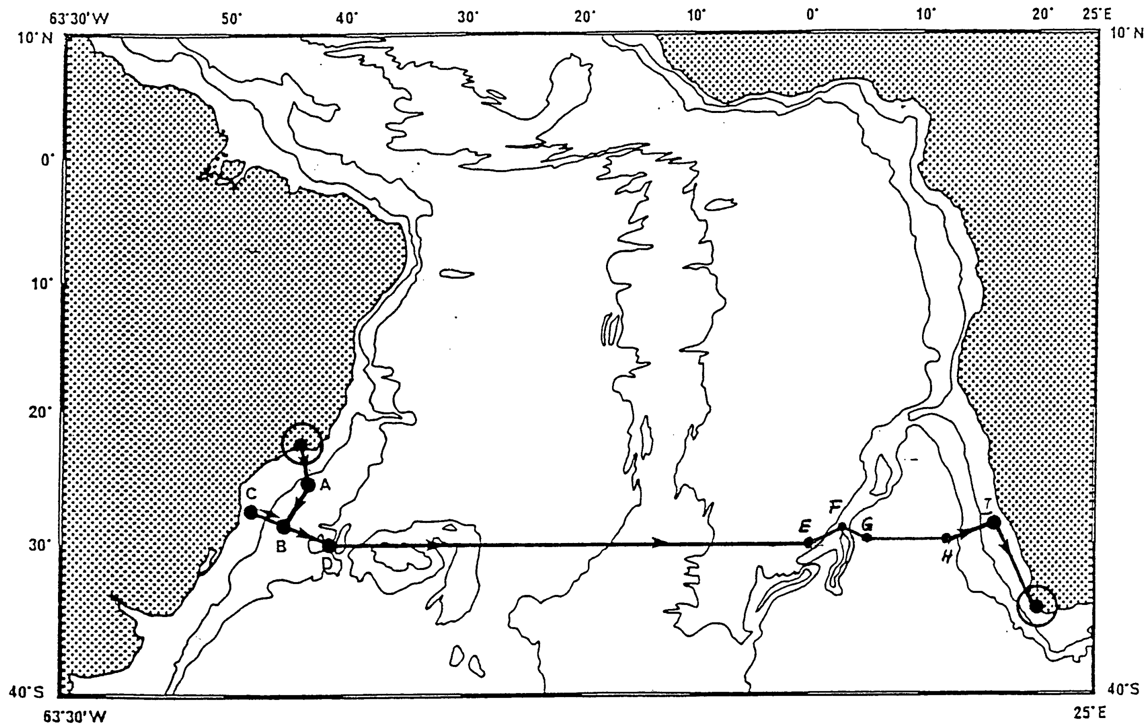

Fig. 6: Cruise track M 22/5. The depth contours represent the 2000 and 4000 m isopleths.

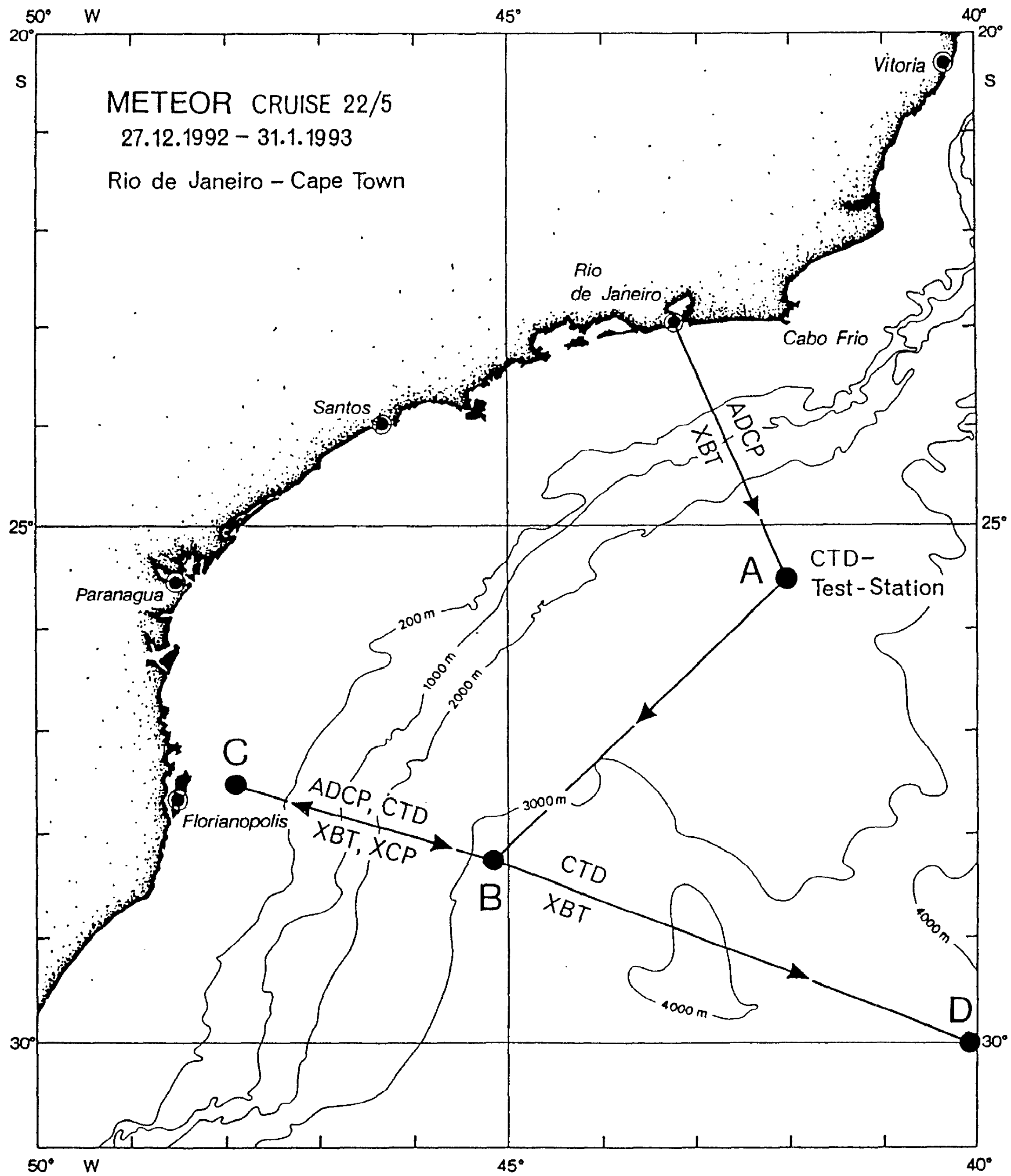

Fig. 7: Cruise track M 22/5 (western part)

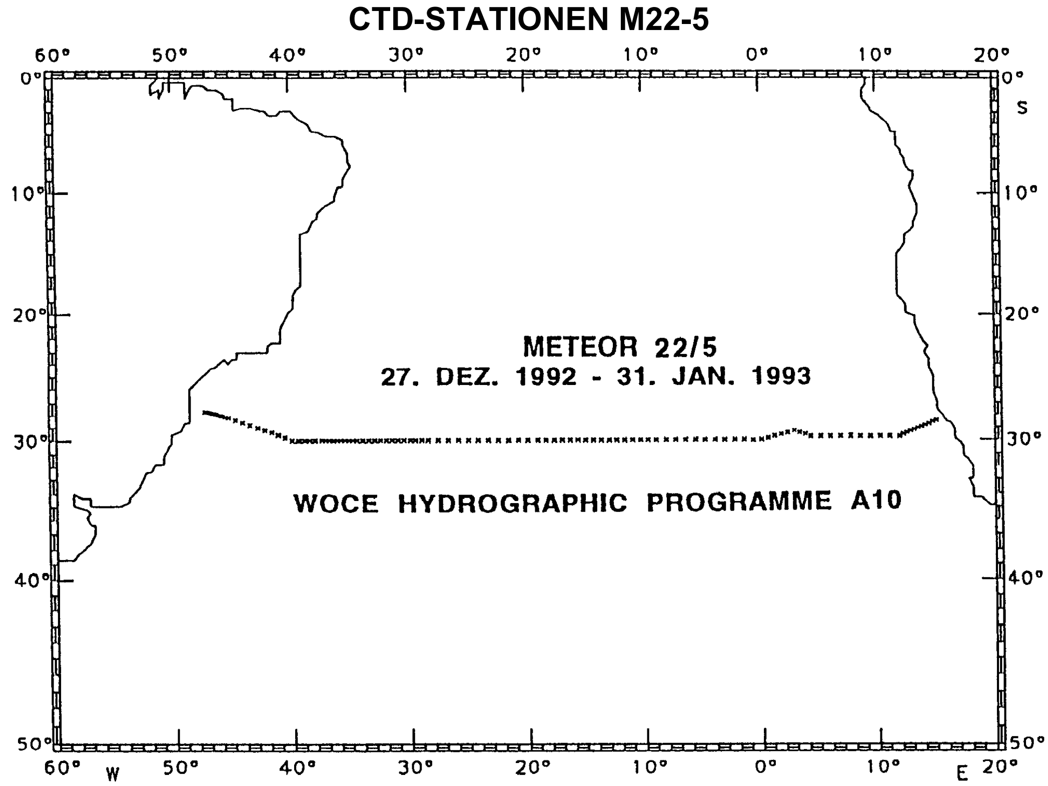

Fig. 8: Stations along WHP section A10, 30˚ 8 S

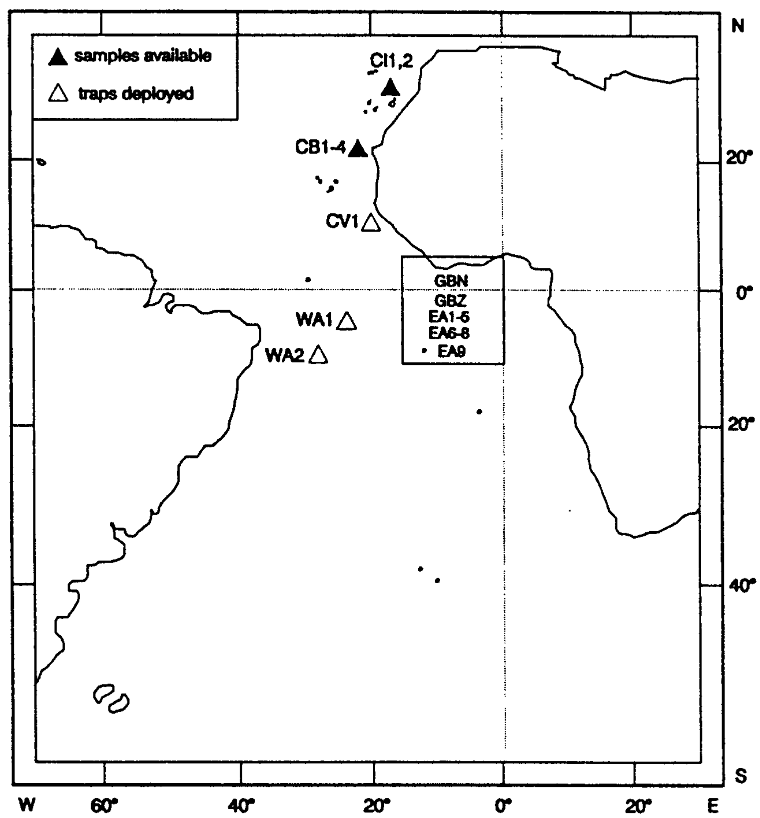

Fig. 9a

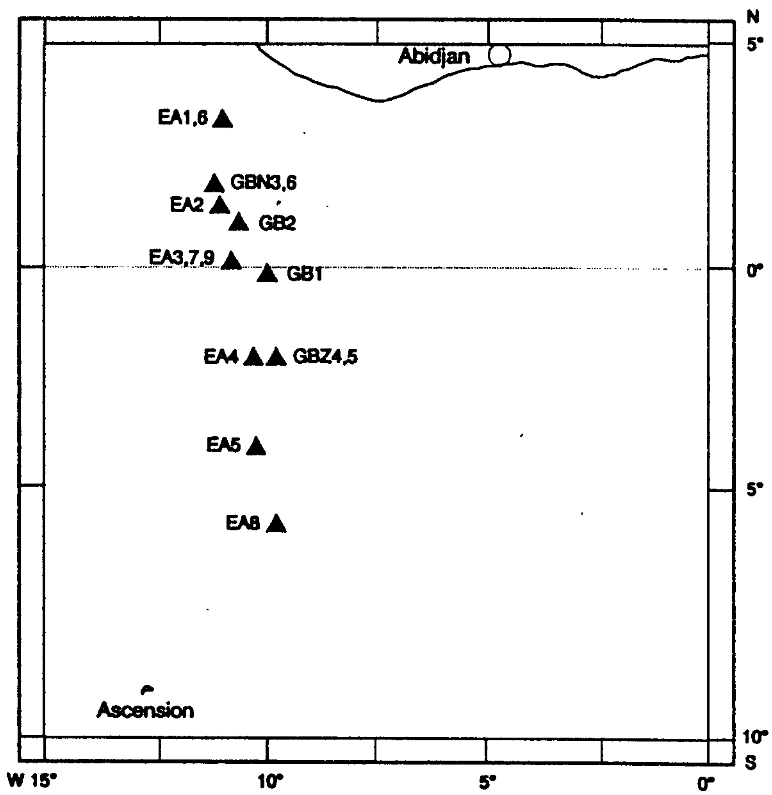

Fig. 9b

Fig. 9a,b: Map of stations where moorings with sediment traps were deployed off NW-Africa and in the equatorial Atlantic. The maps also contain moorings deployed at the same positions during previous cruises.

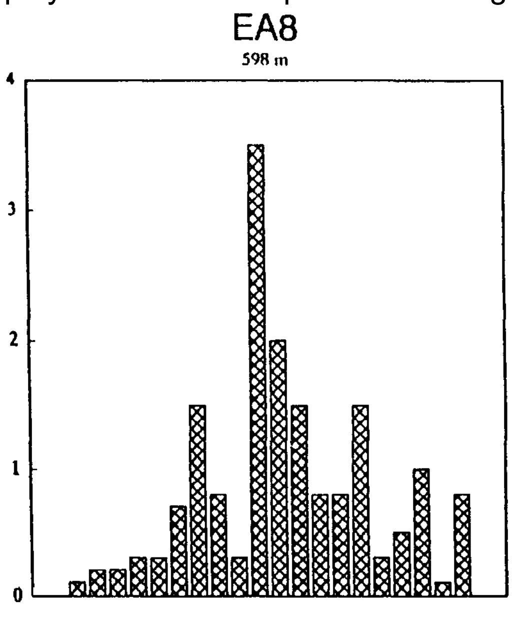

Fig. 10a

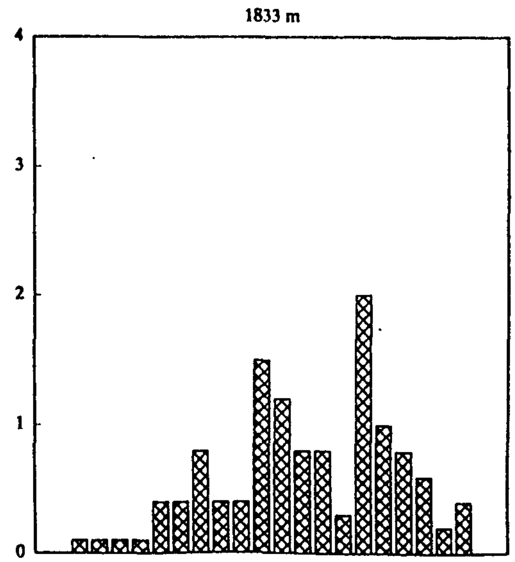

Fig. 10b

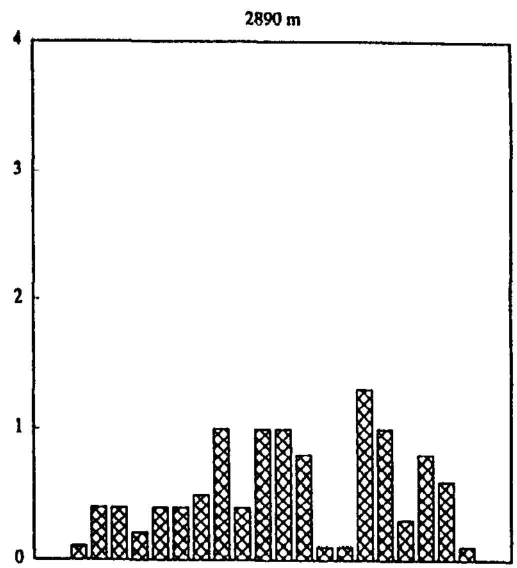

Fig. 10c

Fig. 10a-c: Volume (arbitrary units) of particles in individual cups of the three sediment traps attached to mooring EA8 (recovered at 6˚S in the Gulf of Guinea). The traps started sampling on December 15, 1991 and the last cup stopped sampling at October 6, 1992. For further details see chapter 7.1.2

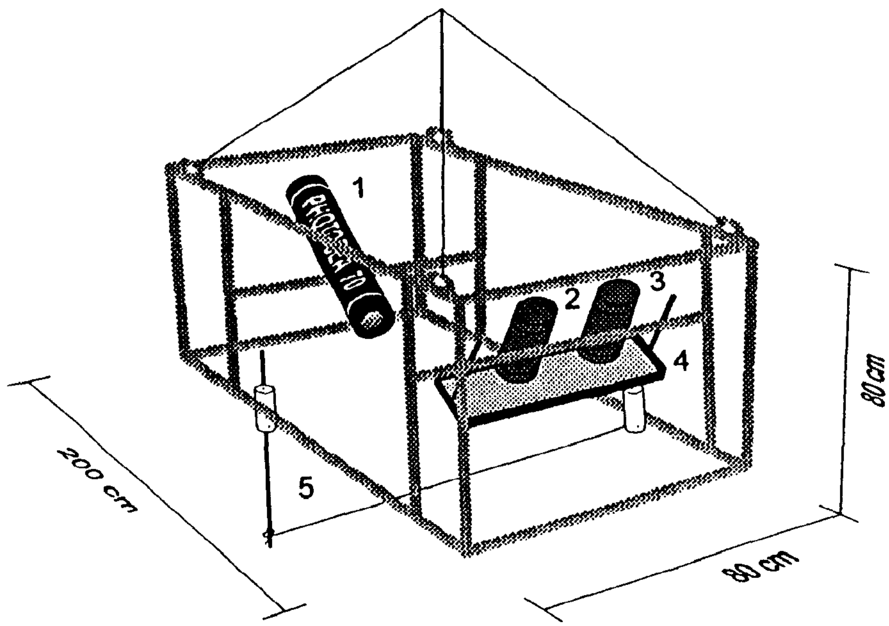

Fig. 11: Perspective view and size of the particle camera system: *1*: 70 mm
2 and 3: 150 W-strobes PHOTOSEA 1500s
4: Collimator, consisting of two 30 x 30 cm highly refractive fresnel lenses, mounted in a steel frame. Distance between fresnel lenses and strobe lights is variable
5: Adjustable holder for a 0.5 mm nylon line used as size standard

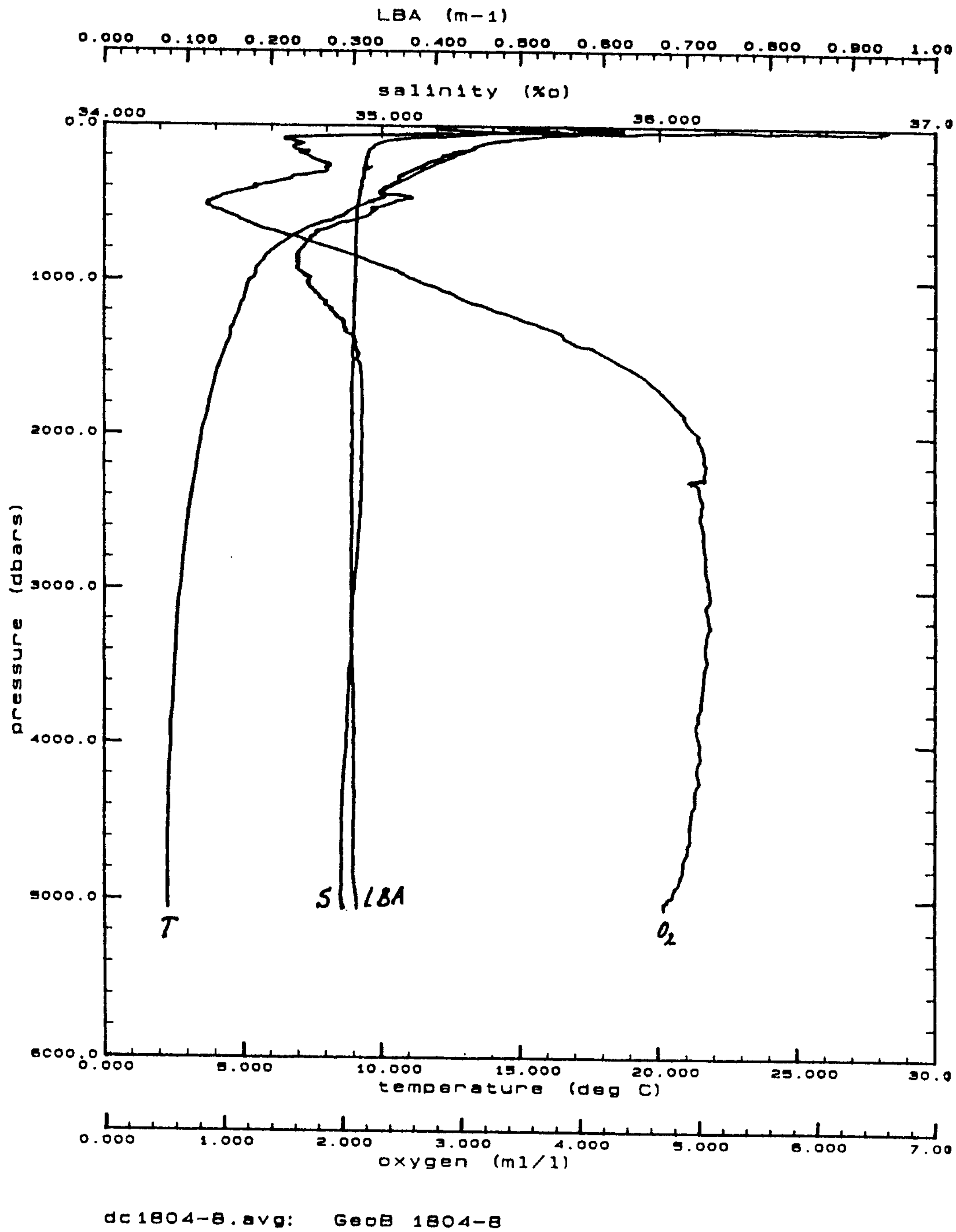

Fig. 12: Profiles of salinity, temperature, oxygen and light beam attenuation (LBA) at station 467-92, south of Cabo Verde Islands

Meteor 22, Salinity, section 35°W

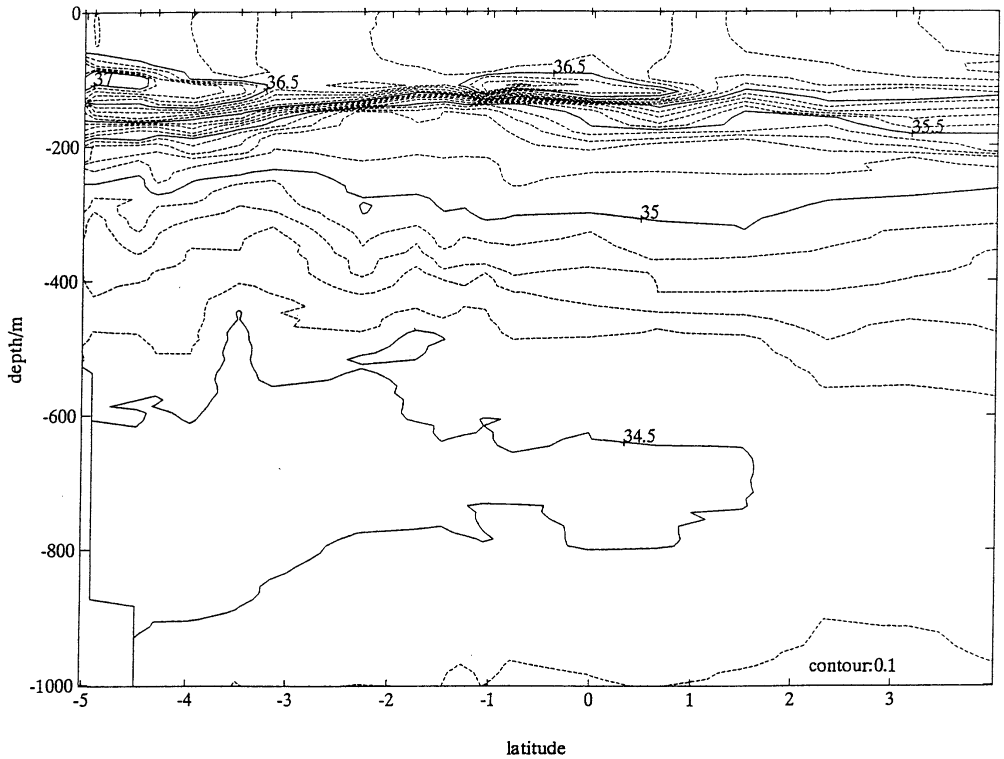

Fig. 13: Salinity distribution along 35˚W between 5˚01'S and 4˚N from November 2 to 7, 1992 for the upper 1000m of the ocean with a contour interval of 0.1.

Meteor 22, profiles: 18-36

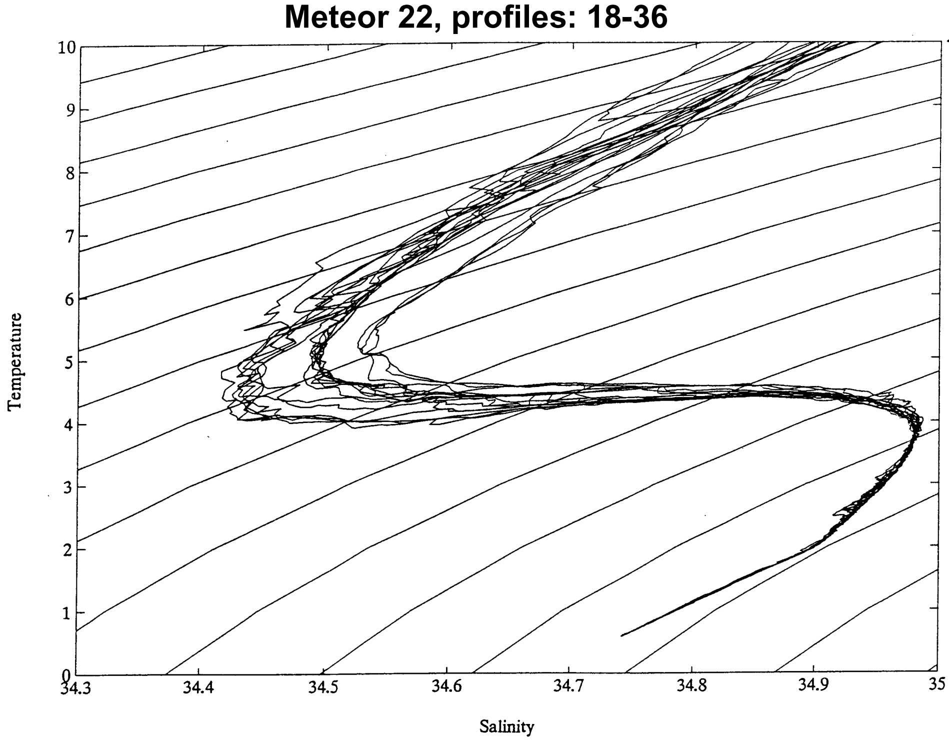

Fig. 14: TS-curves (potential temperature) of all CTD profiles of the 35˚W section for the temperature range 0˚ to 10˚C.

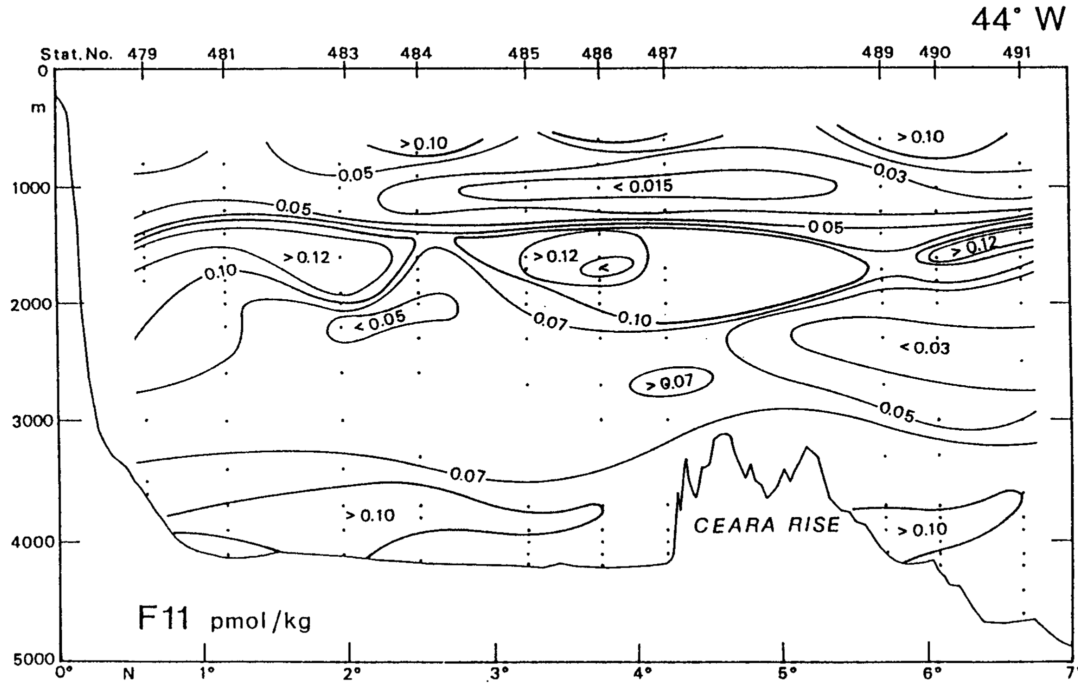

Fig. 15: Freon-11 distribution (pmol/kg) at the 44˚W section.

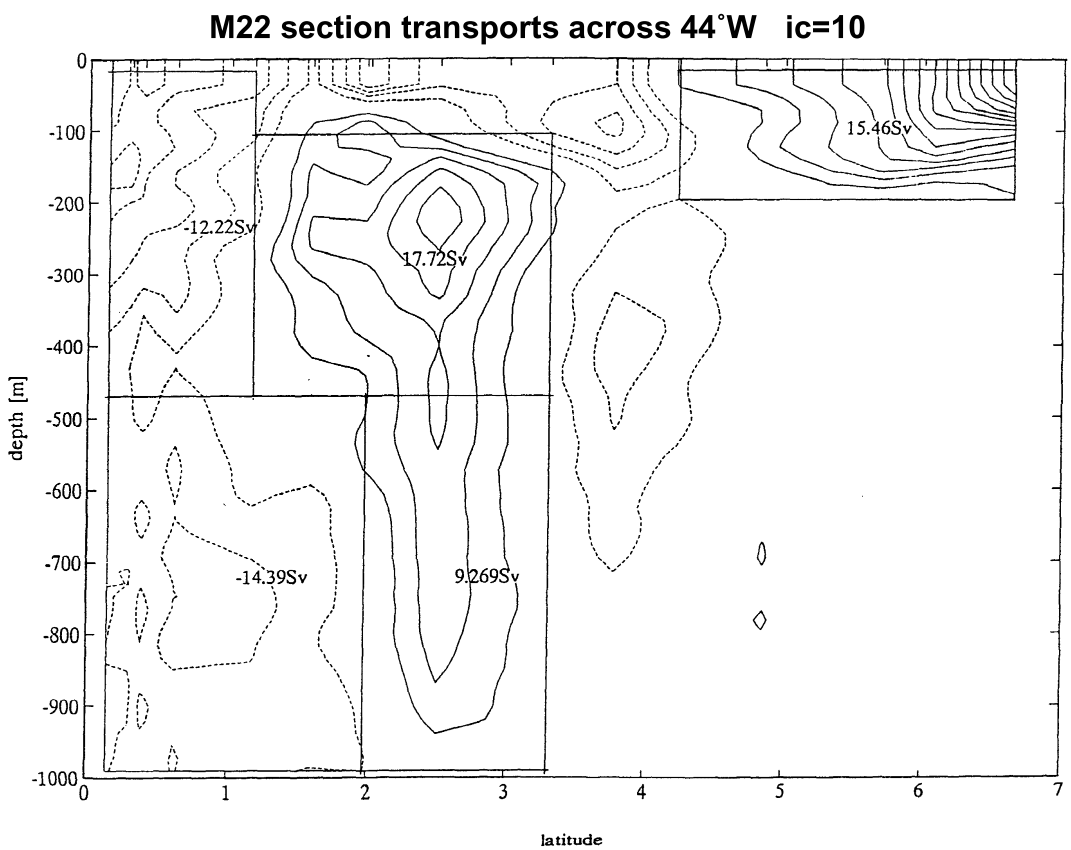

Fig. 16: lADCP: velocity pattern (u-component, cm/s) of the upper 1000 m at 44˚W. Transport calculations for the framed regions are included. Numbers are in Sv, positive is directed east.

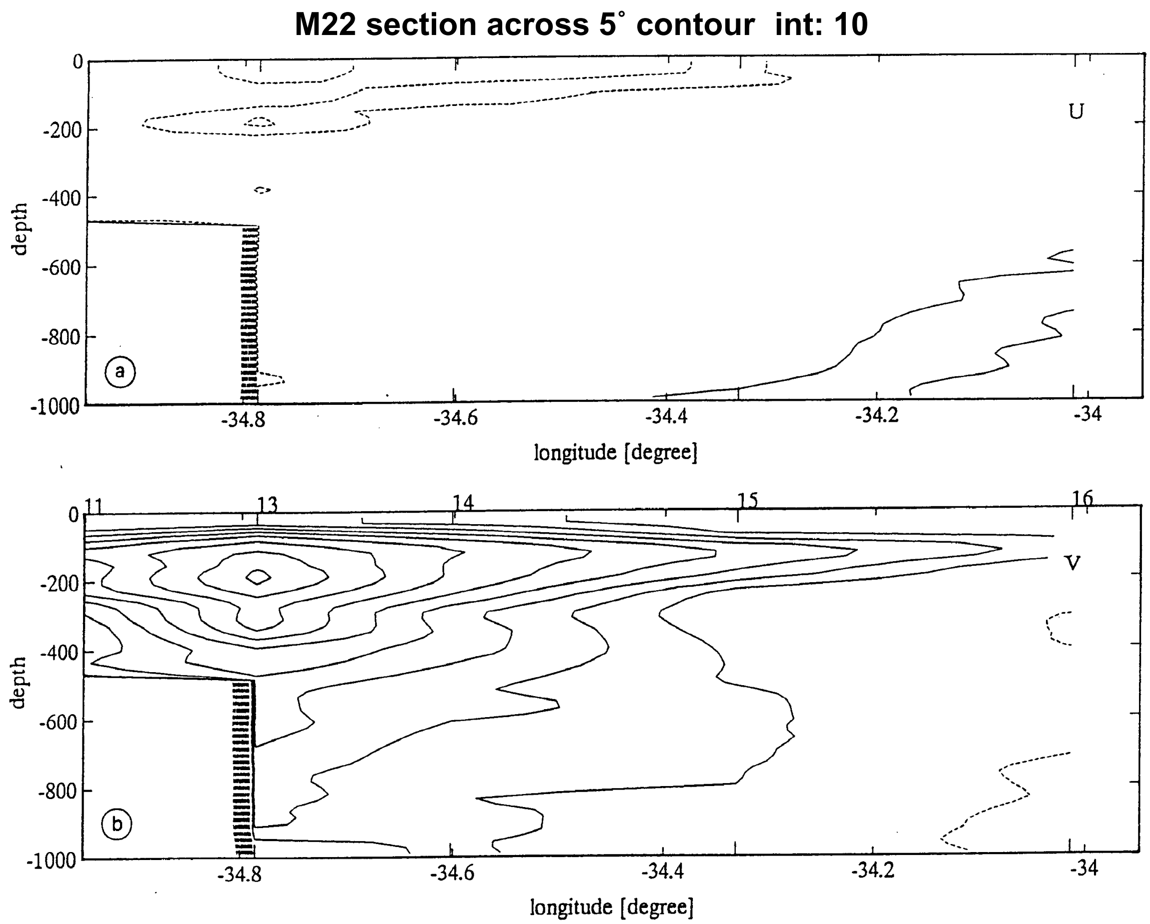

Fig. 17: IADCP: velocity pattern (cm/s) at the 5˚S section

a) u-component

b) v-component

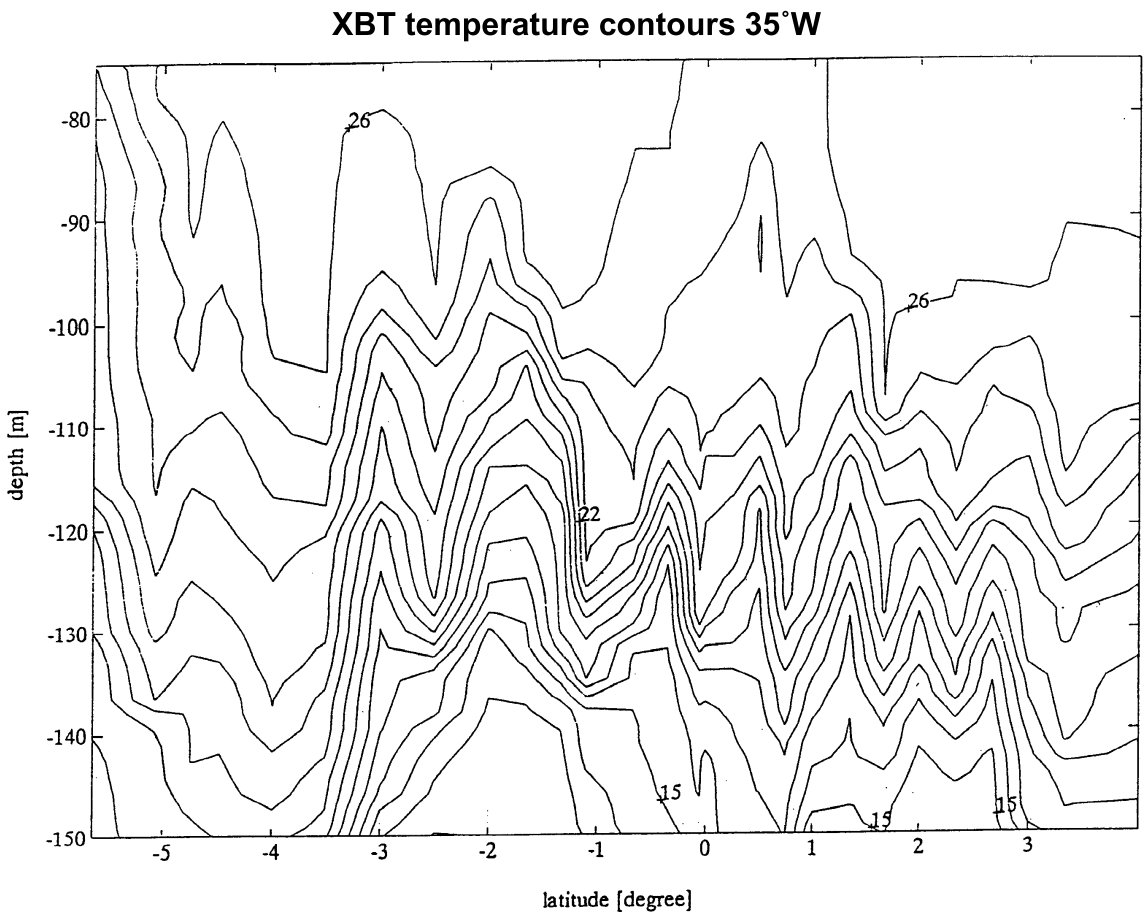

Fig. 18: Temperature distribution from XBT data for the 35˚W section for the depth range of the thermocline between 75 and 150 m with an isotherm spacing of 1˚C.

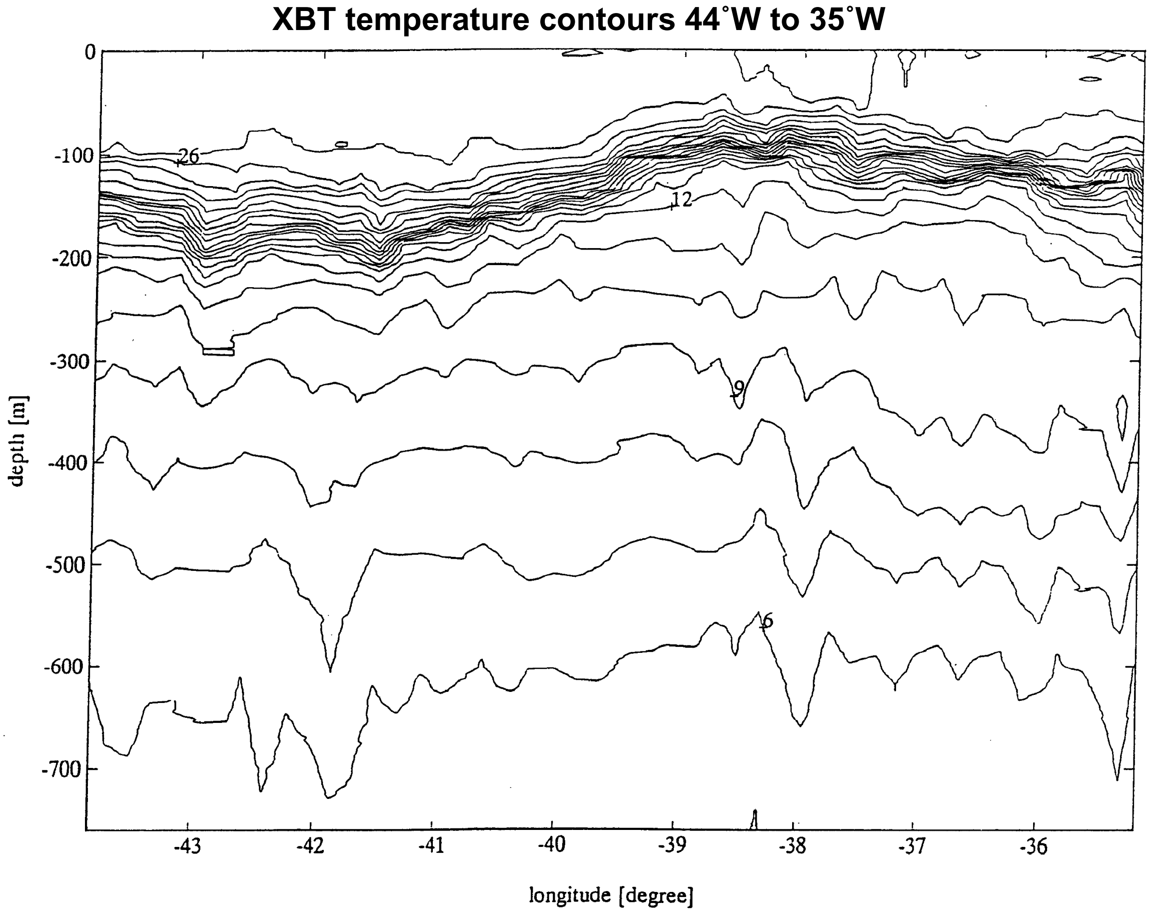

Fig. 19: Temperature distribution from XBT data between 6˚ 40'N, 44˚W and 4˚N, 35˚W with an isotherm spacing of 1˚C.

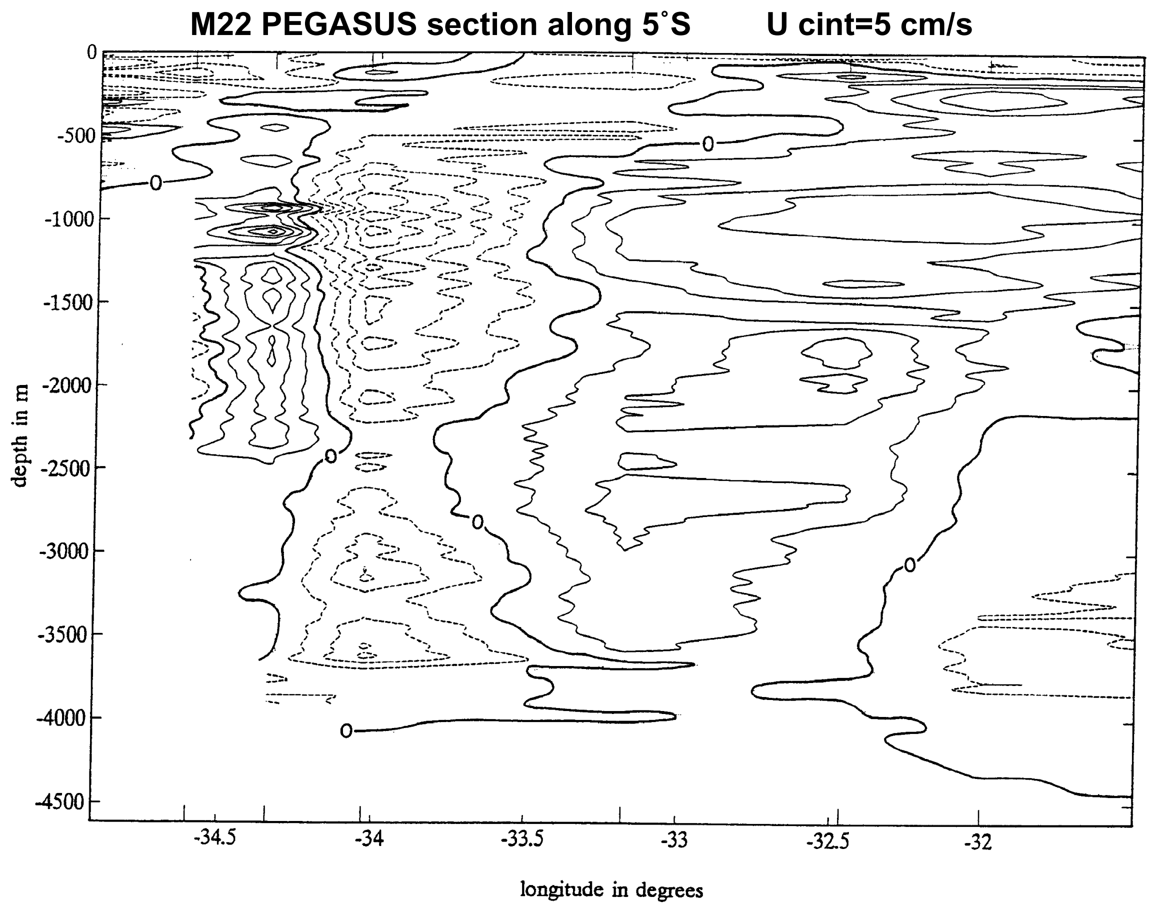

Fig. 20: Pegasus section of the meridional currents at 5˚S. Contour interval is 5 cm/s. Northward contours are solid, southward dashed. The stations are indicated with the longer tick marks at the bottom of the plot.

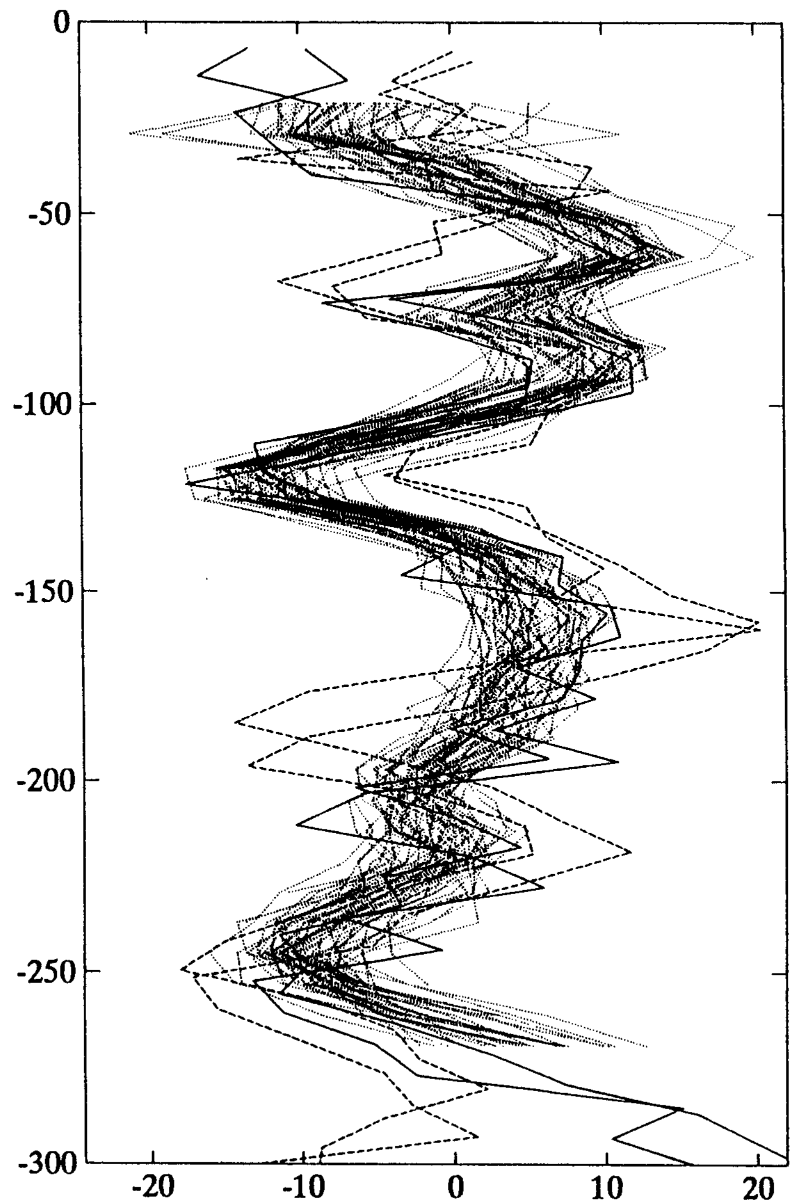

Fig. 21: Zonal current profiles at station S6 (approx.1000m water depth). The solid lines are the Pegasus profile (down and up cast) on 8 Nov. 1992. The family of dotted curves are ship ADCP profiles during the 4 hours on station there. The dashed curves are the corresponding Pegasus profile from 24 Oct. During the 4 hours on station, the profile is remarkably constant. 2 weeks earlier, many of the features are the same, but the direction of jets had changed.

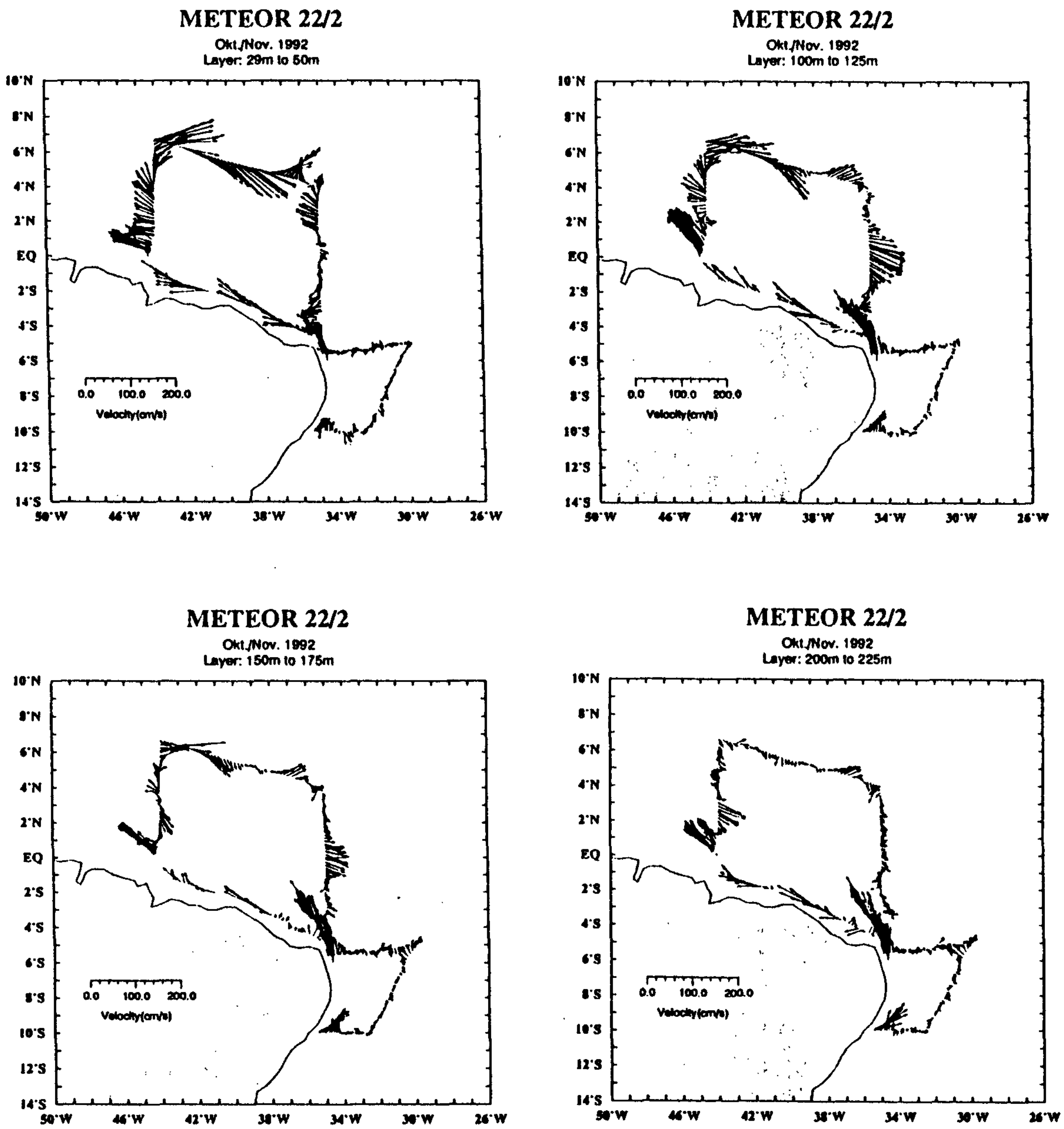

Fig. 22: VM-ADCP: Velocities along the cruise track for different depth layers.

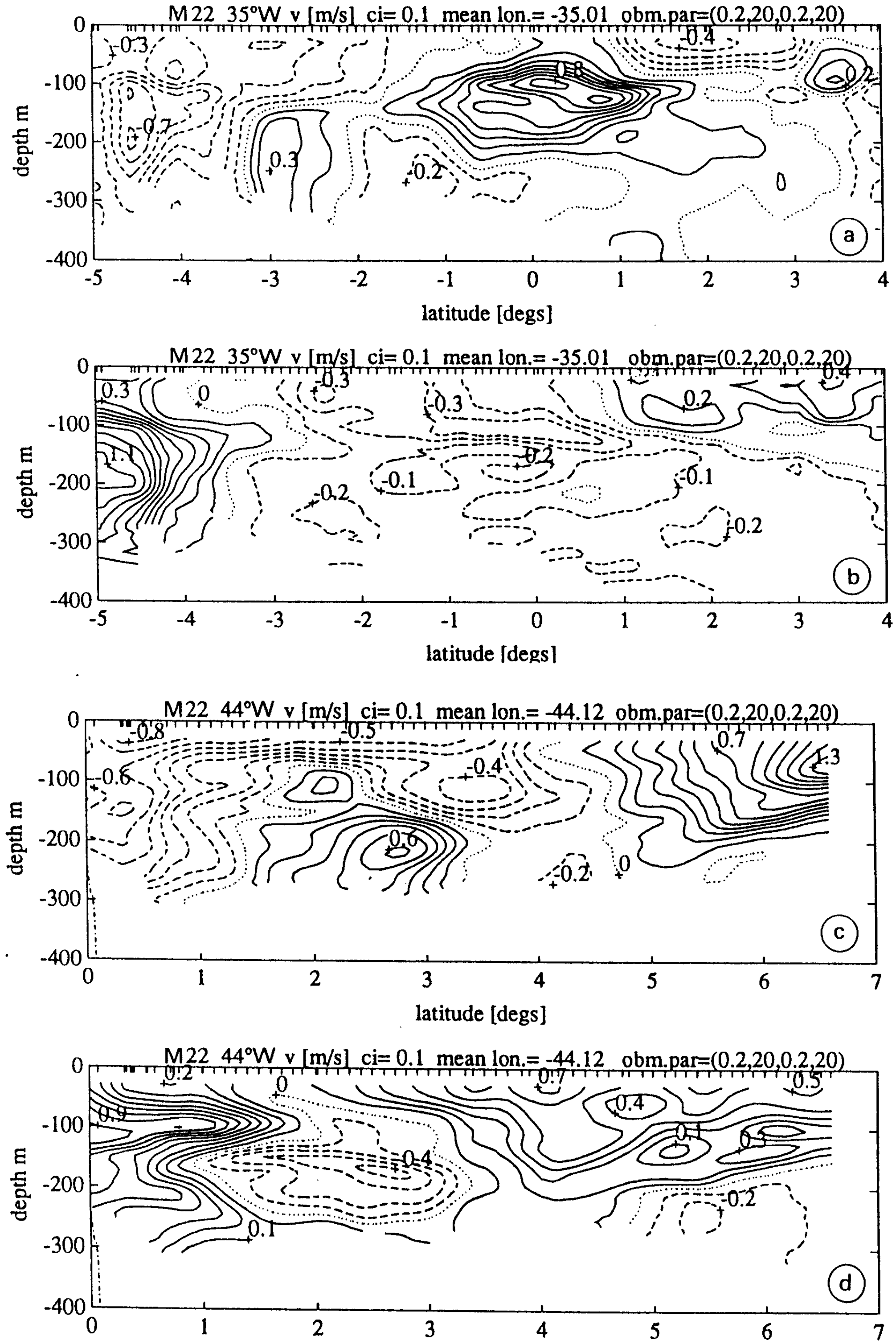

Fig. 23: VM-ADCP: Velocity sections
a)along 35˚W, u-component
b)along 35˚W, v-component
c)along 44˚W, u-component
d)along 44˚W, v-component

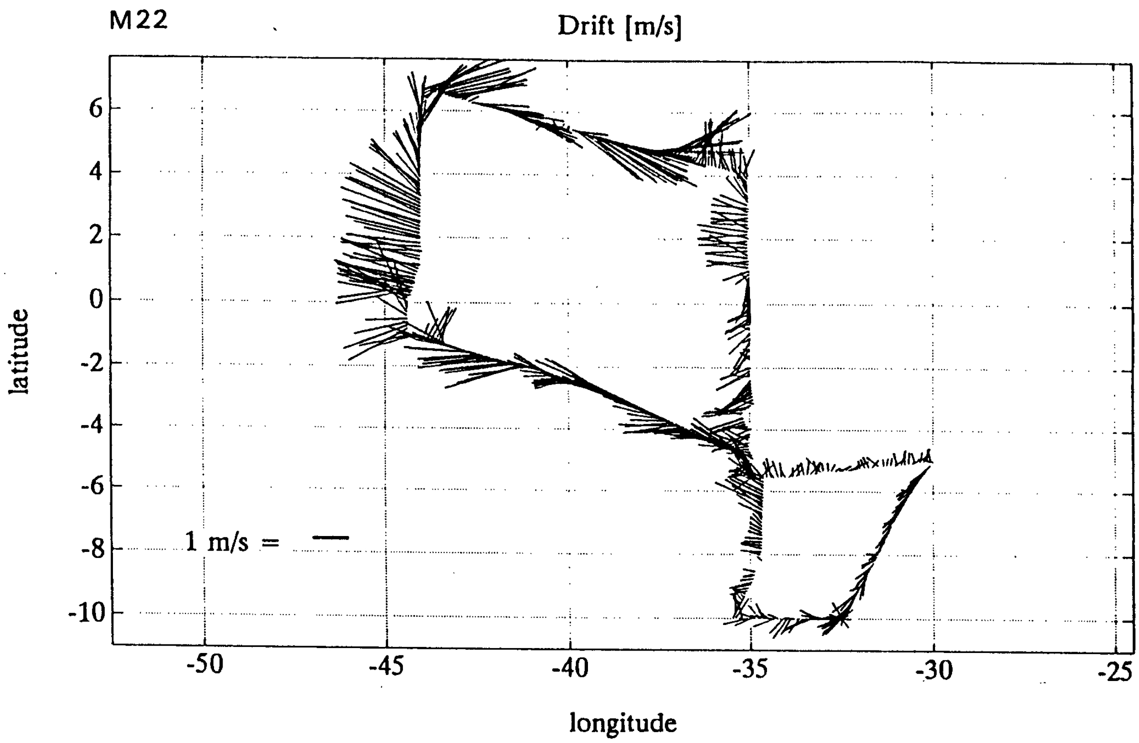

Fig. 24: DVS: ship's drift along cruise track

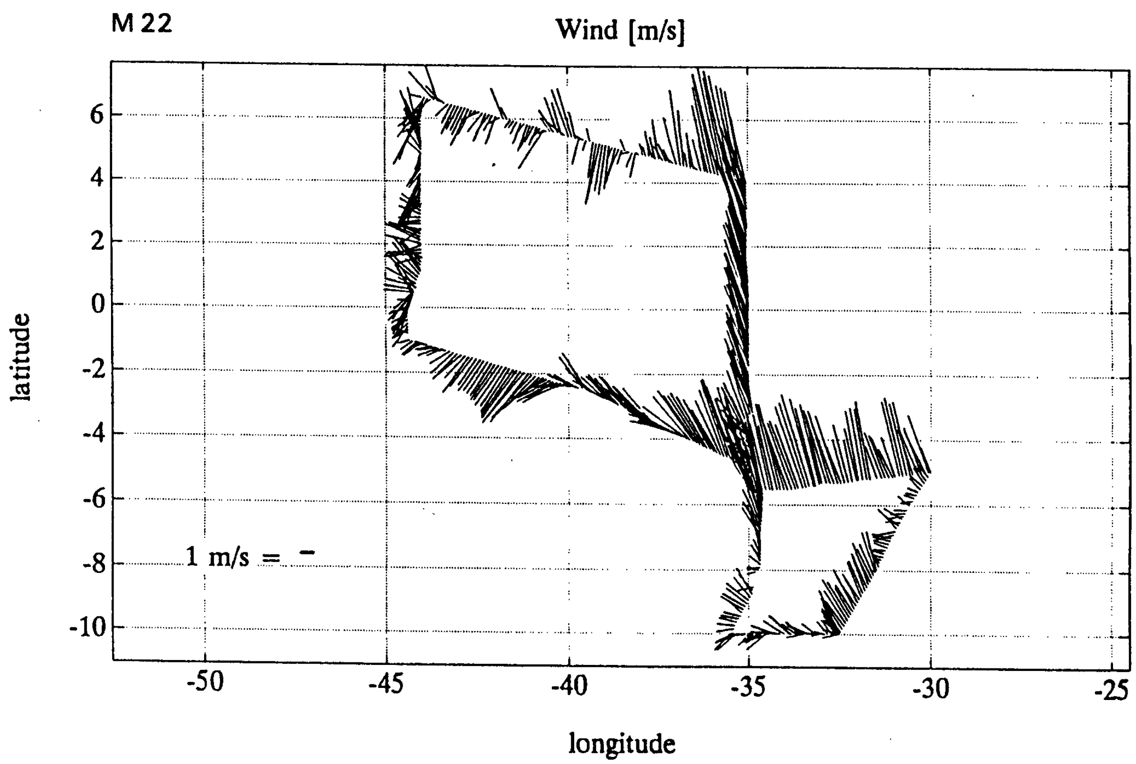

Fig. 25: DVS: winds along cruise track

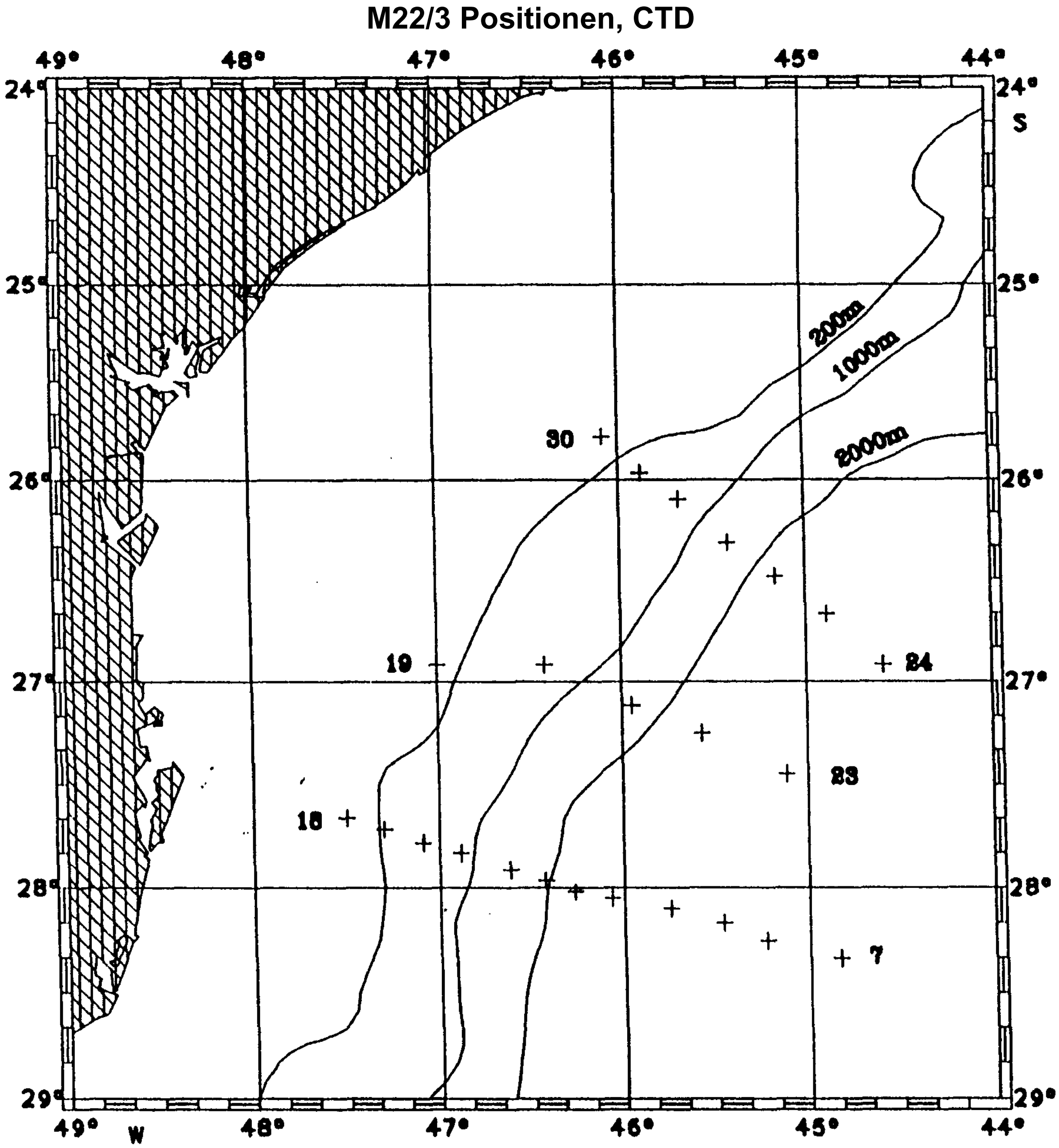

Fig. 26a: Three sections of potential temperature and salinity across the shelf break of the Santos Plateau. (For location see Figure 26b). The upper 1000 m are shown.

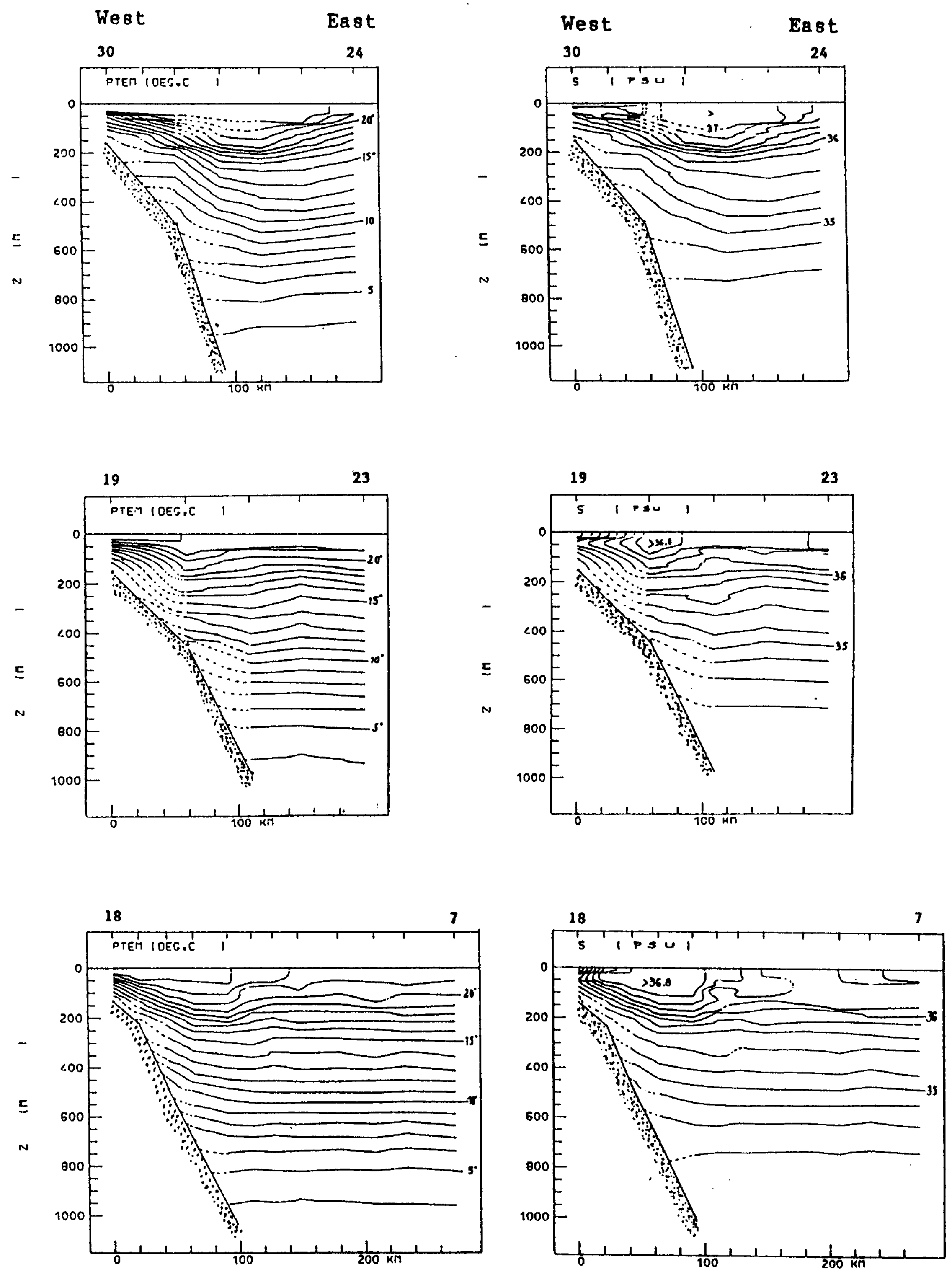

Fig. 26b: Map showing the positions of CTD profiles of 3 sections normal to the shelf break of the Santos Plateau. (For location see Figure 26B). The upper 1000 m are shown.

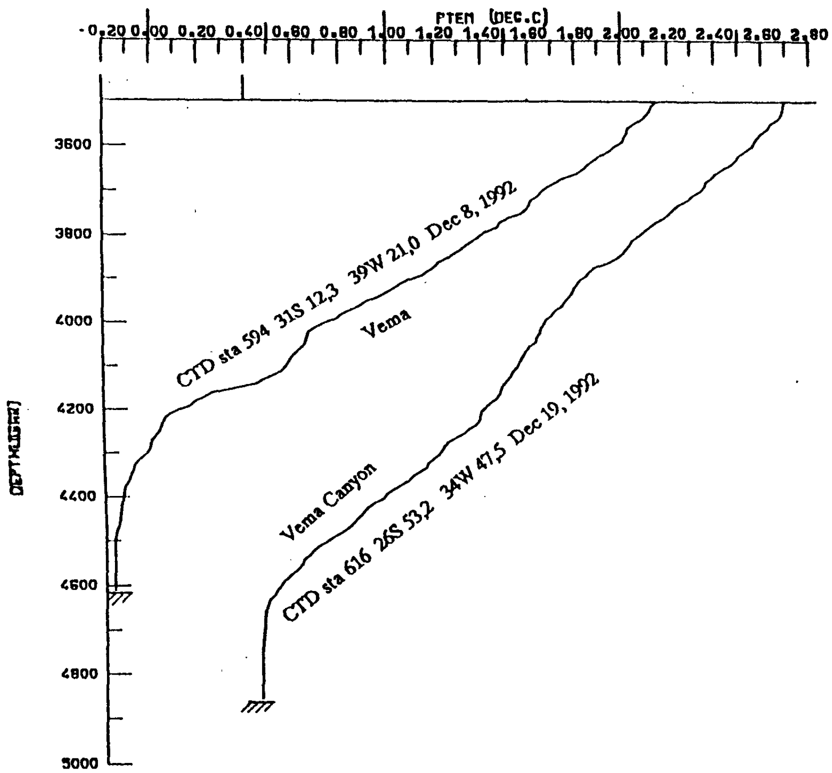

Fig. 27: Vertical profiles of potential temperature near the bottom at the Vema Sill and the northward extention of the Vema Channel, called Vema Canyon. The right curve is shifted by 0.6 K. Both stations were occupied during M 22/4 in December 1992. For locations see Figure 5.

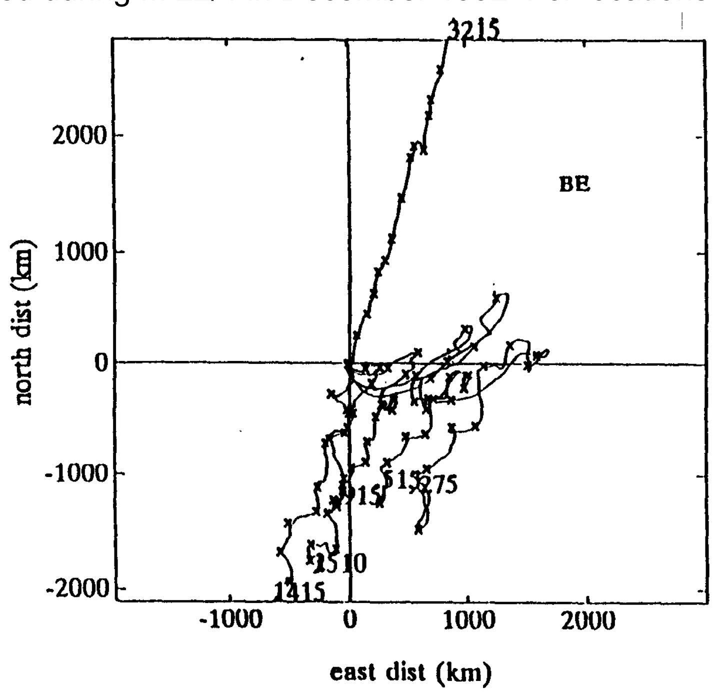

Fig. 28: Progressive vector diagrams from (a) the deepest mooring of the heat flux array ACM3 (BE/335) All curves start at the origin, crosses indicate 50 day intervals, numbers depths in m.

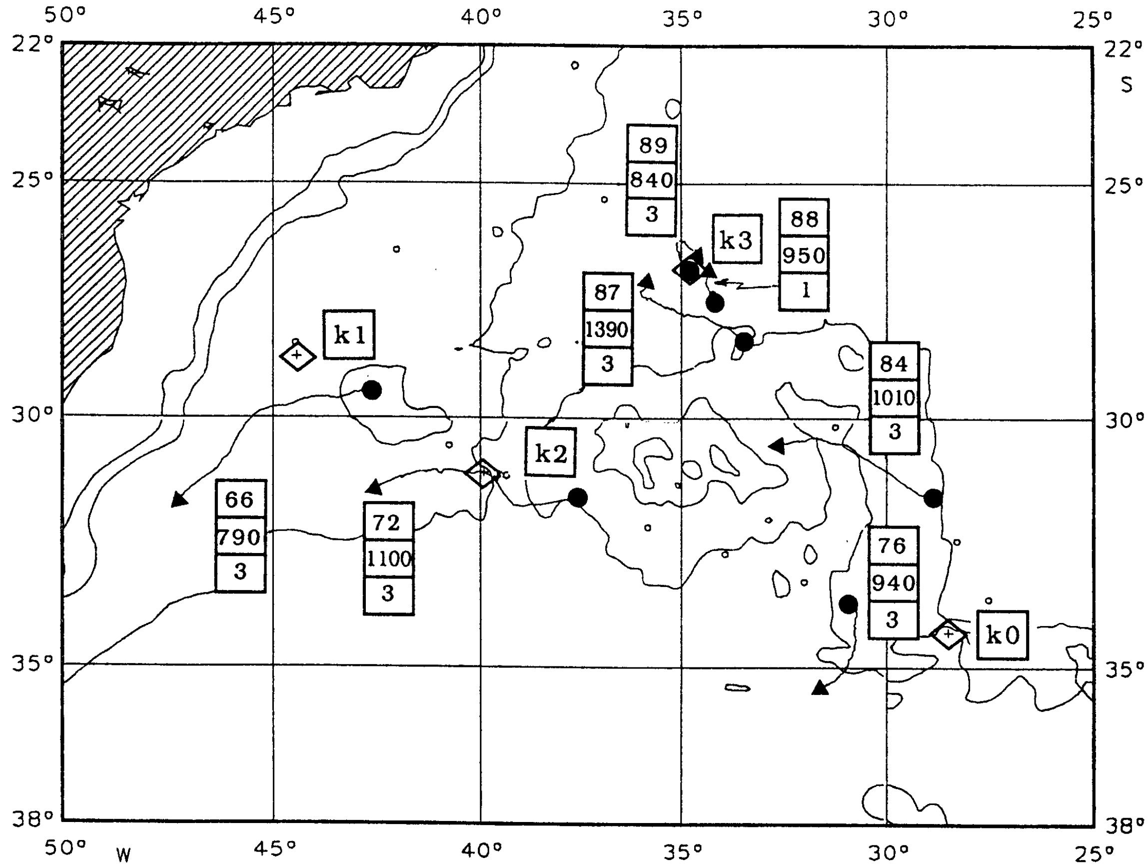

Fig. 29: Trajectories of selected RAFOS floats launched during M 22/4. Numbers indicate IfM serial number, mean depth (m), and mission length (month). Diamonds indicate sound source positions K1, K2, K3, and K0 (from west to east).

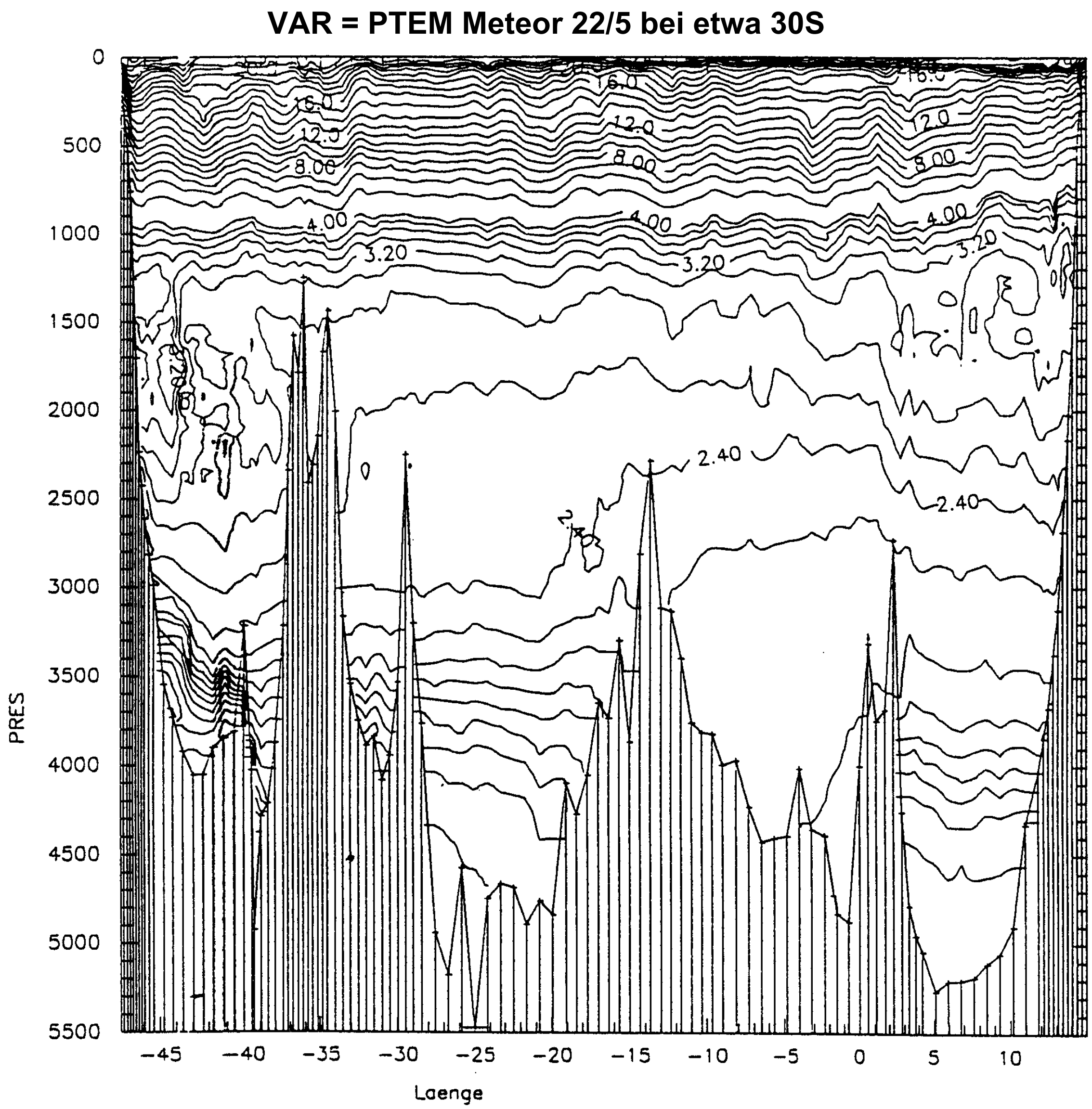

Fig. 30: Potential temperature along 30˚S.
Contour interval 4 - 25˚C: 1˚C
0 - 4˚C: 0,2˚C

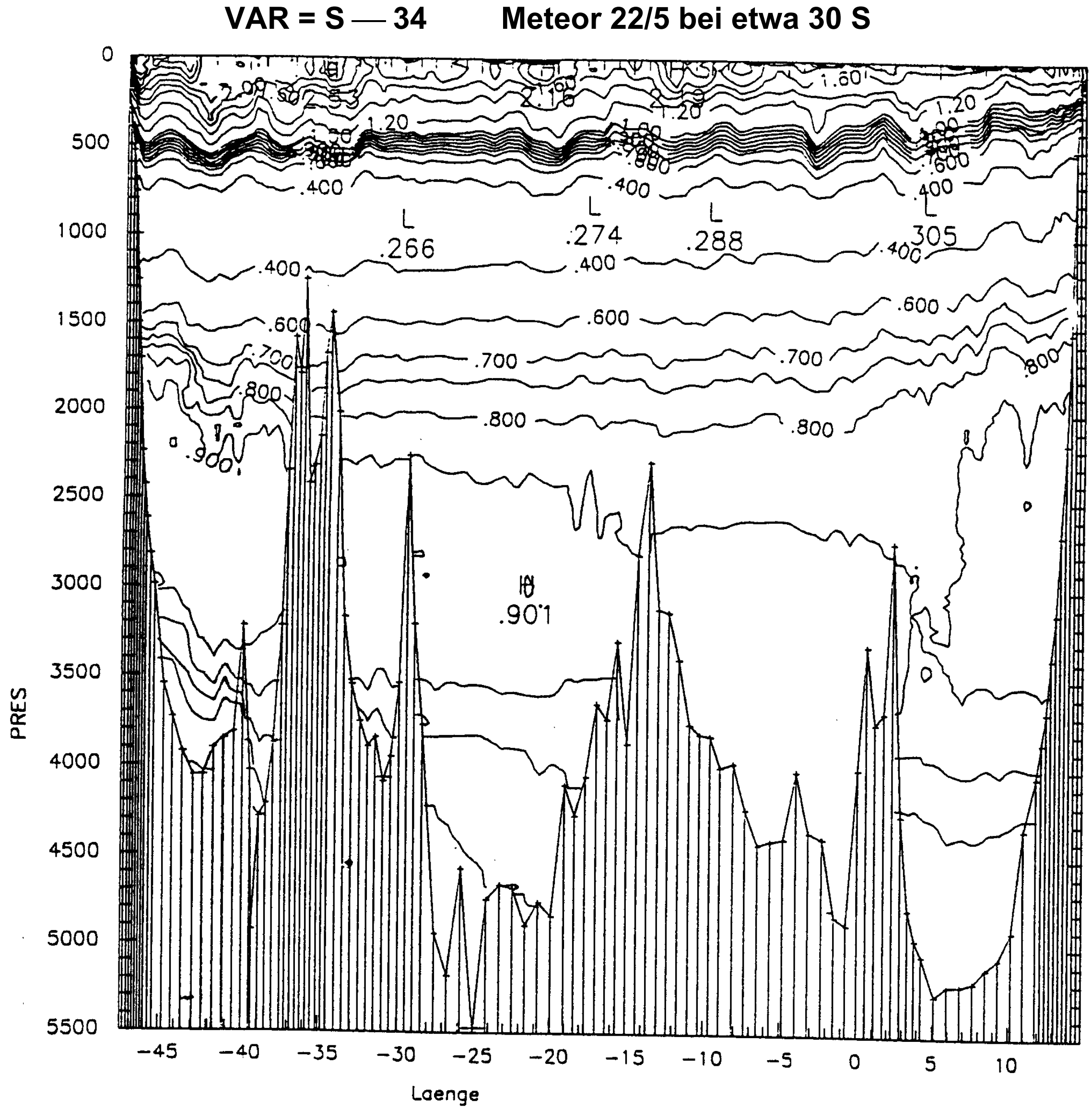

Fig. 31: Salinity-34 along 30˚S.
Contour interval: 0,05

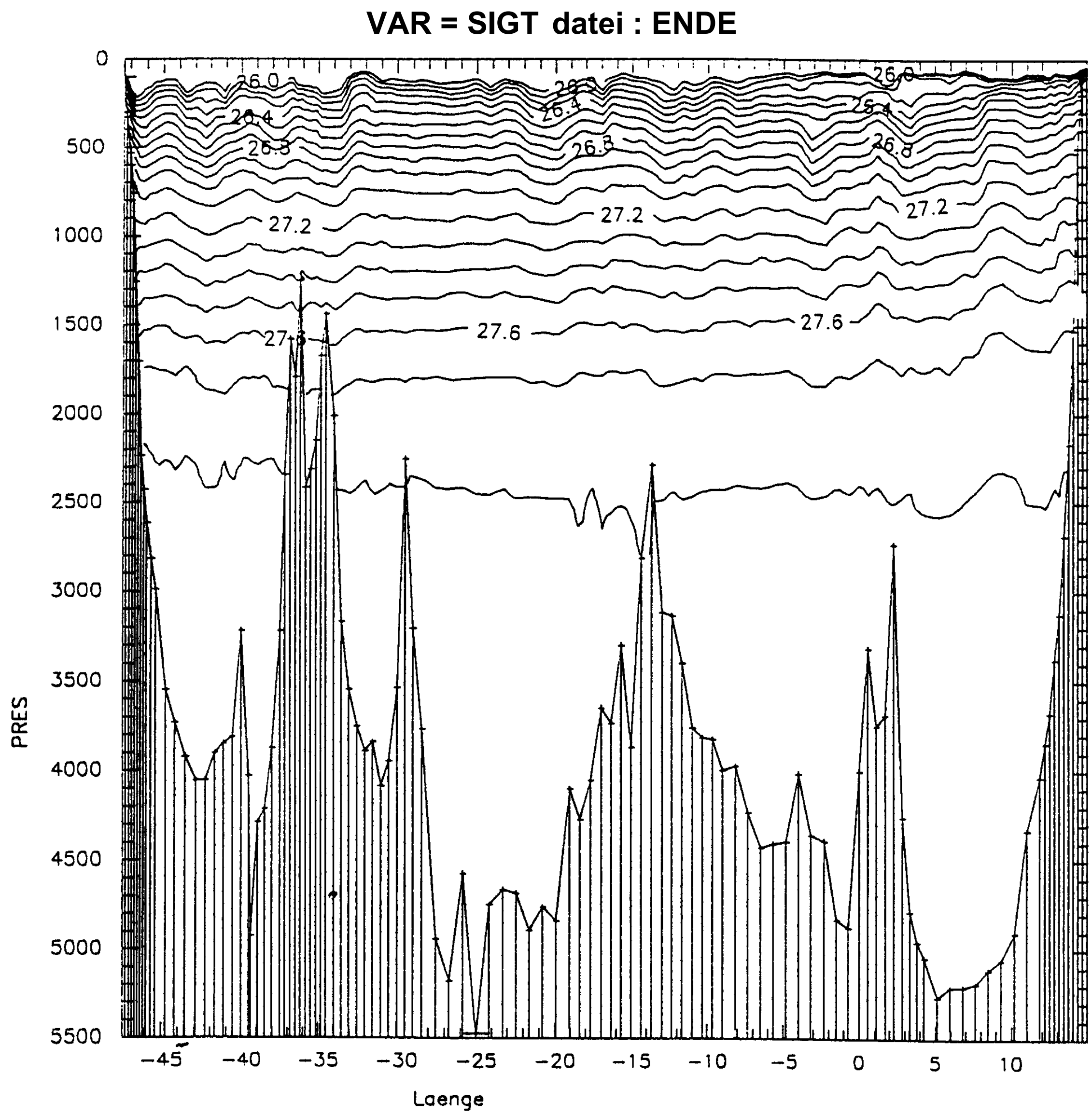

Fig. 32: Sigma-T along 30˚S
Contour interval: 0,1

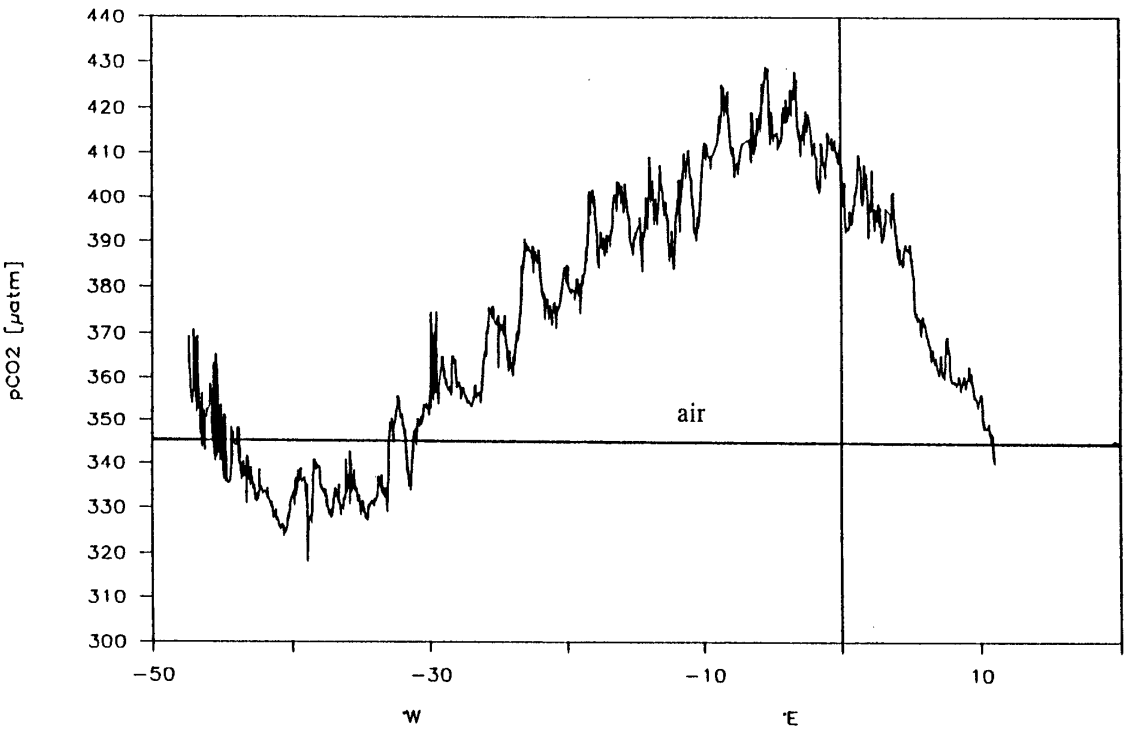

Fig. 33: CO_2 partial pressure in surface water and atmosphere along 30° S

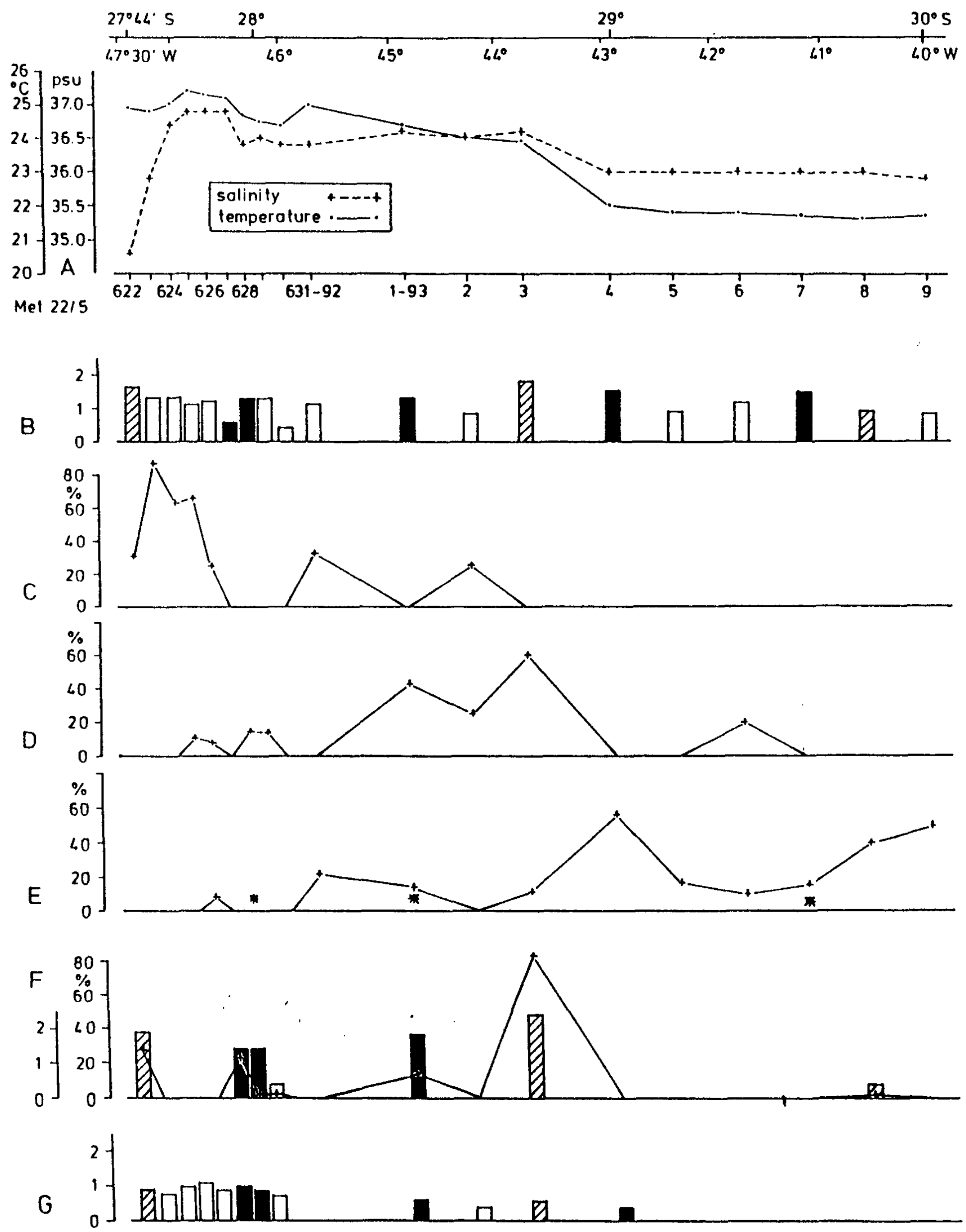

Fig. 34: Hydrographical and biological distribution pattern at the sea surface from Brazil to 40° W.

A) Temperature (lines) and salinity (dashes)

B) Quantitative distribution of the total ichthyoplankton of the upper neuston net ($\log_{10}(n+1)/1000\ m^2$; bar shading indicates the light condition at sample time: white = day, black = night and hatched = dusk/dawn)

C)-E) Percentage of zoogeographical ichthyoplankton groups: C) = neritic; D) = tropical, E) = subtropical taxa and subtropical convergence (see text for species)

F) Quantitative distribution of Synopia (Gammaridae; $\log_{10}(n+1)/1000\ m^2$) and their percentage of total Amphipods.

G) Distribution pattern of Halobates micans (Gerridae, Insecta, $\log_{10}(n+1)/1000\ m^2$)

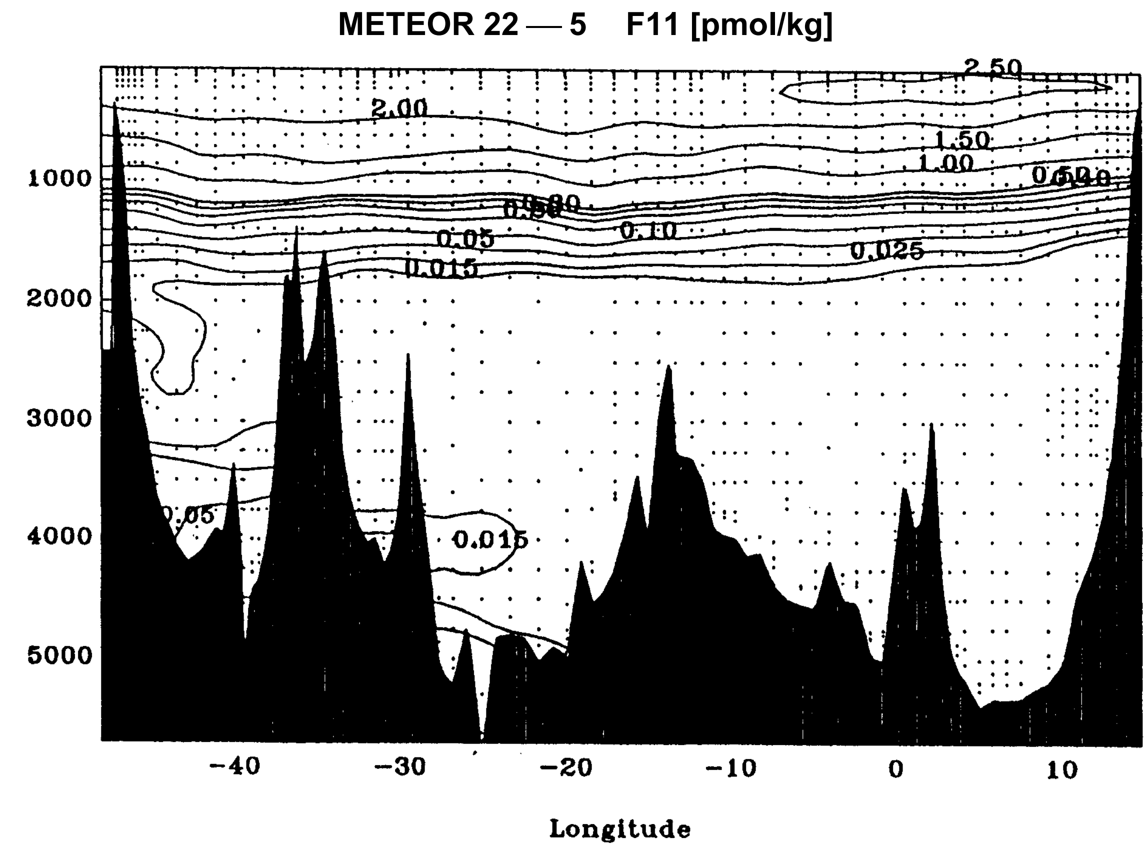

Fig. 35: F-11 section on 30˚S

CFC; HELIUM - NEON ISOTOPE DATA DOCUMENTATION

CRUISE METEOR 22 WHP A10

The data was aquired by

Prof. Dr. Wolfgang Roether
Tracer-Ozeanographie
FB1
Universitaet Bremen
PO.Box. 330 440
28334 Bremen
Tel.: 0421/218-3511 / 4221
Fax: 0421/218-7018
email: wroether@physik.uni-bremen.de

responsible for measurement and data processing of Helium and Neon data:

Christine Rueth
Tel: 0421/218-4317
email: crueth@pacific.physik.uni-bremen.de

responsible for measurement and data processing of CFC data:

Henning Rose
Tel: 0421/218-4562
email: hrose@physik.uni-bremen.de

General comments:

CFC data have been submitted earlier but had wrongly been indicated as being calibrated against SIO scale SIO93 while in reality they had been calibrated against SIO86. This has been corrected in the present version of the data.

F113 measurements during this cruise were seriously contaminated through coelution in the chromatograms and had to be eliminated entirely.

CCL4 measurements in the earlier version had been raised by 17% to match samples of air concentrations. This correction was based on the wrong SIO scale and has not been applied in the present version of the data set. CCL4 concentrations have been increased by 5% to account for the effect that CCL4 is not entirely extracted from the water samples during the measurement process, as noted in the documentation for the data set submitted earlier.

In the beginning of the cruise CFC11 and CFC12 measurements suffered from contamination resulting in large and variable blanks. Low concentrations in the Brasil

Basin have to bee regarded with care. A consistency check with other Woce sections further north was used to eliminate obviously bad data points in the Brasil basin.

The measurements of CFC-11, CFC-12, CFC-113 and CCL4 have been assigned individual errors (CFC-11ER, CFC-12ER, CFC-113ER and CCL4ER). The overall errors are as follows:

- CFC-11 <1% or 0.003 pmol/kg whichever is greater
- CFC-12 <1% or 0.003 pmol/kg whichever is greater
- CCL4 <2% or 0.011 pmol/kg whichever is greater

Quality flags for the CFC measurements are given according to WOCE standards.

- 2 acceptable measurement
- 3 questionable measurement
- 4 bad measurement
- 6 mean of replicate samples
- 9 sample not drawn

- CFC-11 position 1 of quality word
- CFC-12 position 2 of quality word
- CFC-113 position 3 of quality word
- CCL4 position 4 of quality word

Helium isotope and neon concentrations have remained unchanged in comparison to the data set submitted earlier. In the data file we enclose storage time (see below).

Two different sets of samples were taken:

1. Most samples were taken in the usual manner with pinched- off copper tubes. After the gas extraction in Bremen they were measured in the Laboratory with a special Helium - Neon Isotope Mass Spectrometer.
2. Another set was sampled into glas-pipettes and extracted at sea. The glas ampulles with the extracted gas were then transported back to Bremen for measurement.

All samples were calibrated using an air standard (regular air) in the Bremen laboratory. An external standard does not exist.

Please note that the Copper tube samples are NOT corrected for tritium decay during storage time! The storage time is given in the data file, so when the tritium data is available, the correction can be carried out. Because of the very low tritium concentrations in the South Atlantic this will not have a large effect on most of the data. In the upper water column we expect corrections in delta ^{3}He of not more than 0.5% (to be substracted). Below 1000m we do not expect any considerable changes.

Data quality:

Each sample has been assigned an individual error, but the overall errors are as follows. The relative errors for the measured properties can be given as:

- Helium: 0.35 %
- Neon: 0.35 %
- He3/He4: 0.25 % applies to DelHe3

Quality flags for helium and neon both follow a slightly modified WOCE notation.

- 1 sample has been taken but could not be measured
- 2 good data value
- 3 obviously questionable data value
- 4 bad measurement
- 5 correction for air contamination in helium and neon measurements necessary
- 6 average value from replicate samples
- 7 slightly questionable measurement
- 8 sample identification uncertain
- 9 no sample drawn

Helium position 5 of quality word
Delhe3 position 6 of quality word
Neon position 7 of quality word

Evaluation of CTD & Water Sample Salinity and Oxygen data of Woce section A10

The WOCE A10 section was collected in the south Atlantic on METEOR Cruise 22 leg 5 along latitude 30 S from South American to the Africa coast starting in late December 1992 through January 1993. The station numbering is out of sequence begins with 620 through 632, shown in figure 1, followed by stations numbers 1 through 100 collected along 30 degrees South. A chart of beginning station position, created from the summary file of A10, is displayed in the upper panel of figure 1 with a plot of bottom depth versus station number in the lower panel of figure 1. CTD stations 620 & 621 are labeled test stations in summary file. A Bottle file data entry appears for station 620 together with CTD observations but not for 621. No 2 dbar CTD cast was found for either station 620 or 621. The first shallow station group, stations 17 through 25, is on the Rio Grande Plateau while the next rise in topography centered on station 55 is associated with the Mid-Atlantic Ridge showing a minimum bottom depth of less than 3000 meters which blocks (except for flow through deep channels) most of the AABW from reaching the Angola Basin to the East. The shallow feature around station 77 is the Walvis Ridge which separates the Angola Basin from the Namibia Abyssal Plain bounded to the East by the African coast. The deep waters of each basin is examined separately because of distinct water mass characteristics.

A salinity versus potential temperature plot (figure 2) shows all water sample file salinities (water sample and CTD up cast) along with the 2 decibar down-profile CTD data from section A10. The salinities are well matched to the bottle salinities to the resolution of the plot. There are several stations with fresh surface salinities with station 70 particularly fresh with a surface salinity less than 30.0 psu. Stations with fresh surface salts are examined later. The deep water is separated into several basins as mentioned. See the lower panel of figure 1. West of the Mid-Atlantic Ridge the deep waters connect directly to the Antarctic deep waters and presence's of Antarctic Bottom Water (AABW) with a potential temperature for one station less than 0.0°C is seen in figure 3. Figure 4 is a deep water potential Temperature versus salinity plot of stations 56 to 75 taken in the Angola Basin, East of the Mid-Atlantic Ridge. The profiles show a lack of the cold AABW different water mass influence as the minimum Potential temperature is 1.8°C. Figure 5 shows the presence's of AABW in the salinity versus pot. temperature of stations 78 to 90, collected on the Namibia Abyssal Plain to the East of the Walvis Ridge. The CTD salinities in the deep water are well matched to bottle salts in figures 3, 4, and 5 except for a few water sample salinities marked as good "2" in QUALT1 but flagged as questionable in QUALT2. These and are identified on figure 3 with the associated station numbers (stations 14, 40 and 50).

CTD Salinity

A comparison of the up-profile CTD and water sample salinity data in the water sample file (A10.hyd) is shown in figure 6. The up-cast CTD salinities are pretty well matched to the water sample salinities both overall (upper panel) and below 1000 dbars (center panel) exception for the few water sample salinities noted on figure 3 (stations 14, 40 & 50) and deepest salinities of station 29. Examining station 29's water sample data with neighboring stations indicates the salinity mismatch to be within the deep salinity variability with potential temperature of surrounding stations (i.e. the bottle salts fall on station 30 & 31 theta/s) as indicated by the theta/s plot of stations 27 through 31 shown in figure 7. The bottom panel of figure 6 shows the salinity differences to be well behaved in the vertical. Figure 8 shows four histograms of salinity difference (CTD-WS) in various deep intervals. Below 1000 dbars the histograms show a constant standard deviation of salt difference of 0.003 psu and mean differences of less than 0.001 psu.

The down-profile CTD salinity difference is plotted in figures 9 a, b, & c using interpolation at the pressure of the up-profile water sample bottles. Like the up cast CTD salinities, the down cast shows no systematic differences with station but a suggestion that the CTD salinity reads lower than the water sample salts at depths less than 2500 dbars. Figure 10 are four histograms of interpolated down-profile CTD salinity minus bottle salt broken up into 1500 dbar pressure intervals below 1000 dbars. Below 1000 dbars, this summary shows a scatter of from 0.004 (deep) to 0.006 (shallower) psu with mean differences that are within 0.001 psu below 3000 dbars but is -0.0028 psu for pressure intervals between 1000 and 3000 dbars and -0.004 psu from 1000 dbars to the surface. There seems to be mismatch between the down and up salinity of the CTD sensors (form either C, T or P) shallower than 3000 decibars with the salinity fresher than bottle salts.

There are a few stations with low surface salinities mentioned earlier. Using a surface salinity (0 to 2 decibar) edit criteria of ds/dp for the first interval less than the 5*ds/dp of the third interval and the |ds/dp| < 0.5 psu/dbar, the eight stations plotted in figure 11 were flagged. Three stations, 45, 70 and 88, have surface (2 dbars) salinity values less than 34.0 psu while the salt values at 4 dbars are between 2.4 and 6.3 psu higher.

CTD Oxygen

An oxygen versus potential temperature plot shown in figure 12 has all of the good water sample file bottle oxygen data along with the 2 decibar down-profile CTD data from section A10. Note, there are no CTD oxygen data in the water sample file. The down profile CTD oxygen is not as well matched to the bottle oxygen data and even in the coarse scale plotted the CTD oxygen appears to be greater than the bottle oxygen. There is one station (91) which has an excessively high surface oxygen of over 408 micromoles/kg in the upper two pressure intervals. The deep oxygen was examined versus potential temperature for the three basins just as it was earlier for salinity. All three deep water oxygen plots indicate that the CTD oxygen is greater than the water sample value by from 6 to 7 micromoles/kg. Only the oxygen versus potential temperature plot for the Nambia Abyssal Plain is shown in figure 13.

The down-profile CTD oxygen difference with water samples is plotted in figures 14 a, b, & c using an interpolation at the pressure of the up-profile water samples. The down cast difference shows a clear offset between the CTD oxygen and bottle values in all three plots but particularly in the expanded scales of figures 14b and c. The mean difference for all stations and depths is 6.2 micromoles/kg and appears to effect all stations and depths more or less equally. Suggestion that the CTD salinity reads lower than the water sample salts at depths less than 2500 dbars. Figure 15 shows four histograms of oxygen difference (CTD-WS) for various deep intervals. The mean oxygen difference varies by 20 percent between the various pressure intervals represented by the histograms.

There are systematic oxygen differences effecting all CTD oxygen values. Subtracting a constant equal to roughly 6.2 Umoles/kg from all CTD oxygen values will bring the CTD oxygen into much closer agreement with water samples. Station 91 CTD oxygen needs to be edited in the upper 2 pressure bins.

Stability

The stability of the CTD data is checked by looking at the first differences of the potential density anomaly values of the 2 decibar data within a station. Unstable density anomaly differences (i.e. denser above lighter) that exceed -0.0075 kg/dbar and a more stringent -0.005 kg/dbar are plotted in figure 15. The table below indicating stations with observations failing the -0.0075 kg/dbar criteria with additional values failing -0.005 kg/dbars following. A list of stations with density inversions repeats the data shown in figure 15.

Station	Dsg/dp	Pres.	Salt	Dt/dp dsg/dp < -0.0075 kg/dbar
630	-0.09324	100.0	36.5010	-0.03975
630	-0.01719	102.0	36.4202	-0.05025
630	-0.01823	112.0	36.3577	-0.02005
5	-0.00774	4.0	36.1915	0.01000
12	-0.01445	4.0	36.2132	0.02005
15	-0.00767	4.0	35.9952	0.00885
18	-0.00902	4.0	36.1430	0.01155
21	-0.01399	4.0	36.1247	0.02365
22	-0.00910	4.0	36.2692	0.01305

Station	Dsg/dp	Pres.	Salt	Dt/dp dsg/dp < -0.0075 kg/dbar
25	-0.00945	40.0	36.3711	-0.12160
33	-0.00815	8.0	35.8674	0.03555
34	-0.00787	10.0	35.7769	0.01460
39	-0.01156	4.0	35.6508	0.01360
48	-0.03903	14.0	35.5885	0.08415
55	-0.02060	4.0	35.8051	0.06110
56	-0.01228	4.0	36.1198	0.01490
57	-0.01259	4.0	36.0788	0.01940
61	-0.00979	4.0	35.7220	0.02285
76	-0.02018	6.0	35.9259	0.07285
79	-0.00753	10.0	35.8027	0.02425
84	-0.01792	4.0	35.6524	0.00610
90	-0.06800	4.0	35.4913	0.00350
92	-0.01108	4.0	35.6462	0.01750
623	-0.00568	176.0	35.4899	-0.03745
630	-0.00547	114.0	36.3193	-0.03435
5	-0.00631	378.0	35.7421	-0.02770
8	-0.00590	4.0	36.2180	0.00705
49	-0.00509	4.0	35.7092	0.00700
55	-0.00556	634.0	34.5255	-0.02455
81	-0.00520	222.0	35.3172	-0.03020
82	-0.00709	4.0	35.7995	0.00955

Water Sample Salinity checks:

Water sample salinity observations were found for only approximately 1/3 of the total water sample observations.

The following edit criteria comparing CTD and water sample salinity found the following 15 questionable CTD or water sample salinity, both flagged "3". Notice that the deep water edit criteria (0.01) was not sensitive enough to identify questionable salinities of station 29.

|ds| > 0.2 psu for pressure <=500 decibars;
|ds| > 0.02 psu for pressure >500 and <= 1500 decibars;
|ds| > 0.01 psu for pressure > 1500 decibars;

A list of bottle file observations with the QUALT2 salinity quality flags differing from those of the PI QUALT1 are given in file = A10DQE.chg .

Figure number with file names (____. jpg) and figure caption

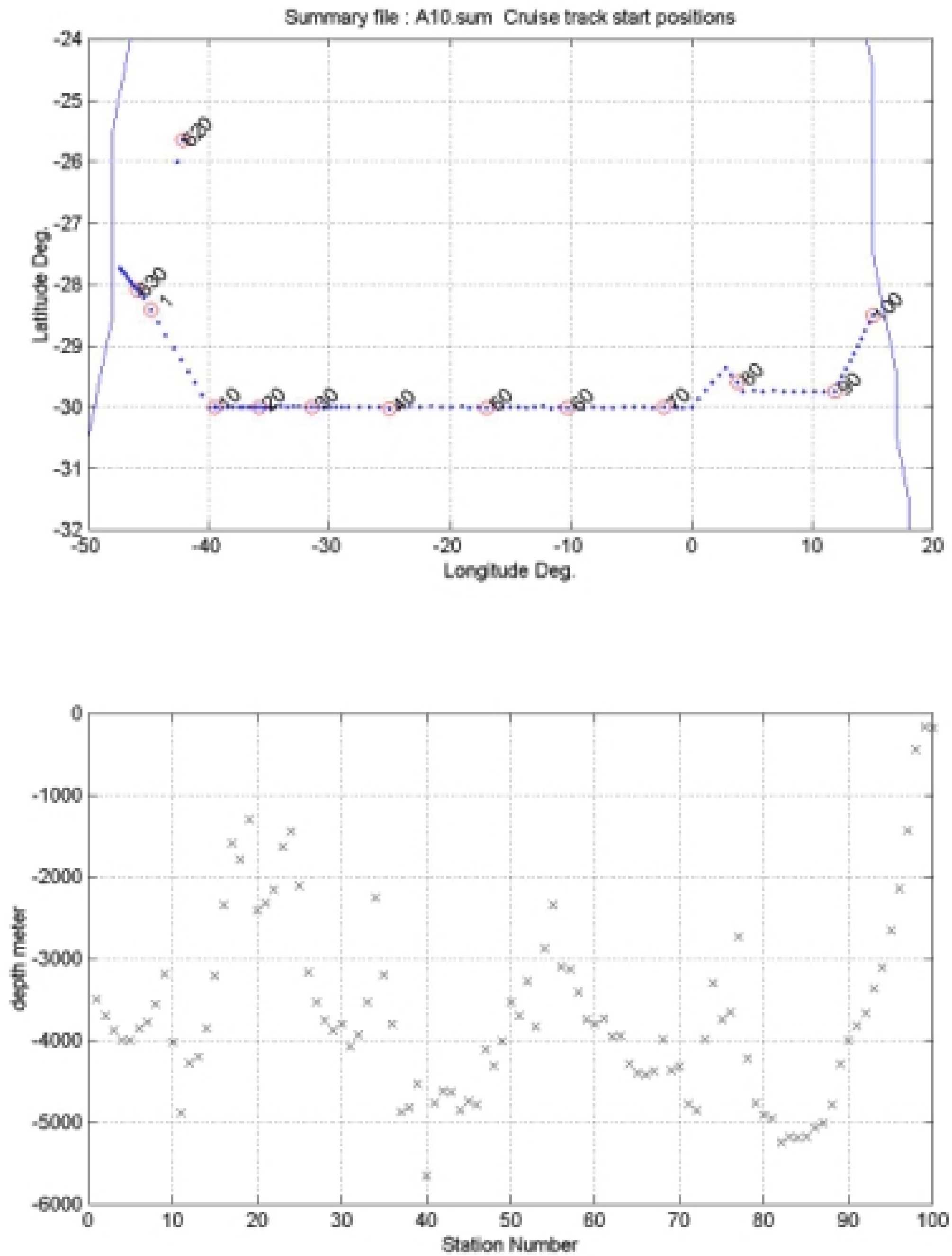

1) fig01_a10.jpg
Plot of annotated beginning station positions from summary file with coastline (upper) and plot of bottom depth (lower).

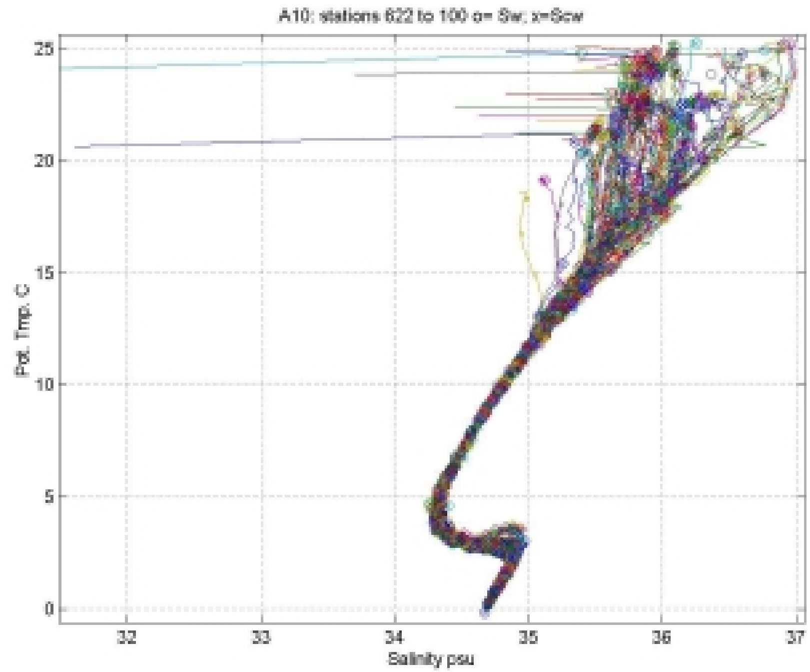

2) fig02_a10.jpg
Overall plot of Salinity versus Potential temperature for all down profile 2-decibar CTD salinities plus QUAL1 "good bottle file water sample (+) and CTD (o).

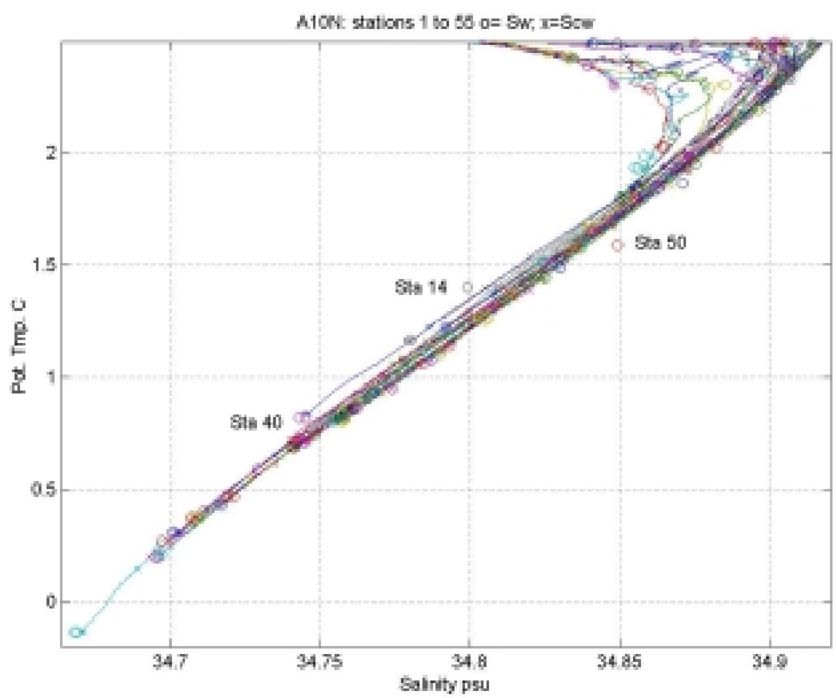

3) fig03_a10.jpg
Deep water plot of Salinity versus Potential temperature West of Mid-Atlantic ridge for all down profile 2-decibar CTD salinities plus QUAL1 "good bottle file water sample (+) and CTD (o).

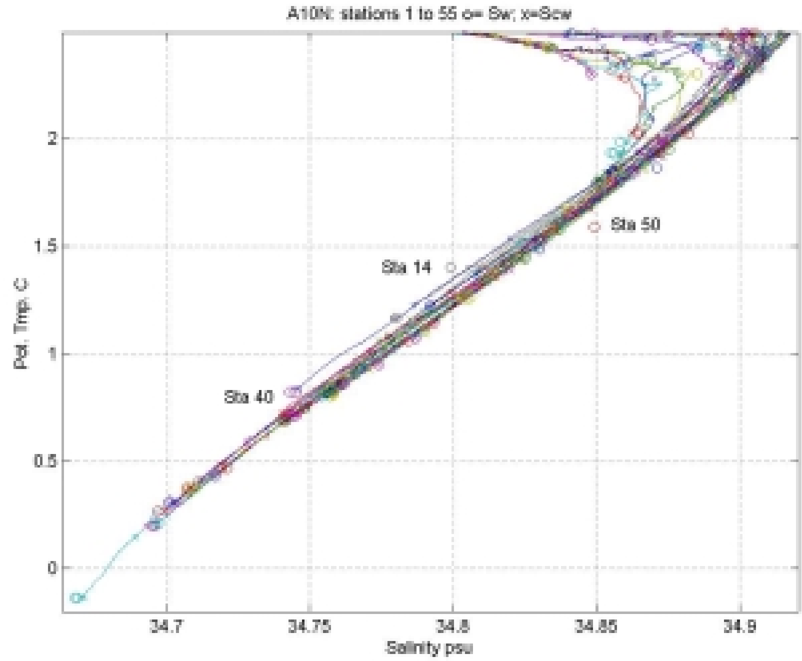

4) fig04_a10.jpg
Deep water plot of Salinity versus Potential temperature in Angola Basin (East of Mid-Atlantic Ridge) for all down profile 2-decibar CTD salinities plus QUAL1 "good bottle file water sample (+) and CTD (o).

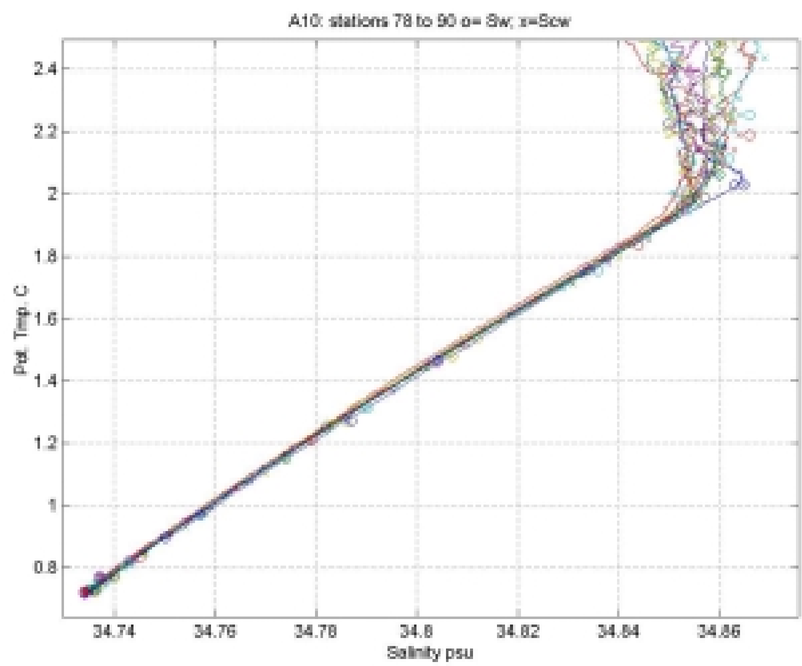

5) fig05_a10.jpg
Deep water plot of Salinity versus Potential temperature on Nambia Abyssal Plain for all down profile 2-decibar CTD salinities plus QUAL1 "good bottle file water sample (+) and CTD (o).

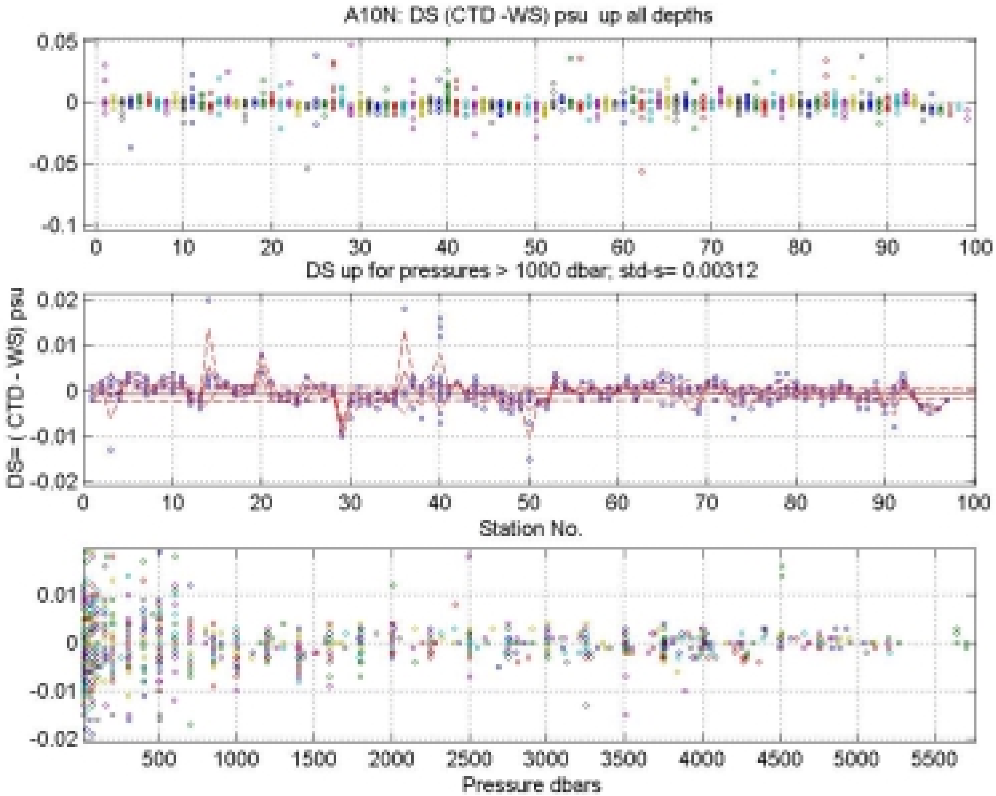

6) fig06_a10.jpg
3 Plot panels of up cast salinity differences Ds = (CTD-WS) psu versus station number (a) all pressures (b) below 1000 dbars and (c) versus pressure.

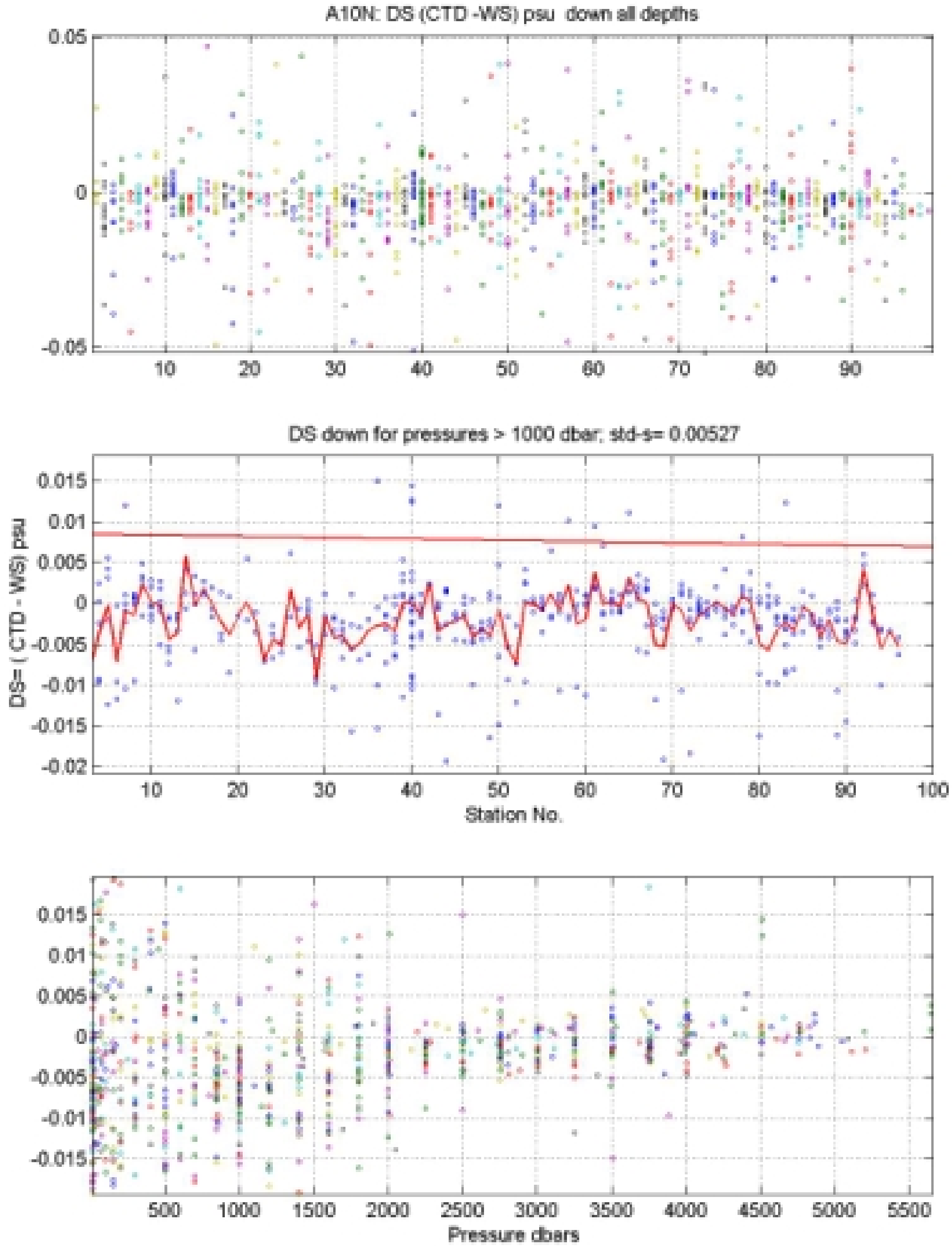

7) fig07_a10.jpg
3 Plot panels of downcast salinity differences Ds = (CTD-WS) psu versus station number (a) all pressures (b) below 1000 dbars and (c) versus pressure.

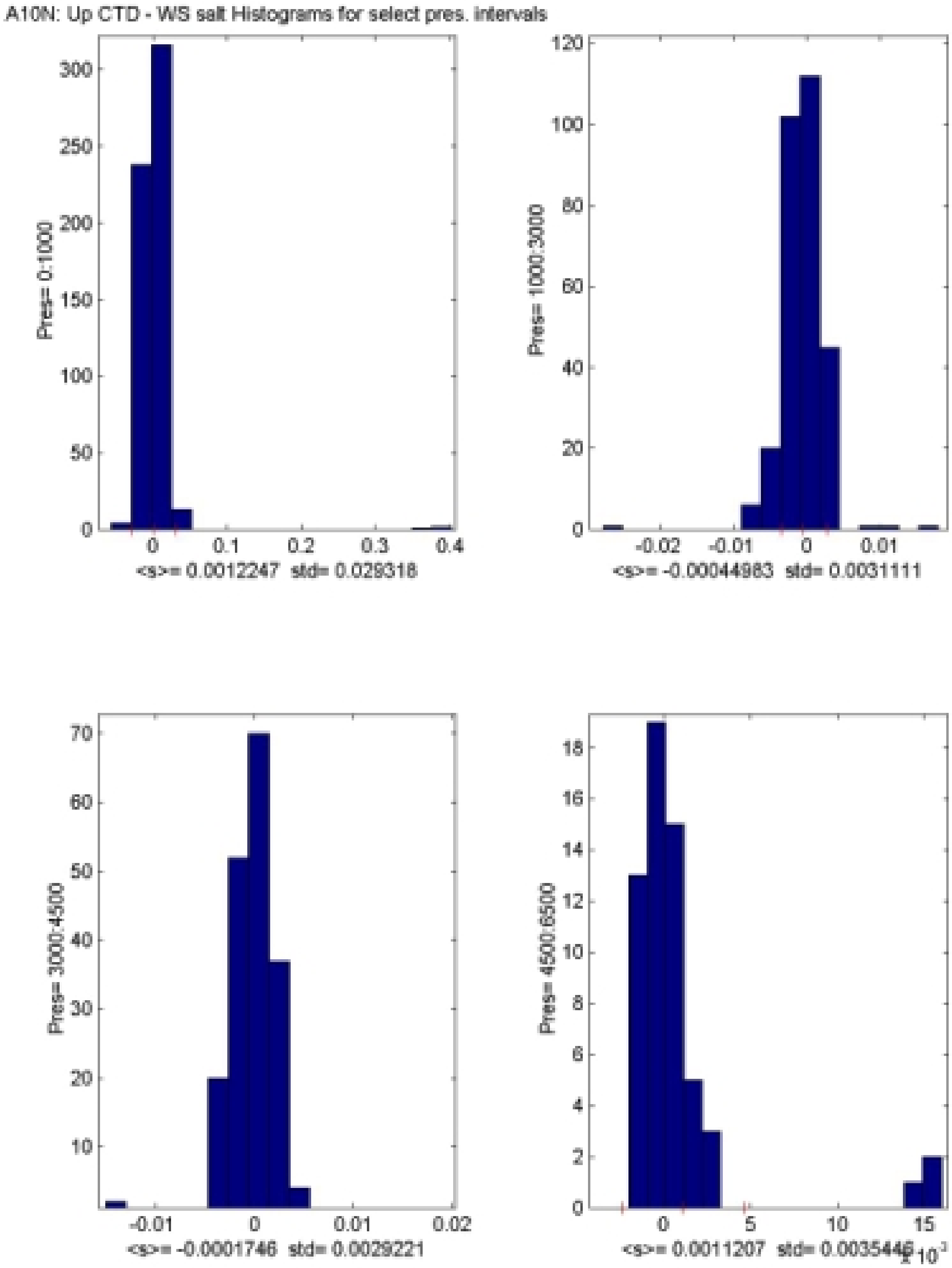

8) fig08_a10.jpg
4 histogram panels of up cast salinity differences Ds = (CTD-WS) psu for various pressure intervals as labeled.

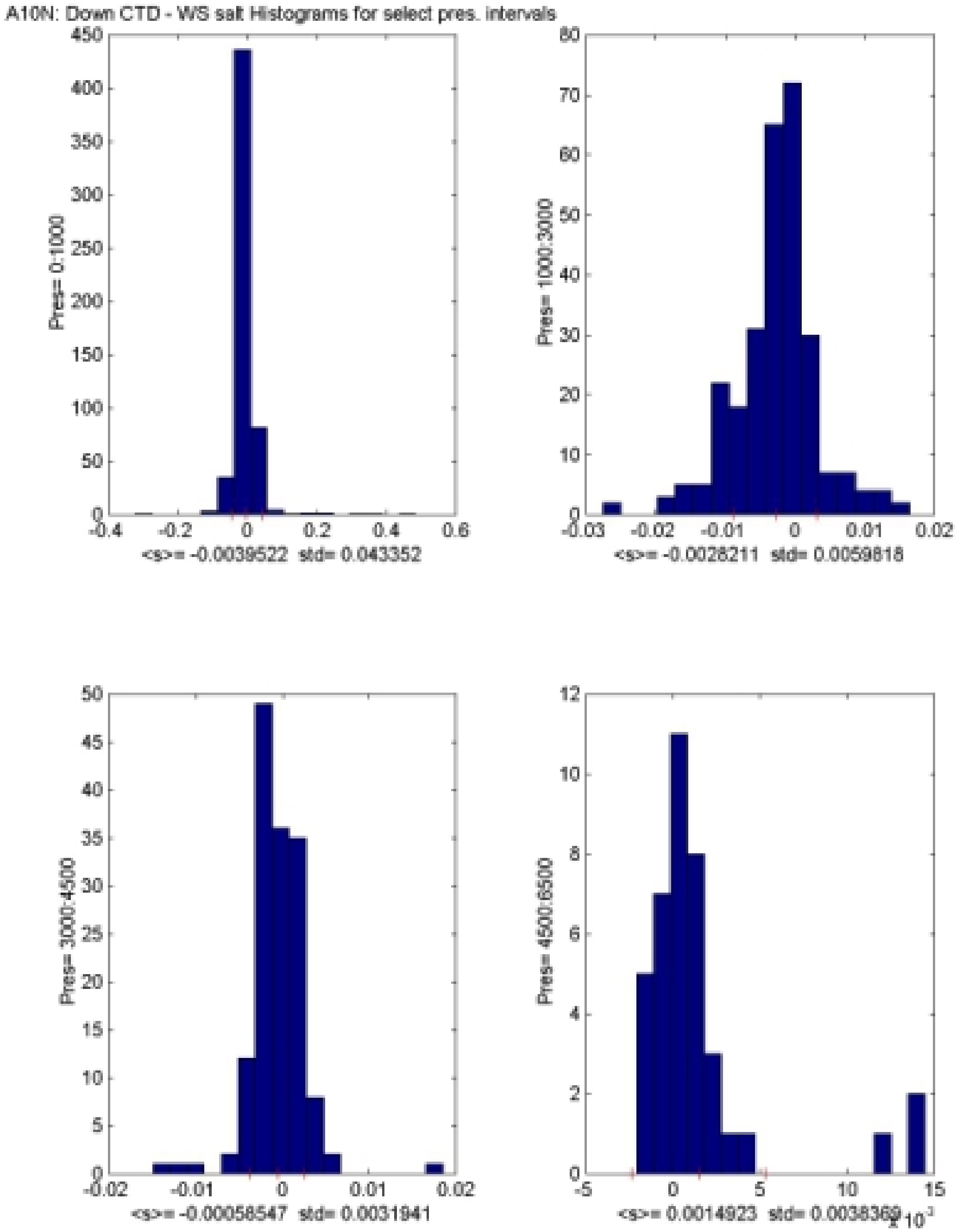

9) fig09_a10.jpg

4 histogram panels of downcast salinity differences Ds=(CTD-WS) psu for various pressure intervals as labeled. Note a much higher standard deviation in 2 shallowest histogram panels compared to up cast.

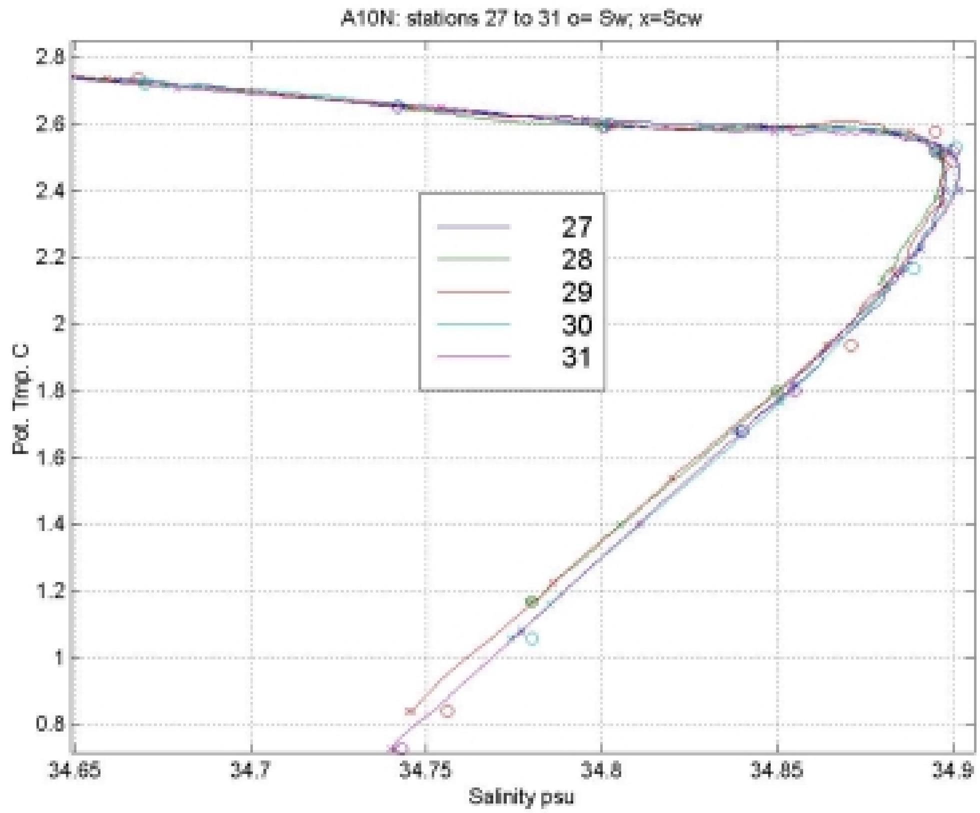

10) fig10_a10.jpg
Deep water plot of Salinity versus Potential temperature for stations 27 through 31 showing CTD station 29 (red) mismatch to water sample (o) data.

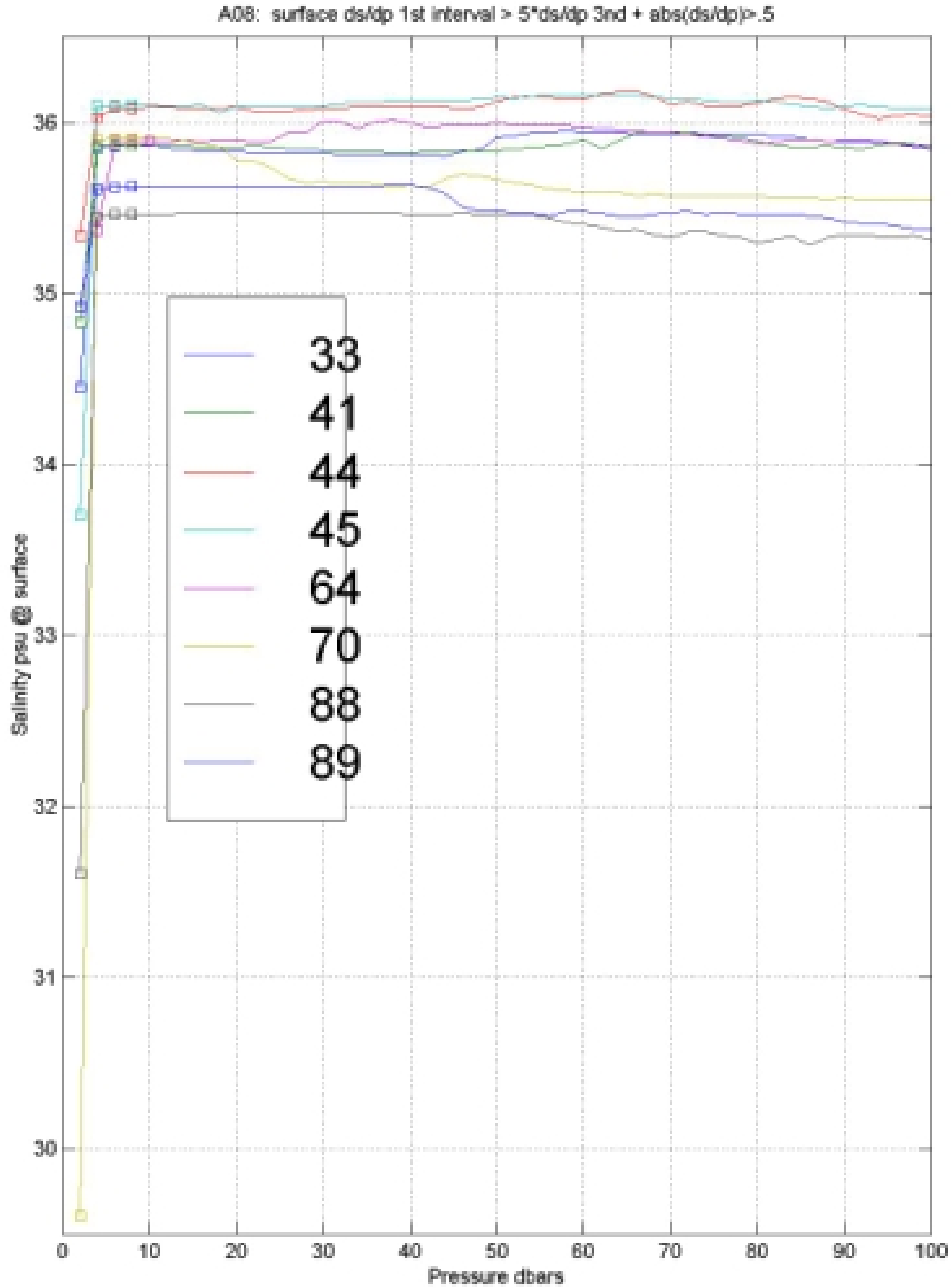

11) fig11_a10.jpg
Plot of salinity versus pressure for upper 100 dbars of stations with questionable surface CTD salinity observations.

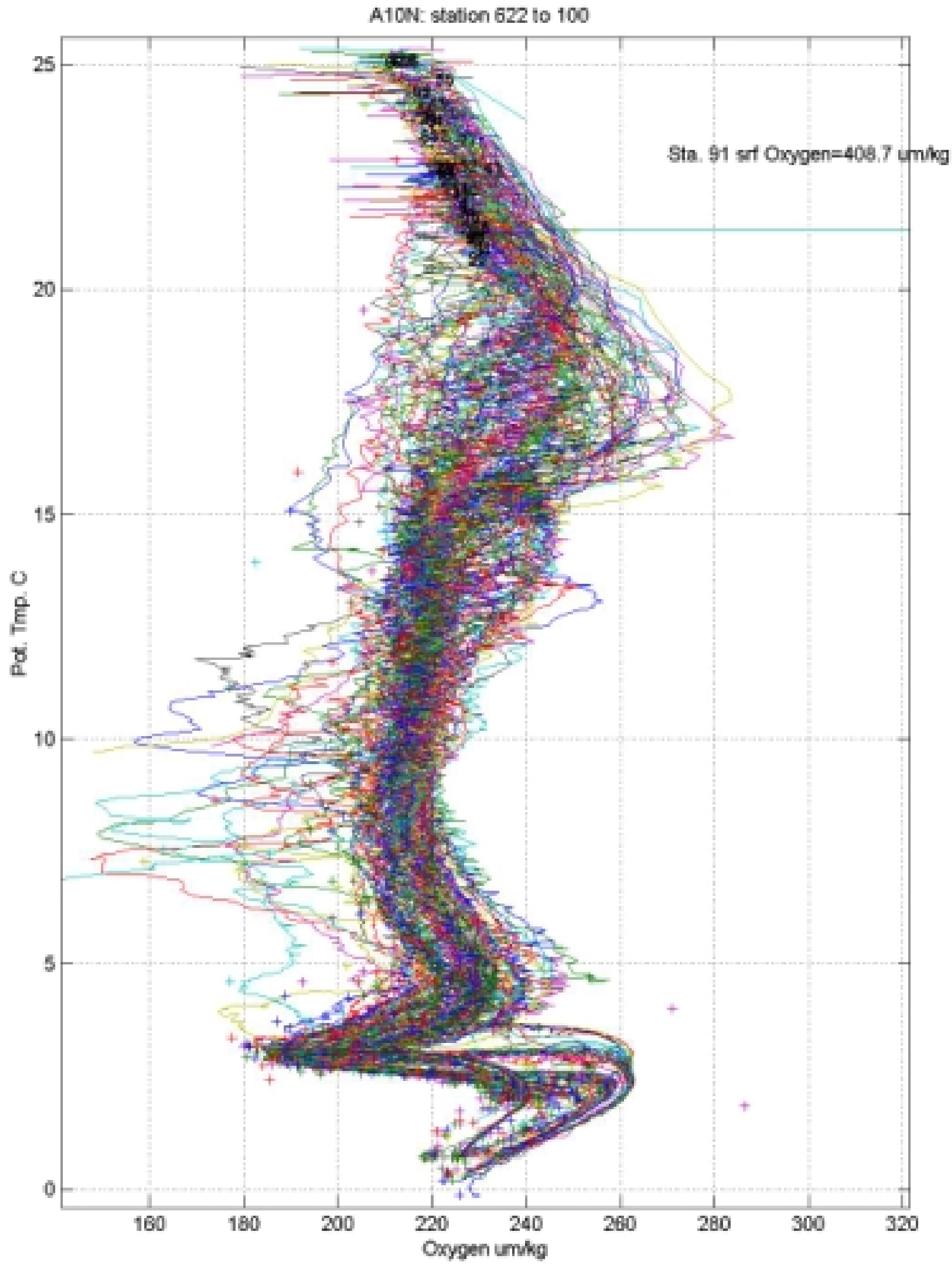

12) fig12_a10.jpg

Overall plot of oxygen versus Potential temperature for down profile 2-decibar CTD oxygen plus QUAL1 "good bottle file water sample (+). Note there is no CTD oxygen data in water sample file.

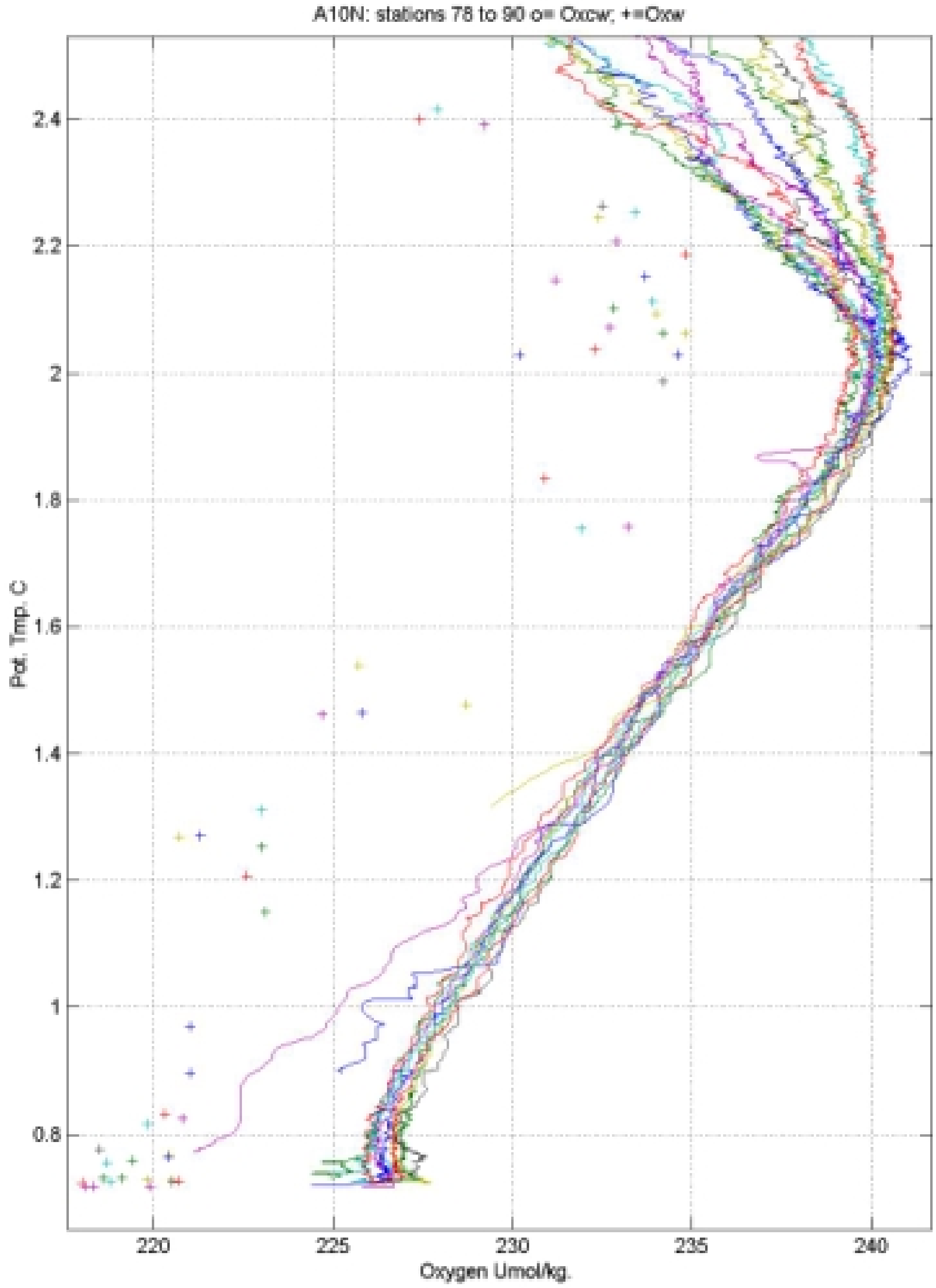

13) fig13_a10.jpg
Deep water plot of oxygen versus Potential temperature for Nambia Abyssal Plain below 2.5 degrees C for down profile 2-dbar CTD oxygen plus QUAL1 "good bottle file water sample (+).

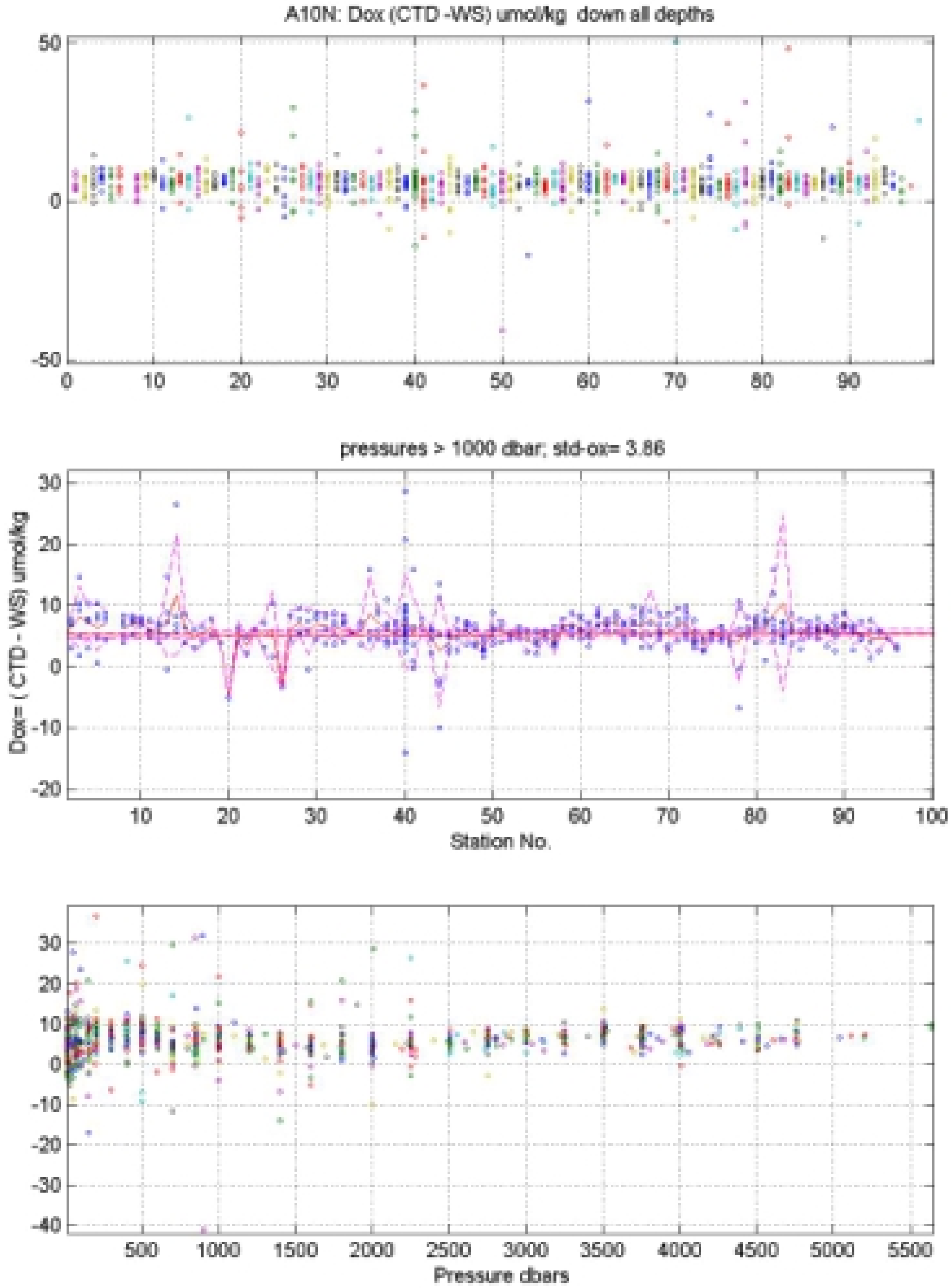

14) fig14_a10.jpg

3 Plot panels of down cast oxygen differences Dox=(CTD-WS) in Umol/) (CTD down cast oxygen observations are interpolated at bottle pressures) versus station number (a) all pressures (b) below 1000 dbars and (c) versus pressure.

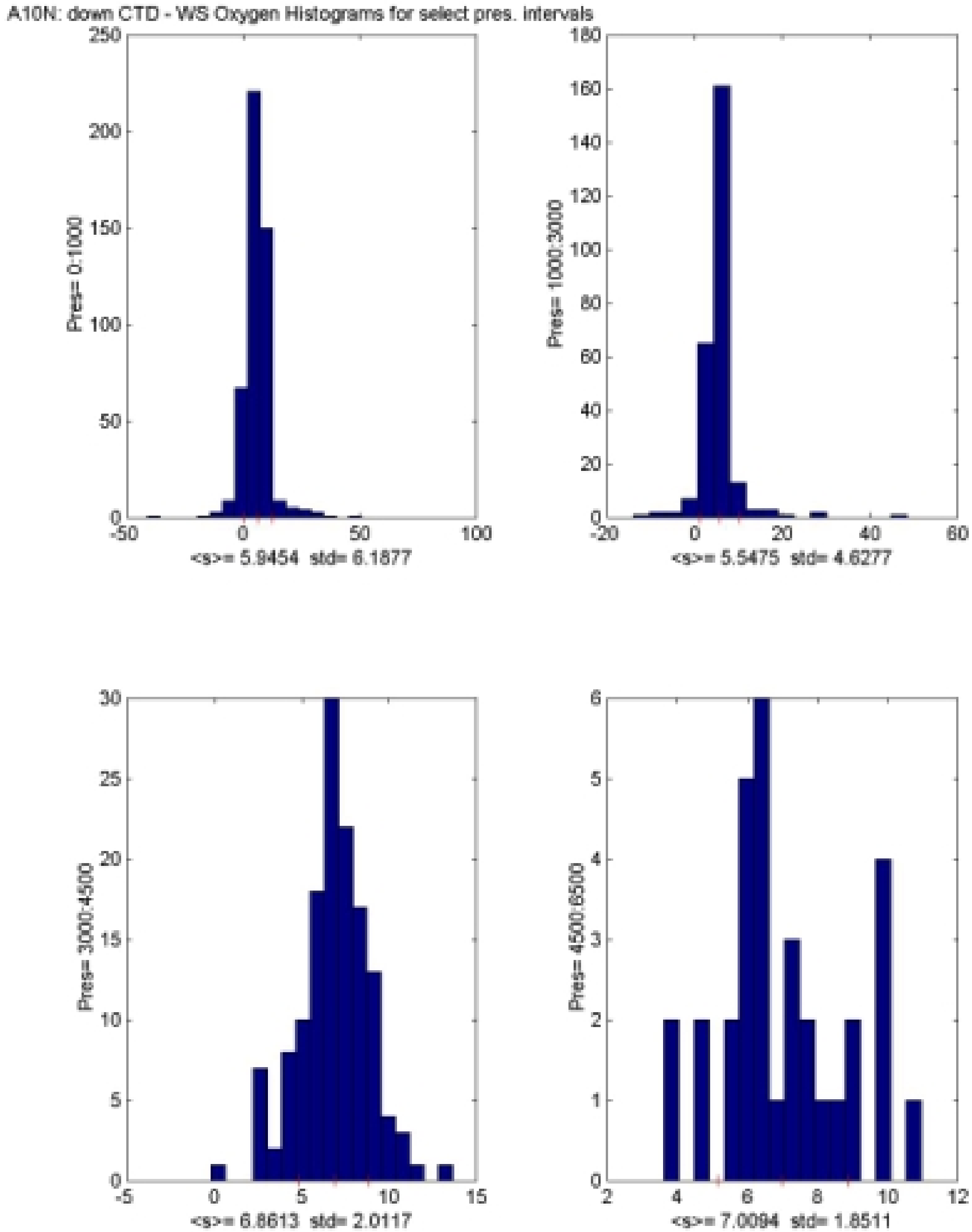

15) fig15_a10.jpg

4 histogram panels of down cast oxygen differences Dox=(CTD-WS) in Umol/kg for various pressure intervals as labeled. CTD down cast oxygen observations are interpolated at bottle pressures.

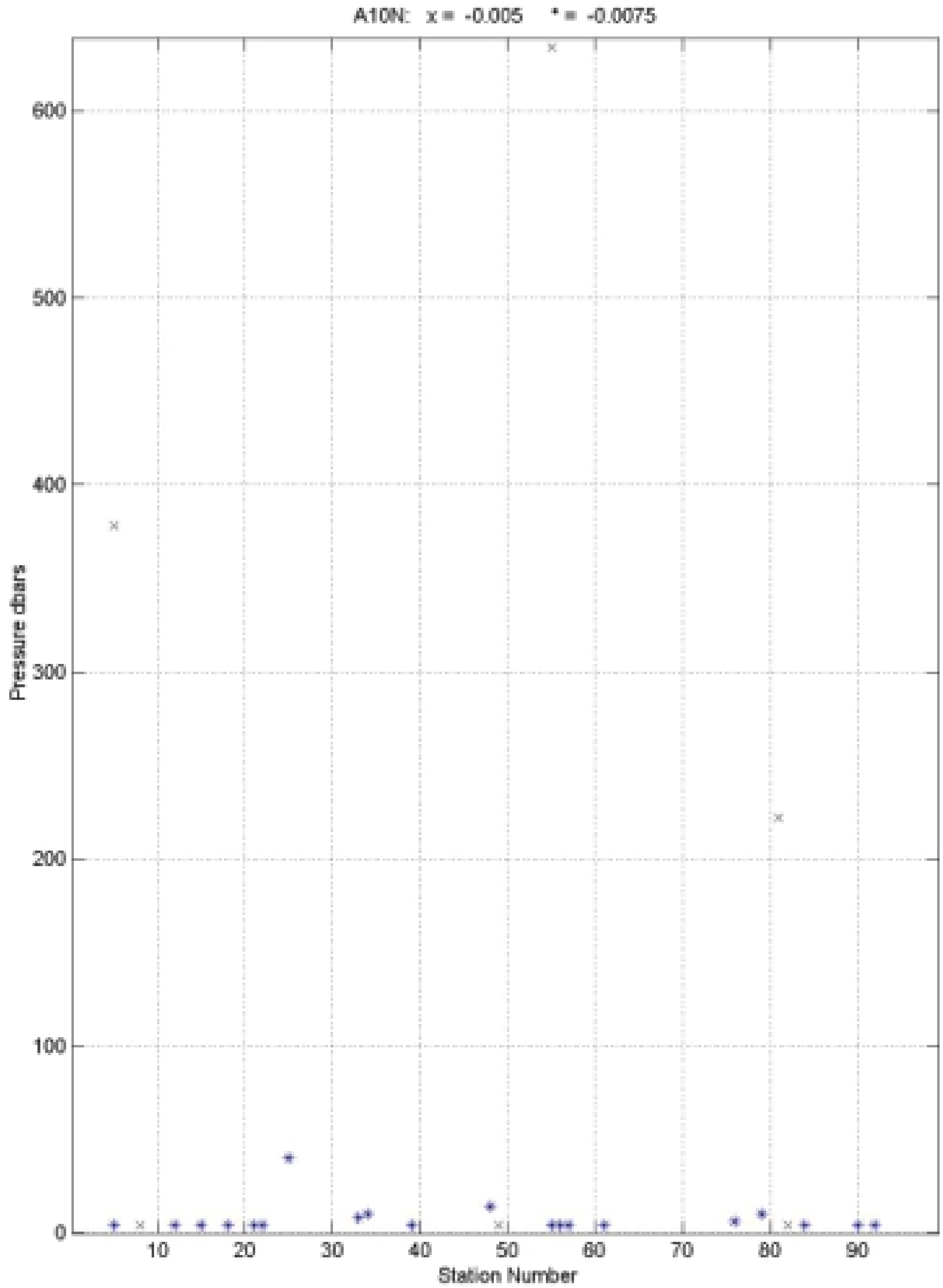

16) fig16_a10.jpg
A plot of pressure versus station indicating unstable values of density change with pressure:

a) x exceeding -0.005 kg/M3/dbar
b) * exceeding -0.0075 kg/M3/dbar

WOCE A10 DQE Notes: Dissolved Oxygen and Nutrients

Joe C. Jennings, Jr. and Louis I. Gordon

Overall impressions:

The A10 section (METEOR Cruise 22, Leg 5) was a zonal transect of the South Atlantic at ca 30° South**.** Stations 621 – 632 were occupied at the end of December 1992, with station numbering changing to 1 – 100 commencing in January 1993. The direction of the Transect was West to East.

CTD oxygen was not reported and so could not be used in evaluating the bottle oxygen data. NO_3+ NO_2 (N+N) was reported, but not a separate NO_2 determination. For most of the water column, the conversion to NO_3 by subtracting NO_2 from N+N would be negligible, but near the bottom of the mixed layer, NO_2 concentrations significantly different from zero could be expected.

As received from the WHPO (and data originator?), the Q1 quality bytes for N+N were all assigned as "9" which indicates that the parameter was not sampled. We have changed the Q1 quality words for all reported N+N values to "2".

The A10 section has a number of noisy oxygen samples, which could have been caused by an inexperienced sampler(s). Overall, the nutrient data are quite good, with few problems.

There are several stations at which it appears that a mis-assignment of bottle depths may have occurred. This affects only the oxygen data in some cases, only the nutrient data in others, and both in still others. At these stations, the vertical profiles and parameter/theta relationships appear offset from those at neighboring stations. Rather than a random offset caused by instrumentation problems, the data appear to be shifted and would agree well with other stations if the values were assigned to the bottle above or below. This could be caused by real mal-functions of the CTD rosette (such as double trips) or by record keeping or file merging errors. We would recommend that the data originators reexamine their records to see if the data may indeed have been shifted.

Comparisons with other WOCE cruises:

The A10 section crosses four other recent WOCE sections that we have examined. We compared vertical profiles and property/theta plots from the three stations in each section closest to the intersection point. A brief summary of these comparisons follows here.

A10/A13: A13 crosses the A10 section at ca. 10°E, 30°S in the eastern Cape basin. This is a highly dynamic region because of the Agulhas Current and it's retroflection zone, so we have confined our comparisons to the deep water (3000 – 5000 m) where the T/S properties of the two cruises were indistinguishable.

There is good agreement between the dissolved oxygen and silicate data from the two cruises, but the nitrate and phosphate data from A10 are higher than on A13. At temperatures below 2°C, the A10 stations are ca. 1.5 µM/kg higher in nitrate and 0.08 µM/kg lower in phosphate than the A13 stations. There is also more noise (or variability) in the A13 data.

A10/A14: The A14 and A10 nutrient and oxygen data largely overlap. Below 2500 m, the A14 nitrate and phosphate data is slightly lower than the A10 data. The A14 nitrate is ca 0.5 – 0.7 µM/Kg lower than the A10 nitrate, while the phosphate is ca 0.04 – 0.08 µM/Kg lower. There are no clear differences in the deep silicates or oxygen. A14 stations 75 and 77 have slightly (0.6 µM/Kg) higher silicates than the A10 stations, but A14 stations 76 and 78 agree well with the A10 data.

A10/A15: The A15 and A10 data sets appear to agree well. Below about 3500 m, the A15 phosphate and nitrate fall within the “envelope” of the A10 data. Dissolved oxygen and silicate mostly overlap although the oxygen at A10 station 46 is higher by ca. 2 – 4 µM/kg below 3500 m than at the other stations and the silicate is lower by 5 – 8 µM/kg. A15 station 104 has higher oxygen and lower nutrients at the oxygen maximum/nutrient minimum (2000 m – 3000 m) than do the other stations at the crossing, but the salinity at this station is also higher in this depth range so these differences are probably real.

A10/A17: These two cruises intersect near the Rio Grande Rise, which separates the Brazil and Argentine basins. There is good overlap of salinity between 2000 and ca. 3300 m. A10 nitrate and phosphate are mostly higher (1.4 µM and 0.07 µM respectively) than the A17 values in this depth interval and the oxygen data are a little higher as well, but the silicate overlap is good. In the bottom waters, the nutrient concentrations at the more southerly A17 stations all increase and become higher than the A10 concentrations. This is probably a real and due to the influence of the Argentine Basin waters, but the offset at mid-depths remains.

Comments on specific stations:

A listing of stations at which specific bottle data seems to be questionable is attached. The “Q2” data quality flags for these data have been set to 3.

Cruise A10 : 06MT22/5

Nutrient and Oxygen DQE: "questionable" flags by Gordon/Jennings (OSU)

Station	Bottle	Pressure	O2	Si	NO3	PO4	Comments
630	316	300	High				
632	307	1799	High				
3	311	1900	Low				Odd Shift in O2.
10	320	399		High	High	High	
10	315	1198	High				
11	316	2501	Low				
11	312	3505	Low				
13	311	2250	High				
20	318	100	*	*	*	*	* 305-318 Nutrients and O2 shifted by one bottle?
20	317	150	*	*	*	*	Looks fine if one depth lower.
20	316	200	*	*	*	*	
20	315	300	*	*	*	*	
20	314	399	*	*	*	*	
20	313	499	*	*	*	*	
20	312	599	*	*	*	*	
20	311	799	*	*	*	*	
20	310	999	*	*	*	*	
20	309	1200	*	*	*	*	
20	308	1400	*	*	*	*	
20	307	1601	*	*	*	*	
20	306	1800	*	*	*	*	
20	305	2001	*	*	*	*	
26	318	100	Low				
26	311	700	Low				No Nutrient shift.
26	309	1200	Low				302-311 All O2 shifted one depth too shallow.
26	308	1400	High				
26	307	1600	High				
26	306	1803	High				
26	305	2000	High				
26	304	2250	High				
26	302	2802	High				
30	312	1801	High				
36	206	102		Low	Low	Low	201-206 Nutrients look too low, probably shifted.
36	205	151		Low	Low	Low	201-206 Nutrients look too low, probably shifted.
36	204	201		Low	Low	Low	
36	203	299		Low	Low	Low	
36	202	402		Low	Low	Low	
36	201	505		Low	Low	Low	

36	319	848	*				* 310-319 Oxygens look one bottle too deep.
36	318	998	*				
36	317	1194	*				
36	316	1397	*				
36	312	1600	*				
36	311	1798	*				
36	310	1998	*				
40	209	300	High				O2 looks high vs. Z and Theta
40	205	1199	High				
40	204	1399	High				
40	203	1598	Low				
40	323	1800			Low		
40	202	1800	Low				
40	201	2004	Low				
41	207	202	Low				
41	206	301		*	*	*	201-206 All Nutrients off by one bottle.
41	205	401		*	*	*	
41	204	500		*	*	*	
41	203	601		*	*	*	
41	202	701		*	*	*	
41	201	851		*	*	*	
41	319	1199	*				* 305-319 All O2s look off by one bottle. If shifted
41	318	1399	*				down the profiles would agree well.
41	317	1600	*				
41	316	1800	*				
41	315	2000	*				
41	314	2251	*				
41	313	2502	*				
41	312	2752	*				
41	311	3003	*				
41	310	3252	*				
41	309	3502	Low				O2 too low, even if bottle depths were shifted.
41	308	3755	*				
41	307	4006	*				
41	306	4255	*				
41	305	4506	*				
44	323	10	Low				
44	320	849	*				* 305-320 O2 look shifted one bottle too shallow.
44	319	1000	*				* 305-320 O2 look shifted one bottle too shallow.

44	318	1199	*				
44	317	1398	*				
44	316	1600	*				
44	315	1800	*				
44	314	2001	*				
44	313	2251	*				
44	312	2501	*				
44	311	2752	*				
44	310	3003	*				
44	309	3252	Low				Low beyond shift noted above.
44	308	3504	*				
44	307	3754	*				
44	306	4003	*				
44	305	4256	*				
46	205	401	High				
46	206	302	High				
46	313	2250	Low				
48	307	3253	Low				
50	317	900	High				
50	307	2852	High				
50	302	3653	High				
52	306	2250	Low	High	High	High	
53	319	601		Low	Low	Low	
55	312	602	Low Y				
58	314	849	Low				
58	313	999	High				
60	316	897	Low				
61	304	3508				High	
62	315	1200	High				
63	307	3002		High			
67	311	2251	High				
70	204	252	Low				
70	304	4017	High				
74	322	50	Low				
74	304	2754			High		
78	306	3502	*				* Poor duplicates, O2 above and below looks shifted.
78	307	3502	*				
81	306	4255	Low				
83	314	2502	Low				
86	320	1198	High				
89	202	501	Low				
93	204	504	Low				